

7  
ADA035843

# NAVAL POSTGRADUATE SCHOOL Monterey, California



## THESIS

FINITE ELEMENT SOLUTION OF THE NONLINEAR  
COUPLED NEUTRONIC-ENERGY EQUATIONS  
FOR A FAST REACTOR FUEL CELL

by

Roy Edward Kasdorf

December 1976

Thesis Advisor:  
Thesis Advisor:

D. Nguyen  
D. Salinas

Approved for public release; distribution unlimited.

REPRODUCED BY  
NATIONAL TECHNICAL  
INFORMATION SERVICE  
U.S. DEPARTMENT OF COMMERCE  
SPRINGFIELD, VA. 22161

156P

REPORT DOCUMENTATION PAGE		READ INSTRUCTIONS BEFORE COMPLETING FORM
1. REPORT NUMBER	2. GOVT ACCESSION NO.	3. RECIPIENT'S CATALOG NUMBER
4. TITLE (and Subtitle) Finite Element Solution of the Non-linear Coupled Neutronic-Energy Equations for a Fast Reactor Fuel Cell		5. TYPE OF REPORT & PERIOD COVERED Master's & Mechanical Engineer's Thesis; December 1976
7. AUTHOR(s) Roy Edward Kasdorf		6. PERFORMING ORG. REPORT NUMBER
9. PERFORMING ORGANIZATION NAME AND ADDRESS Naval Postgraduate School Monterey, California 93940		8. CONTRACT OR GRANT NUMBER(s)
11. CONTROLLING OFFICE NAME AND ADDRESS Naval Postgraduate School Monterey, California 93940		10. PROGRAM ELEMENT, PROJECT, TASK AREA & WORK UNIT NUMBERS
14. MONITORING AGENCY NAME & ADDRESS (if different from Controlling Office) Naval Postgraduate School Monterey, California 93940		12. REPORT DATE December 1976
		13. NUMBER OF PAGES
		15. SEC. 1 Unclassified
		15a. SEC. 1 Unclassified
16. DISTRIBUTION STATEMENT (of this Report)  Approved for public release; distribution unlimited.		
17. DISTRIBUTION STATEMENT (of the abstract entered in Block 20, if different from Report)		
18. SUPPLEMENTARY NOTES		
19. KEY WORDS (Continue on reverse side if necessary and identify by block number)		
20. ABSTRACT (Continue on reverse side if necessary and identify by block number) A transient overpower (TOP) accident in a Liquid Metal Fast Breeder Reactor (LMFBR) is considered. The analysis is formulated to model the dynamic response of the reactor fuel subassembly during the initial period of the postulated overpower transient. An equivalent cylindrical cell is used to model the fuel subassembly. The governing neutronic and heat transport equations for each region (fuel, clad, and		

coolant) of the equivalent cylindrical cell are developed. Nuclear Doppler broadening feedback is included in the dynamic model making the coupled equations non-linear. The resulting non-linear partial differential field equations are transformed into a system of ordinary differential equations by the finite element method. An isoparametric, quadratic, rectangular element is used for the discretization of the spatial domain. When using the finite element method, large system matrices may result. To facilitate solution of these large systems, an optimum compacting scheme is utilized. The implicit Gear's method is used for the solution of the system of ordinary differential equations. The results for a sample problem are presented.

Finite Element Solution of the Nonlinear  
Coupled Neutronic-Energy Equations  
for a Fast Reactor Fuel Cell

by

Roy Edward Kasdorf  
Lieutenant, United States Navy  
B.S.M.E., New Mexico State University, 1970

Submitted in partial fulfillment of the  
requirements for the degrees of

MASTER OF SCIENCE IN MECHANICAL ENGINEERING

and

MECHANICAL ENGINEER

from the

NAVAL POSTGRADUATE SCHOOL  
December 1976

Author

Roy E. Kasdorf

Approved by:

Dong H. Nguyen Thesis Advisor

David Salinas Thesis Advisor

Richard Frank Second Reader

Allen E. Fuchs  
Chairman, Department of Mechanical Engineering

Robert P. Johnson  
Dean of Science and Engineering

## ABSTRACT

A transient overpower (TOP) accident in a Liquid Metal Fast Breeder Reactor (LMFBR) is considered. The analysis is formulated to model the dynamic response of the reactor fuel subassembly during the initial period of the postulated overpower transient. An equivalent cylindrical cell is used to model the fuel subassembly. The governing neutronic and heat transport equations for each region (fuel, clad, and coolant) of the equivalent cylindrical cell are developed. Nuclear Doppler broadening feedback is included in the dynamic model making the coupled equations non-linear. The resulting non-linear partial differential field equations are transformed into a system of ordinary differential equations by the finite element method. An isoparametric, quadratic, rectangular element is used for the discretization of the spatial domain. When using the finite element method, large system matrices may result. To facilitate solution of these large systems, an optimum compacting scheme is utilized. The implicit Gear's method is used for the solution of the system of ordinary differential equations. The results for a sample problem are presented.

## TABLE OF CONTENTS

I.	INTRODUCTION - - - - -	13
II.	DESCRIPTION OF PROBLEM - - - - -	16
	A. PHYSICAL SYSTEM - - - - -	16
	B. SYSTEM MODEL - - - - -	18
	C. NUMERICAL SOLUTION - - - - -	20
III.	MODEL DEVELOPMENT - - - - -	22
	A. NEUTRONIC ANALYSIS - - - - -	22
	1. Fuel Region - - - - -	23
	2. Cladding Region - - - - -	25
	3. Coolant Region - - - - -	26
	4. Infinite Multiplication Factor - - - - -	26
	5. Boundary Conditions - - - - -	30
	B. HEAT TRANSFER ANALYSIS - - - - -	32
	1. Fuel Region - - - - -	32
	2. Cladding Region - - - - -	33
	3. Coolant Region - - - - -	33
	4. Interface Conditions - - - - -	34
	5. Boundary Conditions - - - - -	36
IV.	FINITE ELEMENT FORMULATION - - - - -	39
	A. BASIC THEORY - - - - -	39
	B. SHAPE FUNCTIONS - - - - -	42
	C. COORDINATE TRANSFORMATIONS - - - - -	43
V.	APPLICATION OF FEM TO GOVERNING FIELD EQUATIONS - - - - -	48
	A. GAUSSIAN QUADRATURE - - - - -	48

B.	NEUTRONIC FIELD EQUATIONS	- - - - -	49
1.	Fuel Region	- - - - -	49
2.	Clad Region	- - - - -	53
3.	Coolant Region	- - - - -	53
C.	HEAT TRANSPORT FIELD EQUATIONS	- - - - -	54
1.	Fuel Region	- - - - -	54
2.	Clad Region	- - - - -	57
3.	Coolant Region	- - - - -	58
D.	DISCRETIZATION OF THE SPATIAL DOMAIN	- - - - -	60
E.	OPTIMUM COMPACTING SCHEME	- - - - -	63
VI.	NUMERICAL SOLUTION	- - - - -	66
A.	SELECTION OF METHOD	- - - - -	66
B.	USER SUPPLIED SUBROUTINES TO IMPLEMENT THE IMPLICIT GEAR'S METHOD	- - - - -	67
1.	DIFFUN	- - - - -	67
2.	JACMAT	- - - - -	68
3.	NUITSL	- - - - -	69
VII.	PROCEDURE	- - - - -	71
A.	INPUT DATA	- - - - -	72
VIII.	RESULTS	- - - - -	75
IX.	RECOMMENDATIONS	- - - - -	87
	APPENDIX A: DEVELOPMENT OF TRANSFORMATIONS	- - - - -	89
	APPENDIX B: REDUCTION OF SECOND ORDER TERM	- - - - -	92
	APPENDIX C: LIST OF RELATIONS FOR MATERIAL THERMAL PROPERTIES	- - - - -	93
	COMPUTER PROGRAM	- - - - -	95
	LIST OF REFERENCES	- - - - -	153
	INITIAL DISTRIBUTION LIST	- - - - -	155

LIST OF T ES

I. Physical Parameters - - - - - 73

## LIST OF FIGURES

1. Equivalent Cylindrical Cell - - - - -	17
2. Doppler Broadening of a Resonance Peak - - - - -	28
3. Gap Heat Transfer Coefficient - - - - -	35
4. Element Transformation - - - - -	44
5. Normalized Shape Functions - - - - -	45
6. Finite Element Discretization - - - - -	62
7. Sample Data Deck - - - - -	74
8. Convergence of the Finite Element Method - - - - -	76
. Determination of the Critical Fission Cross Section - - - - -	77
10. Flux Profile ( $\rho = \$10$ ) - - - - -	79
11. Temperature Profile ( $\rho = \$10$ ) - - - - -	80
12. Radial Flux ( $\rho = \$10$ ) - - - - -	82
13. Axial Flux ( $\rho = \$10$ ) - - - - -	83
14. Radial Temperature Profile ( $\rho = \$10$ ) - - - - -	84
15. Axial Temperature Profile ( $\rho = \$10$ ) - - - - -	85

## LIST OF SYMBOLS AND NOTATION

### A. NOTATION

$\langle \rangle$	Row vector
$\{ \}$	Column vector
$[ ]$	Square matrix or indicates a reference
$[ ]^{-1}$	Inverse of a square matrix
$\nabla$	Del operator
$\frac{\partial}{\partial x}$	Partial derivative with respect to x
$\Delta x$	Change in x
$\int_V$	Volume integral
$\int_x$	Integration with respect to x
$\det [x]$	Determinant of x

### B. SYMBOLS

$b$	Nuclear Doppler constant
$C$	Concentration of delayed neutron precursors
$C_p$	Specific heat [cal/gm °C]
$D(\underline{r})$	Neutron diffusion coefficient [cm]
$e$	Nuclear energy released per fission [cal/fission]
$h$	Heat transfer coefficient [cal/cm <sup>2</sup> sec °C]
$J$	Jacobian matrix
$J(\underline{r}, t)$	Neutron current [ $\frac{\text{neutrons}}{\text{cm}^2 \text{ sec}}$ ]
$k_\infty$	Infinite multiplication factor
$K_D$	Doppler constant
$k(\underline{r})$	Thermal conductivity [cal/cm sec °C]
LMFBR	Liquid Metal Fast Breeder Reactor

LOCA	Loss of Coolant Accident	
N	Shape function	
n	Number of delay neutron groups	
$n(\underline{r}, t)$	Neutron density	$[\frac{\text{neutrons}}{\text{cm}^3}]$
$H, x$	Derivative of H with respect to x	
$\dot{q}(\underline{r}, t)$	Nuclear generation	$[\text{cal}/\text{cm}^3 \text{sec}]$
R	Residual	
$\underline{r}$	Spatial coordinate	$[\text{cm}]$
$r, z$	Global coordinates	
$S(\underline{r}, t)$	Neutron production	$[\frac{\text{neutrons}}{\text{cm}^3 \text{sec}}]$
T	Temperature	$[^\circ\text{C}]$
t	Time	$[\text{sec}]$
TOP	Transient Overpower	
v	Neutron velocity	$[\text{cm}/\text{sec}]$
$V_{\text{co}}$	Velocity of coolant flow	$[\text{cm}/\text{sec}]$
W	Weighting function	
B	Fraction of fission neutrons which appear as delayed neutrons	
$\phi(\underline{r}, t)$	Neutron flux	$[\frac{\text{neutrons}}{\text{cm}^2 \text{sec}}]$
$\lambda$	Decay constant of the delayed neutron precursors	$[1/\text{sec}]$
$\eta, \xi$	Local coordinates	
$\nu$	Average number of neutrons released per fission	
$\rho$	Reactivity	
$\rho(\underline{r})$	Density	$[\text{gm}/\text{cm}^3]$
$\Sigma$	Neutron cross section	$[\text{cm}^{-1}]$

### C. SUBSCRIPTS

a	Absorption
c	Clad
co	Coolant
CR	Critical
D	Delayed, Doppler
f	Fission
F	Fuel
gap	Fuel-clad interface
i,j	Group, equation
P	Prompt
s-c	Clad-coolant interface

### D. SUPERSSCRIPTS

e	Element
e*	Adjacent element
0	At time zero
.	Derivative with respect to time

## ACKNOWLEDGEMENTS

The author wishes to express his appreciation to Dr. Dong Nguyen and to Dr. David Salinas, Professors of Mechanical Engineering, for their advice and guidance throughout the course of this work.

The author is obligated to Dr. Richard Franke, Professor of Mathematics, for his assistance in implementing the integration procedure and for his assistance as second reader.

The author wishes to thank Dr. Gilles Cantin, Professor of Mechanical Engineering, for his invaluable discussions concerning the finite element method.

Finally, the author wishes to thank his wife, Gail, for her encouragement and understanding throughout the course of this study.

## I. INTRODUCTION

As the world's fossil fuel resources are depleted, more emphasis is being placed on the breeder reactor as a potential means of solving the coming energy crisis. While the development of new energy sources is being pushed, equal effort is being given to the maintenance of an environmentally clean world. To this end, the safety of breeder reactors is receiving a considerable amount of attention before assuming that the breeder reactor is the answer to the energy problem.

The Liquid Metal Fast Breeder Reactor (LMFBR) appears to be one of the most promising breeder reactors. Most engineers will concede there is little probability of a nuclear explosion occurring in the operation of a nuclear reactor. Of major concern to engineers is the loss of coolant accident (LOCA) and the transient overpower accident (TOP). The present analysis is concerned with a TOP accident in a LMFBR. The analysis is formulated to model the dynamic response of the reactor fuel subassembly during the initial period of the postulated overpower transient. The primary consideration is given to the early response of this fuel subassembly to various conditions of disturbances. The phenomenon which occurs after core disassembly (i.e., clad melting) is not the concern of this analysis. Only the time prior to clad melting is being considered.

No consideration is given here as to how the overpower transient occurs or to why the safety features of the reactor did not operate properly. It is postulated that the accident has occurred. In this analysis, the TOP accident is created by either a step increase in reactivity, a ramp increase in reactivity, or a combination of both.

An inherent safety feature of most reactors, nuclear Doppler broadening feedback, is included in the dynamic model of the fuel subassembly. The Doppler feedback acts to reduce the effect of the excursion. Consideration of this feedback creates a non-linear system model which is described by a non-linear, initial-boundary-value problem.

The conventional method of solution uses the standard point kinetics formulation. Recent studies have pointed out a non-negligible error in this model [1], particularly with asymmetric disturbances [2], or space-dependent feedback [3]. In Ref. [4], a somewhat novel approach of using the finite element method (FEM) for the space-time dependent solution of the reactor dynamics problem was demonstrated. The FEM is effective in handling these asymmetric disturbances and space-dependent feedbacks. Therefore, the finite element method was used so that the spatial effects on the postulated problem may be studied further.

The purpose of this work was to demonstrate further the applicability of the FEM to the non-linear reactor dynamics problem as well as to investigate the dynamic response of the reactor fuel subassembly. The analysis required a novel

approach to handle the gap conductances present at the interfaces of the equivalent cell model of the fuel subassembly; this will be clarified in the analysis.

## II. DESCRIPTION OF PROBLEM

### A. PHYSICAL SYSTEM

The typical Liquid Metal Fast Breeder Reactor (LMFBR) core consists of many hexagonal modules, each containing several hundred fuel pins. For this analysis, an equivalent cylindrical cell is used to model the fuel subassembly; see Figure 1. The use of equivalent cells as models for larger systems has been common practice in nuclear analysis (i.e., the well known Wigner-Sietz method). In using an equivalent cell, the actual shape of the reactor core is not important, and the analysis is applicable to any reactor which has the same equivalent cell.

The equivalent cell considered in this analysis, Figure 1, is fueled with enriched uranium dioxide, has a stainless steel cladding, and has liquid sodium for a coolant. The dimensions used are

$$a = 0.254 \text{ cm,}$$

$$b = 0.292 \text{ cm,}$$

$$c = 0.365 \text{ cm,}$$

and

$$H = 33.0 \text{ cm.}$$

The gap between the fuel and cladding is very small and, in fact, may be nonexistent as in bonded fuels. The dimension of this gap has been assumed negligible. The height,  $H$ , of the fuel rod is shorter than many proposed systems (Fast Flux Testing Facility and Clinch River Breeder Reactor). However,

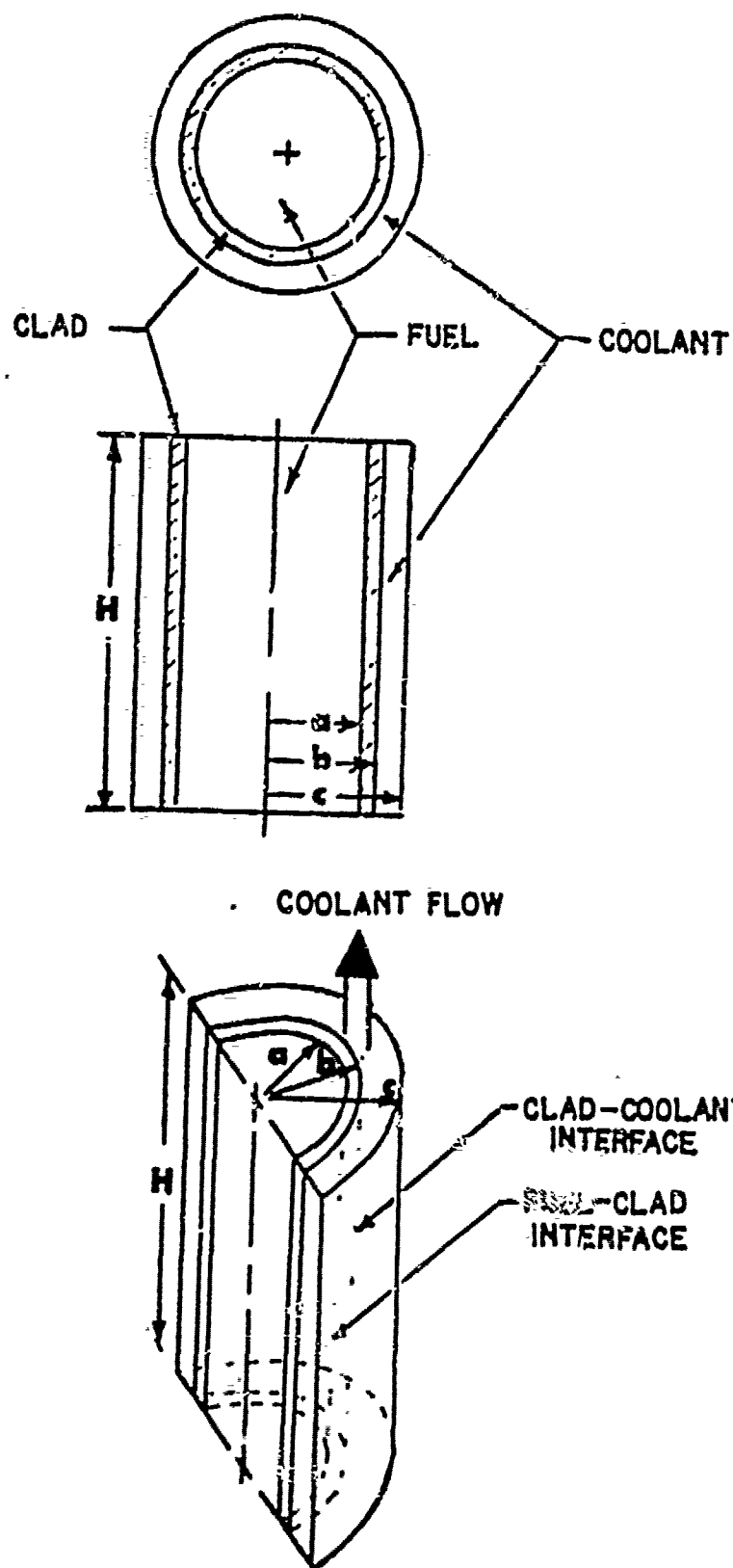


Figure 1. Equivalent Cylindrical Cell

to facilitate the numerical solution a smaller rod was used. The dynamic behavior prior to fuel pin failure for this system should be similar to the behavior of larger systems.

The treatment of this problem in three dimensions would be prohibitive in computer usage. Therefore, azimuthal symmetry is assumed, and the problem becomes a two-dimensional cylindrical  $(r,z)$  problem.

## 8. SYSTEM MODEL

The analysis considers the monoenergetic neutron diffusion approximation to model the transient neutron transport problem. A simple conduction-convection heat transfer model is used for the energy transport problem. The temperatures in the model are directly coupled to the neutron flux through the nuclear heat generation within the fuel. The neutron population is in turn coupled to the temperature through any of a number of reactivity feedback mechanisms. The nuclear Doppler effect is perhaps the most important of these mechanisms since it provides a negative temperature coefficient which increases the inherent stability of the reactor. Prior to core disassembly and fuel melting, the nuclear Doppler effect is the most dominant feedback and is, therefore, the only feedback mechanism considered in this analysis.

For irradiated, mixed-oxide fuels, a phenomenon of fuel restructuring has been commonly observed. This restructuring, essentially a change of phase of the fuel material, presents a unique heat transfer problem particularly during transient conditions. The problem has not been fully characterized and

is beyond the scope of this analysis. The fuel was, therefore, assumed to be a homogeneous mixture of enriched uranium dioxide.

At the fuel-cladding interface, there exists a gap which produces a thermal resistance. This thermal resistance is one of the most significant deterrents to the energy transfer to the coolant. The interface may be in physical contact or an actual gap may exist. The prediction of the thermal resistance is extremely complicated and must take into consideration many parameters: initial dimensions, type of bond, fill gas composition, fuel restructuring, fuel swelling, prior fuel life cycle, to mention a few. Reference [5] documents a computer program which attempts to predict the gap conductance,  $h_{\text{gap}}$ . This treats the thermal resistance at the interface in the same manner as a convection heat transfer coefficient when considering convection heat transfer. Since it is not the objective of this analysis to predict the gap coefficient, a representative set of values for gap coefficient, as given in Ref [6], is used in this analysis. These values are assumed to remain static during the transient. The gap conductance profile actually varies with time and will have an effect upon the transient, as noted in Ref. [7]. The prediction of this variance was not considered important for this analysis; therefore, the static assumption was made.

An average convection heat transfer coefficient was used to determine the heat transfer from the cladding to the coolant. The value used was determined from an empirical formula given in Ref. [5] and repeated in Appendix C.

In this work, consideration is given to step and ramp increases in reactivity, although any reactivity transient may easily be considered. The step and ramp increases in reactivity probably represent the most realistic physical reactivity inputs in a reactor. Once the reactivity has been inserted, the transient overpower excursion begins. Unless the Doppler feedback can override the inserted reactivity, the excursion will continue until there is physical core disassembly.

### C. NUMERICAL SOLUTION

The system of equations which models the proposed problem is a non-linear, initial-boundary-value problem. The conventional method of solution of the reactor dynamics is the point kinetics formulation. It was pointed out in Refs. [1], [2], [3], and [4], that there is a non-negligible error in this model, particularly under conditions of asymmetric disturbances or space-dependent feedback. Reference [4] demonstrates the somewhat novel approach of using the finite element method (FEM) to solve the space-time dependent reactor dynamics problem. As shown in Ref. [4], the FEM is quite effective in handling localized perturbations and space-dependent feedback. In this work, only uniform disturbances were considered; however, the feedback model was space-dependent. Therefore, the finite element method is used to solve the non-linear, coupled, space-time dependent neutronic and heat transport field equations. The solution technique results in a large computer storage requirement; therefore, an optimum compact storage scheme, Ref. [8], is utilized for storage of the discretized matrices.

Once the domain has been discretized by the FEM, the solution of the resulting ordinary differential equations was to be accomplished by the implicit Gear's method, Ref. [9].

### III. MODEL DEVELOPMENT

#### A. NEUTRONIC ANALYSIS

In this section the governing field equations for the neutron population (flux) for each of the three regions (fuel, clad, and coolant) of the domain will be formulated. The monoenergetic, diffusion theory will be used.

Consider an arbitrary volume of material within a reactor. Applying the condition of conservation to the monoenergetic neutrons leads to the neutron equation of continuity [10]

$$\frac{\partial n(\underline{r}, t)}{\partial t} = S(\underline{r}, t) - \Sigma_a(\underline{r})\phi(\underline{r}, t) - \text{div } J(\underline{r}, t) \quad (1)$$

where

$\underline{r}$  - spatial point

$t$  - time

$n(\underline{r}, t)$  - neutron density

$S(\underline{r}, t)$  - neutron production

$\Sigma_a(\underline{r})$  - neutron absorption cross section

$\phi(\underline{r}, t)$  - neutron flux

$J(\underline{r}, t)$  - neutron current

The left-hand side of equation (1) represents the time rate of change of the neutron density which is related to flux,  $\phi$ , by

$$n(\underline{r}, t) = \frac{1}{v} \phi(\underline{r}, t) \quad (2)$$

where

$v$  - neutron velocity

On the right-hand side of equation (1), the first term is neutron production, the second term is a neutron loss through absorption, and the third term is a neutron loss through leakage from the control volume.

Using equation (2) and applying Fick's Law to the equation of continuity results in the classical neutron diffusion equation

$$\nabla \cdot (D(\underline{r}) \nabla \phi(\underline{r}, t)) - \Sigma_a(\underline{r}) \phi(\underline{r}, t) + S(\underline{r}, t) = \frac{1}{v} \frac{\partial \phi(\underline{r}, t)}{\partial t} \quad (3)$$

where  $D(\underline{r})$  - neutron diffusion coefficient

The vector notation used here is intended to include only two dimensions ( $r, z$ ) since azimuthal symmetry has been assumed.

Equation (3) is applicable to each of the three regions of the equivalent cylindrical cell. The subscripts F (fuel), c (cladding), and co (coolant), will be used to denote these regions.

#### 1. Fuel Region

In applying equation (3) to the fuel region the material properties of the fuel must be used. Within the fuel the neutron source term is due to the nuclear fission process. During fission, neutrons are released as both prompt neutrons and delayed neutrons so that

$$S(\underline{r}, t) = s_p(\underline{r}, t) + s_d(\underline{r}, t) \quad (4)$$

where  $S_p(r, t)$  - prompt neutron source  
 $S_D(r, t)$  - delayed neutron source

The neutron sources are commonly represented as [10]

$$S_p = k_{\infty} \bar{\Sigma}_{aF} \phi_F (1 - \beta) \quad (5)$$

and

$$S_D = \sum_{i=1}^n C_i \lambda_i \quad (6)$$

where

- $k_{\infty}$  - infinite multiplication factor
- $\beta$  - fraction of fission neutrons which appear as delayed neutrons
- $n$  - number of delayed neutron groups
- $C_i$  - concentration of delayed neutron precursors in the  $i$ th group
- $\lambda_i$  - decay constant of the delayed neutrons

The space and time variables,  $r$  and  $t$ , will be dropped except where needed for clarification.

The concentration of delayed neutron precursors,  $C_i$ , is given by the following first order partial differential equation [10]

$$\frac{\partial C_i}{\partial t} = \beta_i k_{\infty} \Sigma_{aF} \phi_F - \lambda_i C_i \quad (7)$$

where

- $\beta_i$  - fraction of delayed neutrons which appear as delayed neutrons in the  $i$ th group

The solution of equation (7) is

$$C_i = \beta_i \int_0^t e^{-\lambda_i(t-t')} k_\infty(r, t') \Sigma_{aF} \phi_F dt' + C_i^0 e^{-\lambda_i t} \quad (8)$$

$C_i^0$  - concentration of delayed neutron precursors of the ith group at time zero

Reference [10] develops an expression for the initial concentration of delayed neutrons

$$C_i^0 = \beta_i k_\infty^0 \Sigma_{aF} \phi^0 / \lambda_i \quad (9)$$

where

$k_\infty^0$  - initial finite multiplication factor

$\phi^0$  - initial neutron flux

Combining equations (3), (4), (5), (6), (8), and (9), yields the governing equation for the fuel region

$$\begin{aligned} \nabla \cdot (D_F \nabla \phi_F) + \Sigma_{aF} \phi_F [k_\infty (1 - \beta) - 1] \\ + \sum_{i=1}^n \lambda_i [\beta_i \int_0^t e^{-\lambda_i(t-t')} k_\infty(r, t') \phi_F \Sigma_{aF} dt' \\ + \beta_i k_\infty^0 \Sigma_{aF} \phi_F / \lambda_i e^{-\lambda_i t}] = \frac{1}{v} \frac{\partial \phi_F}{\partial t} \end{aligned} \quad (10)$$

## 2. Cladding Region

The cladding separates the fuel and coolant and contains the fuel and the fission by-products. Equation (3) governs the neutron flux in the clad. Since the clad contains

no fissile material, the neutron source term is zero. The field equation is, then,

$$\nabla \cdot (D_c \nabla \phi_c) - \Sigma_{ac} \phi_c = \frac{1}{v} \frac{\partial \phi_c}{\partial t} \quad (11)$$

### 3. Coolant Region

The annular region around the cladding of the equivalent cell contains the coolant. As in the clad, there is no fissile material in the coolant and, therefore, no neutron source term. The equation governing the neutron flux in the coolant is

$$\nabla \cdot (D_{co} \nabla \phi_{co}) - \Sigma_{aco} \phi_{co} = \frac{1}{v} \frac{\partial \phi_{co}}{\partial t} \quad (12)$$

Equations (10), (11), and (12) are the one-velocity, diffusion approximation used to model the neutron transport problem.

### 4. Infinite Multiplication Factor

The infinite multiplication factor,  $k_{\infty}$ , may be expressed as the infinite multiplication factor at time zero (start of transient),  $k_{\infty}^0$ , plus the postulated reactivity insertion (such as a step or a ramp),  $\rho$ , minus the change in the Doppler reactivity feedback,  $\Delta \rho_D$ . Other feedback mechanisms are normally not as significant as the Doppler broadening feedback prior to fuel melting and have been neglected in this analysis. Therefore,

$$k_{\infty} = k_{\infty}^0 + \rho - \Delta \rho_D \quad (13)$$

For a fast reactor,  $k_{\infty}^0$  may be approximated as

$$k_{\infty}^0 = \nu \frac{\Sigma_{fF}}{\Sigma_{aF}} \quad (14)$$

where

$\nu$  - average number of neutrons released per fission

$\Sigma_{fF}$  - fission cross section of the fuel

$\Sigma_{aF}$  - absorption cross section of the fuel

The nuclear Doppler effect is a very important safety feature in a nuclear reactor. Nuclei in an atom are in continual motion due to their own thermal energy. As a result of this motion, even when monoenergetic neutrons interact with the atom, there appears to be a spread in the energy of the neutron - the Doppler effect. It can be shown that the cross section of a resonance becomes less in magnitude and wider as the motion of the nuclei increases [10]. As the temperature increases, the motion increases, and the shape of a resonance cross section broadens. This broadening increases the average cross section, thus, providing a negative temperature coefficient. This effect is shown in Figure 2. It is this nuclear Doppler broadening effect which provides one of the few inherent, reliable, negative reactivity feedbacks which slows an overpower transient and possibly stops a mild overpower transient.

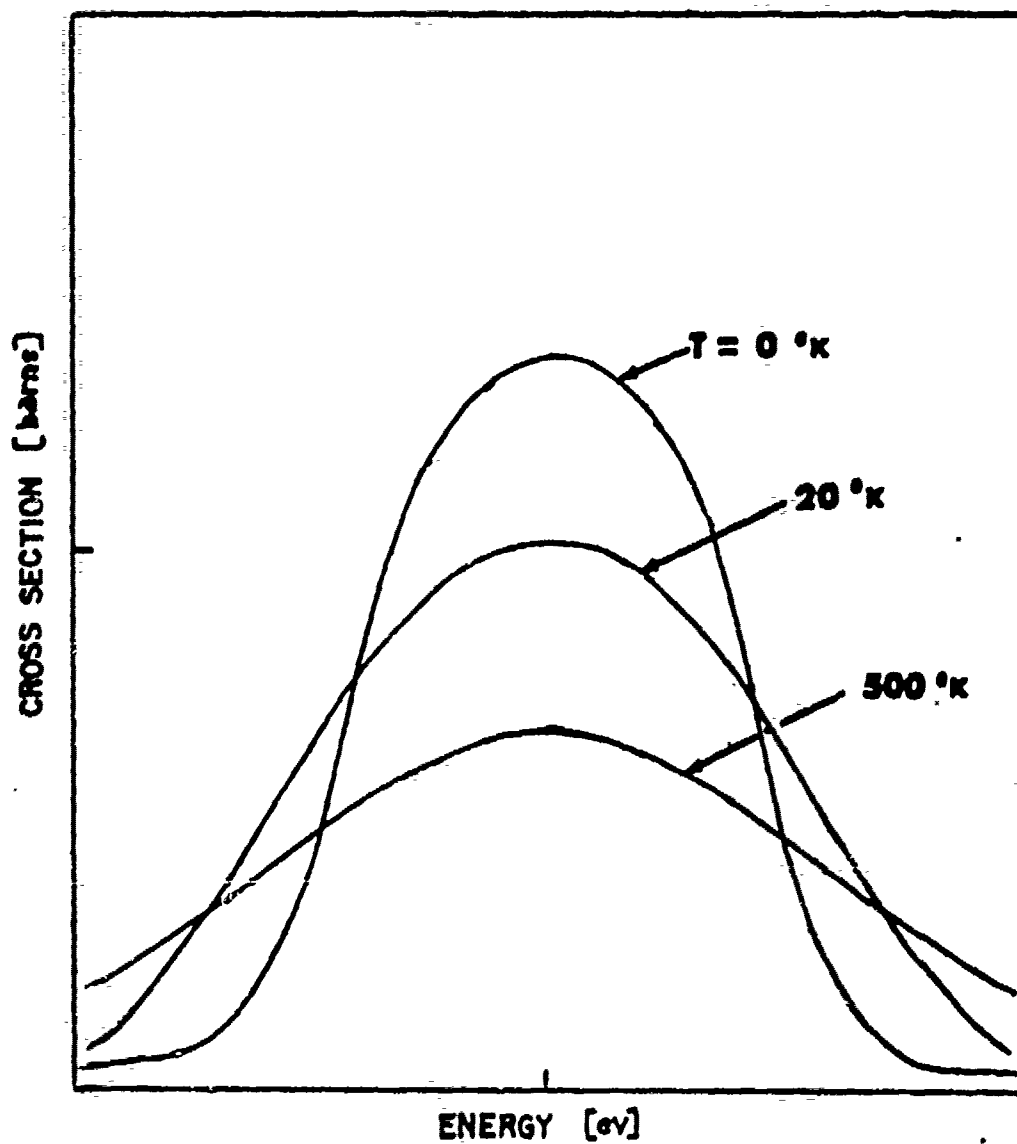


Figure 2. Doppler Broadening of a Resonance Peak

The Doppler reactivity change with respect to fuel temperature changes should be written as [6]

$$\frac{d\rho_D}{dT} = aT^{-3/2} + bT^{-1} + cT^{m-1} \quad (15)$$

where  $a$ ,  $b$ , and  $c$  are parameters determined from experimental work and  $m$  is an integer. However, as noted in Ref. [6], a substantial amount of work has shown that  $T \frac{d\rho_D}{dT}$  is very nearly constant over the temperature range under consideration. Therefore, the coefficients  $a$  and  $c$  have been set equal to zero, and  $b$  is defined as

$$b = K_D = T \frac{d\rho_D}{dT} \quad (16)$$

The constant,  $K_D$ , is commonly called the Doppler constant. Solving equation (16) for  $\rho_D$  yields

$$\rho_D = b \ln T_F + K \quad (17)$$

where  $K$  is an integration which may be obtained from initial conditions.

$$K = \rho_D^0 - b \ln T_F^0 \quad (18)$$

where

$\rho_D^0$  - Doppler effect at time zero

$T_F^0$  - fuel temperature at time zero

Substituting for  $K$  in equation (17) will give

$$\rho_D - \rho_D^0 = \Delta\rho_D = b \ln(T_F/T_F^0) \quad (19)$$

The infinite multiplication factor now becomes

$$k_\infty = k_\infty^0 + \rho - b \ln(T_F/T_F^0) \quad (20)$$

The effect of delayed neutrons is small compared to the prompt neutron effect; therefore, it may be assumed that the Doppler effect on delayed neutrons is insignificant to the overall problem. The  $k_\infty$  of equation (8) is, then, assumed to be  $k_\infty^0$ . With this assumption and equation (20), the neutron diffusion equation in the fuel, equation (10), may be rewritten as

$$\begin{aligned} \nabla \cdot (D_F \nabla \phi_F) + \Sigma_{aF} \phi_F [k_\infty^0(1-\beta) - 1 + \rho(1-\beta) - b(1-\beta) \ln(T_F/T_F^0)] \\ + \sum_{i=1}^n \lambda_i \{ \beta_i \Sigma_{aF} \int_0^t e^{-\lambda_i(t-t')} [k_\infty^0 + \rho] \phi_F dt' + C_i^0 e^{-\lambda_i t} \} = \frac{1}{v} \frac{\partial \phi_F}{\partial t} \end{aligned} \quad (21)$$

To facilitate the present analysis, the number of delayed neutron groups is taken as one averaged group. So that,  $\lambda_i$  and  $\beta_i$  become  $\bar{\lambda}$  and  $\bar{\beta}$ , respectively. This approximation should have little effect on the problem under consideration.

##### 5. Boundary Conditions

The neutron diffusion problem involves solution of the partial differential equations (11), (12), and (21), with the following boundary, interface, and initial conditions:

- 1)  $\frac{\partial \phi_F}{\partial r} (0, z, t) = 0$
- 2)  $\phi_F (a, z, t) = \phi_C (a, z, t)$
- 3)  $D_F \frac{\partial \phi_F}{\partial r} (a, z, t) = D_C \frac{\partial \phi_C}{\partial r} (a, z, t)$
- 4)  $\phi_C (b, z, t) = \phi_{Co} (b, z, t)$
- 5)  $D_C \frac{\partial \phi_C}{\partial r} (b, z, t) = D_{Co} \frac{\partial \phi_{Co}}{\partial r} (b, z, t)$
- 6)  $\frac{\partial \phi_{Co}}{\partial r} (c, z, t) = 0$
- 7)  $\phi_F (r, \pm \frac{H}{2}, t) = \phi_C (r, \pm \frac{H}{2}, t) = \phi_{Co} (r, \pm \frac{H}{2}, t) = 0$
- 8)  $\phi_F (\underline{r}, 0) = \phi_F^o (\underline{r})$
- 9)  $\phi_C (\underline{r}, 0) = \phi_C^o (\underline{r})$
- 10)  $\phi_{Co} (\underline{r}, 0) = \phi_{Co}^o (\underline{r})$

Boundary condition 1) results from the assumed azimuthal symmetry. Interface conditions 2), 3), 4), and 5) are continuity conditions of the flux. Boundary condition 6) results from the use of an equivalent cell and basically indicates there is an equal number of neutrons transferred in and out of the cell at the outer boundary. This should be valid unless the cell is located near the outer edge of the reactor. Boundary condition 7) is an assumption that the flux is zero at the axial boundaries of the cell. Initial conditions 8), 9), and 10) are the assumed initial distributions of the neutron flux.

## B. HEAT TRANSFER ANALYSIS

In this section, the principle of conservation of energy will be used to formulate the governing field equations for the heat transport in each of the three regions. A simple heat conduction model with convection heat transfer to the coolant is used to model the heat transport problem. A gap conductance model is used to describe the heat transport across the gap at the fuel-clad interface.

### 1. Fuel Region

Conservation of energy within the fuel region yields the unsteady heat conduction equation with a generation term

$$\nabla \cdot (k_F(\underline{r}) \nabla T_F(\underline{r}, t)) + \dot{q}(\underline{r}, t) = \rho_F(\underline{r}) c_{pF}(\underline{r}) \frac{\partial T_F}{\partial t}(\underline{r}, t) \quad (22)$$

where

- $k_F(\underline{r})$  - thermal conductivity of the fuel
- $T_F(\underline{r}, t)$  - fuel temperature
- $\dot{q}(\underline{r}, t)$  - nuclear energy generation per unit volume
- $\rho_F(\underline{r})$  - fuel density
- $c_{pF}(\underline{r})$  - fuel specific heat

As in the neutronic analysis, the vector notation is intended to include only two dimensions,  $(r, z)$ . The  $\underline{r}$  and  $t$  will be dropped except where needed for clarification.

The nuclear generation term may be expressed as

$$\dot{q} = e \Sigma_{ff} \phi_F \quad (23)$$

where  $e$  - nuclear energy released per fission

As can be seen, it is through the nuclear generation term that the temperature is directly coupled to the neutron flux. This coupling and the temperature dependent Doppler reactivity feedback combine to make the coupled problem nonlinear.

Substituting equation (23) into equation (22) yields the governing thermal equation for the fuel

$$\nabla \cdot (k_F \nabla T_F) + e \Sigma_{fF} \phi_F = \rho_F C_{pF} \frac{\partial T_F}{\partial t} \quad (24)$$

## 2. Cladding Region

Conservation of energy within the clad will yield the heat conduction equation. With nuclear generation, a relatively small amount (~5%) of the energy will be released in the cladding and the coolant. However, in this analysis it is assumed that the total energy release is in the fuel region. This should not create any significant error. Using this assumption, the unsteady heat conduction equation for the cladding becomes

$$\nabla \cdot (k_C \nabla T_C) = \rho_C C_{pC} \frac{\partial T_C}{\partial t} \quad (25)$$

## 3. Coolant Region

Once again, conservation of energy will lead to the heat conduction equation plus an additional term which

takes into consideration the coolant flow. The governing equation is

$$\nabla \cdot (k_{co} \nabla T_{co}) - V_{co} \frac{\partial}{\partial z} (\rho_{co} C_{pco} T_{co}) = \rho_{co} C_{pco} \frac{\partial T_{co}}{\partial t} \quad (26)$$

where  $V_{co}$  - coolant flow velocity

Equations (24), (25), and (26) are the governing equations used to model the energy transport problem.

#### 4. Interface Conditions

The interface between the fuel and the cladding may be an actual gap with a finite distance, or the surfaces may be in intermittent contact on a microscopic scale. To model the heat transfer across this interface, a gap heat transfer coefficient is introduced. The gap coefficient must take into consideration many items (e.g., radiation heat transfer across the gap, heat transfer by solid-to-solid contact, heat conduction across a gas filled gap). The prediction of this gap coefficient is extremely complicated and beyond the scope of this work. In Ref. [6], a set of values for  $H_{gap}$  is given and the axial variation of  $H_{gap}$  in this analysis is approximately the same. A cosine curve has been fitted to the sample data to determine the gap coefficient, see Figure 3. The heat flux across the fuel-clad interface is, then,

$$q = H_{gap} (T_F - T_C) \quad (27)$$

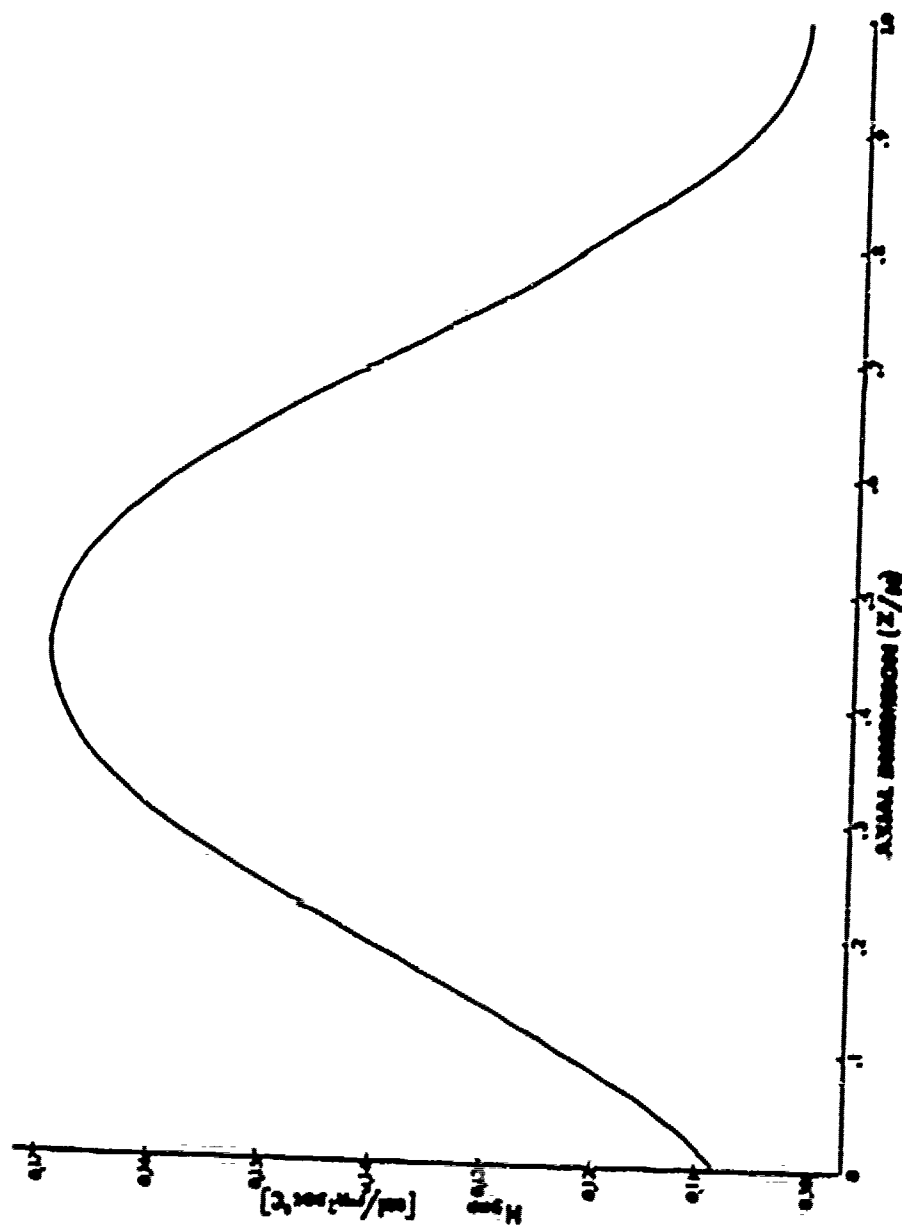


Figure 3. Gap Heat Transfer Coefficient

The heat conducted out of the fuel is governed by Fourier's equation and is equal to the heat transferred across the gap

$$q = -k_F \frac{\partial T_F}{\partial r} \quad (28)$$

Equating equations (27) and (28) gives the fuel-clad interface condition

$$T_F(a,z,t) + \frac{k_F(a,z)}{h_{gap}(z)} \frac{\partial T_F}{\partial r}(a,z,t) = T_C(a,z,t) \quad (29)$$

and from continuity

$$k_F(a,z) \frac{\partial T_F}{\partial r}(a,z,t) = k_C(a,z) \frac{\partial T_C}{\partial r}(a,z,t) \quad (29a)$$

As is common practice in convection heat transfer analysis, a coolant surface heat transfer coefficient,  $h_{surf}$ , is used to account for the thermal resistance at the clad-coolant interface. Similar to the fuel-clad interface analysis, the clad-coolant interface conditions may be determined

$$T_C(b,z,t) + \frac{k_C(b,z)}{h_{surf}} \frac{\partial T_C}{\partial r}(b,z,t) = T_{co}(b,z,t) \quad (30)$$

and

$$k_C(b,z) \frac{\partial T_C}{\partial r}(b,z,t) = k_{co}(b,z) \frac{\partial T_{co}}{\partial r}(b,z,t) \quad (30a)$$

## 5. Boundary Conditions

The boundary and initial conditions for the heat transport problem are:

- 1)  $\frac{\partial T_F}{\partial r} (0, z, t) = 0$
- 2)  $T_{co}(r, -\frac{H}{2}, t) = T_{PLENUM}$
- 3)  $\frac{\partial T_{co}}{\partial z} (r, \frac{H}{2}, t) = 0$
- 4)  $\frac{\partial T_{co}}{\partial r} (c, z, t) = 0$
- 5)  $\frac{\partial T_F}{\partial z} (r, \pm \frac{H}{2}, t) = \frac{\partial T_c}{\partial z} (r, \pm \frac{H}{2}, t) = 0$
- 6)  $T_F(r, 0) = T_F^{\circ}(r)$
- 7)  $T_c(r, 0) = T_c^{\circ}(r)$
- 8)  $T_{co}(r, 0) = T_{co}^{\circ}(r)$

Boundary condition 1) results from the assumed azimuthal symmetry. The coolant has been assumed to enter the flow channel at a constant temperature,  $T_{PLENUM}$ . This results in condition 2). Boundary conditions 3) and 5) result from an assumption that no heat is transferred axially from the fuel rod. Boundary condition 4) is the result of the use of the equivalent cell. Conditions 6), 7), and 8) are the assumed initial conditions.

Solution of the nonlinear coupled neutronic and energy transport problem involves the solution of the partial differential equations (11), (12), (21), (24), (25), and (26), with the appropriate boundary, interface, and initial conditions.

Several works, Refs. [4], [11], [12], have demonstrated the feasibility and success of the finite element method in solving nuclear reactor dynamics problems. The FEM

is used to reduce the partial differential equations developed in this analysis to a system of ordinary differential equations. Integration of these ordinary differential equations (ODE) yields the solution.

#### IV. FINITE ELEMENT FORMULATION

In this section, the basic theory underlying the finite element method is formulated. Selection of the finite elements and the shape functions for the elements are given. Some simple transformations which facilitate the integration necessary in the FEM are also presented.

##### A. BASIC THEORY

To obtain a numerical solution, the governing partial differential field equations are transformed into a system of ODE in finite dimensional vector space. This may be accomplished in several manners such as the finite-difference method, the variational method, or the weighted residual method. In this work, the Galerkin method (a weighted residual method) is utilized for the discretization of the spatial domain. The Galerkin procedure will be applied to each of the governing field equations. Any of these equations may be considered to be in the following form

$$\frac{\partial \psi}{\partial t}(\underline{r}, t) - \mathcal{L} \psi(\underline{r}, t) = f(\underline{r}, t) \quad (31)$$

where  $\psi$  represents the unknown function, e.g., in equation (21),  $\psi$  represents  $\phi_F$ ,  $\mathcal{L}$  represents the operator for each individual equation, and  $f$  is a forcing function. In the finite element method the solution is approximated as

$$\psi(\underline{r}, t) \approx \tilde{\psi}(\underline{r}, t) = \sum_{i=1}^N N_i(\underline{r}) \psi_i(t) = \langle N_i \rangle \{ \psi_i \} \quad (32)$$

where

$N$  - the number of degrees of freedom

$N_i$  - the element shape function

$\psi_i$  - unknown coordinate function

$\langle \rangle$  - matrix notation for a row vector

$\{ \}$  - matrix notation for a column vector

$\langle N_i \rangle = \langle N_1 \ N_2 \ \dots \ N_i \ \dots \ N_N \rangle$

$\{ N_i \} = \begin{pmatrix} N_1 \\ N_2 \\ \vdots \\ N_i \\ \vdots \\ N_N \end{pmatrix}$

The residual,  $R(\underline{r}, t)$ , is a measure of the error in this finite element approximation. The residual may be considered as

$$R = \frac{\partial \psi}{\partial t} - \mathcal{L}\psi - f \quad (33)$$

The best solution for  $\tilde{\psi}$  is one which "minimizes" this residual. Various "minimums" are obtained by the weighted residual method by setting

$$\int_V W_i(\underline{r}) R \, dV = 0 \quad i=1, 2, \dots, N \quad (34)$$

$W_i(\underline{r})$  - weighting functions

With the Galerkin method, the weighting functions are the shape functions defining the approximation of equation (32) (i.e.,  $W_i = N_i$ ). A noteworthy attribute of the Galerkin method is the opportunity of using an integration-by-parts

of the terms involving the second order spatial derivatives. A lower order finite element may be used than would have been possible otherwise. Once the weighting functions have been chosen, the problem becomes

$$\int_V N_i \left\{ \frac{\partial \psi}{\partial t} - \mathcal{L} \psi - f \right\} dV = 0 \quad i=1,2,\dots,N \quad (35)$$

The integration involved in equation (35) is carried out on the element level, taking advantage of the use of a "local" coordinate system. Once the integration is accomplished, the results are merged into a system using "global" coordinates. On the element level

$$\tilde{\psi}^e = \langle N_j \rangle^e \{\psi_j\}^e \quad j=1,2,\dots,N \quad (36)$$

where the superscript  $e$  indicates the element level. Substituting  $\tilde{\psi}^e$  into equation (35) and noting  $\{\psi_j\}^e$  is not a function of the spatial domain yields

$$\int_V \langle N_i \rangle^e \{N_j\}^e dV^e \{\psi_j\}^e - \int_V [\langle N_i \rangle^e \mathcal{L} \{N_j\}^e - \langle N_i \rangle^e f^e] dV^e \{\psi_j\}^e = 0 \quad (37)$$

where  $i, j = 1, 2, \dots, N^e$   
 $N^e$  - number of degrees of freedom for an element

The operator  $\mathcal{L}$  will vary depending upon which governing equation is under consideration.

## B. SHAPE FUNCTIONS

The shape functions,  $N_i$ , are chosen to satisfy certain completeness and convergence criteria [13] and will depend upon the finite-element used for the spatial discretization.

Many previous works, Refs. [4], [11], and [12], utilized linear triangular shaped elements to discretize the spatial domain. This element was the first element considered. However, because the width of the cladding is very thin, elements in the cladding region would have extremely large aspect ratios (ratio of base to height) unless an extremely large number of elements in the axial direction were used. A large number of elements becomes numerically untractable. Previous experience with triangular elements had shown that large aspect ratios yield inaccurate results. Zlamal, Ref. [14], showed the error,  $e$ , when using triangular elements, is proportional to the square of the longest side,  $h$ , and inversely proportional to the sine of the smallest angle,  $\gamma$

$$e \propto h^2/\sin\gamma$$

A triangular element with a large aspect ratio necessarily must have a small related angle which adversely affects the error in the FEM. Hopefully to alleviate the problem, an isoparametric, quadratic, rectangular element was selected. The aspect ratio would still be large, but experience, Ref. [15], with the use of rectangular elements indicated that a large aspect ratio is not always a detrimental factor.

The shape functions for this element are well documented, Ref. [13]. Utilizing a "local" coordinate system (See Figure 4), the shape functions may be written as

Corner nodes  $i = 1, 3, 5, 7$

$$N_i = \frac{1}{4}(1+\xi_0)(1+\eta_0)(\xi_0+\eta_0-1) \quad (38)$$

Midside nodes  $N_i = \frac{1}{2}(1-\xi^2)(1+\eta_0) \quad i=2,6 \quad (38a)$

$$N_i = \frac{1}{2}(1+\xi_0)(1-\eta^2) \quad i=4,8 \quad (38b)$$

where

$$\xi_0 = \xi \xi_i$$

$$\eta_0 = \eta \eta_i$$

These normalized shape functions are shown in Figure 5.

The local and global coordinates are related by the following

$$r = \langle N_i \rangle^e \{r_i\}^e \quad (39)$$

and

$$z = \langle N_i \rangle^e \{z_i\}^e \quad (39a)$$

### C. COORDINATE TRANSFORMATIONS

When using a local coordinate system, some simple transformations facilitate the integrations required by equation (37). In cylindrical coordinates with azimuthal symmetry

$$dV = 2\pi r dr dz \quad (40)$$

The derivative terms may be transformed by the following

$$\begin{pmatrix} \frac{\partial N_i}{\partial r} \\ \frac{\partial N_i}{\partial z} \end{pmatrix} = [J]^{-1} \begin{pmatrix} \frac{\partial N_i}{\partial \xi} \\ \frac{\partial N_i}{\partial \eta} \end{pmatrix} \quad (41)$$

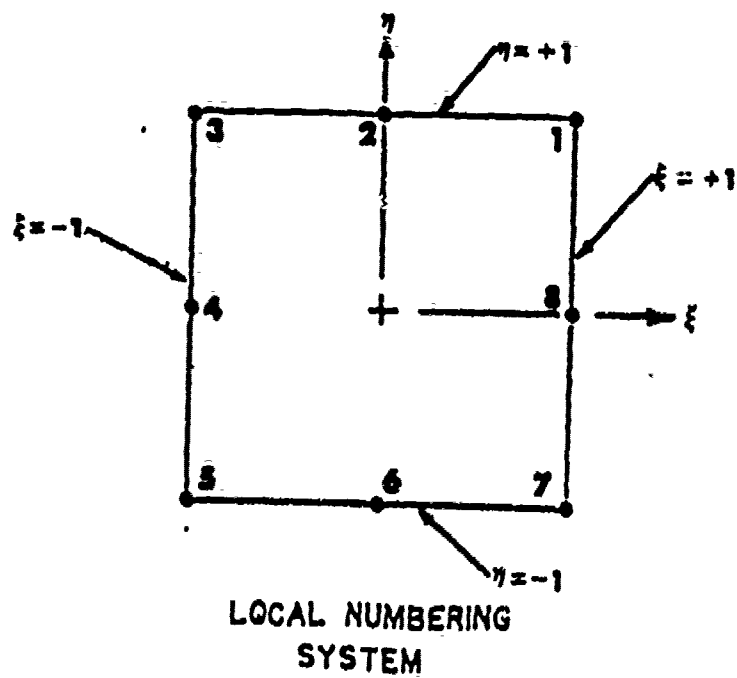
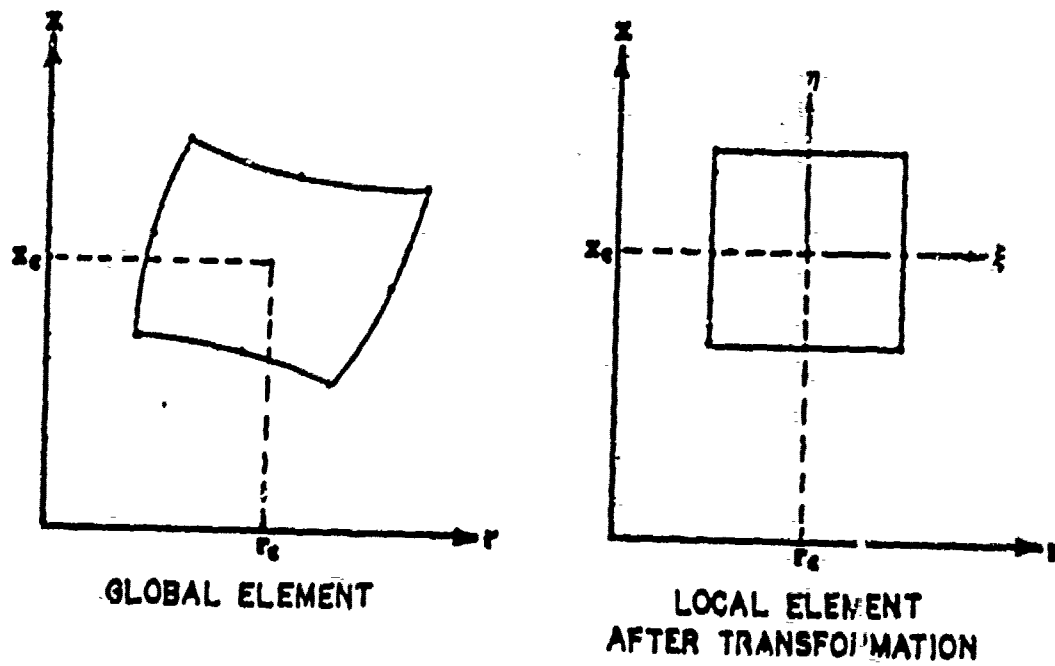
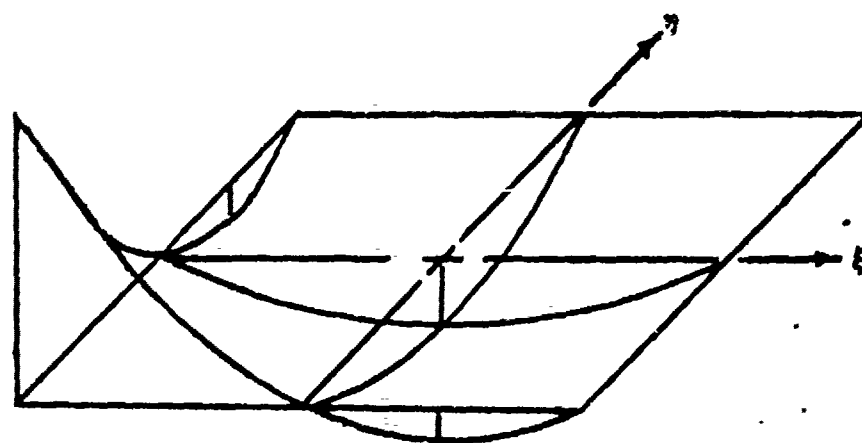
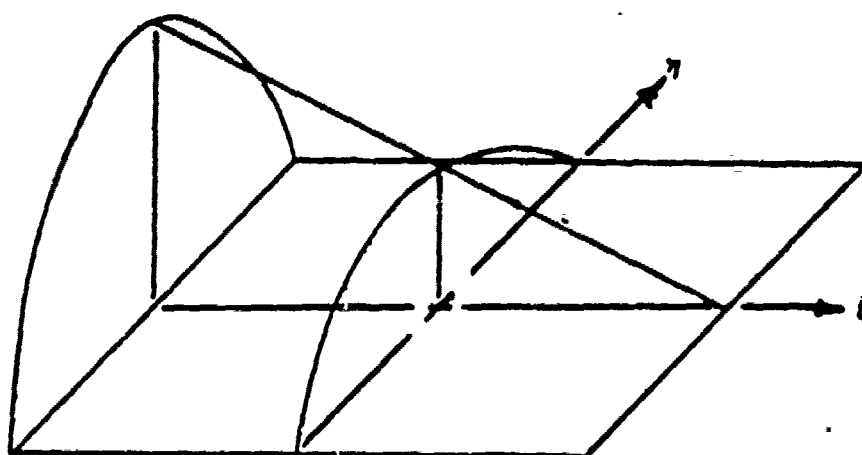


Figure 4. Element Transformation



CORNER NODE



MIDSIDE NODE

Figure 5. Normalized Shape Functions

where  $[J]^{-1}$  is the inverse of the 2x2 Jacobian matrix defined in Appendix A. As shown in Appendix A, this inverse can be easily shown to be (for this problem)

$$[J]^{-1} = \begin{bmatrix} J_{11}^* & J_{12}^* \\ J_{21}^* & J_{22}^* \end{bmatrix} \quad (42)$$

where

$$\begin{aligned} J_{11}^* &= 2/\Delta r, & J_{12}^* &= 0 \\ J_{21}^* &= 0, & J_{22}^* &= 2/\Delta z \\ \Delta r &- \text{radial length of the element} \\ \Delta z &- \text{axial length of the element} \end{aligned}$$

Elements of area transform as

$$drdz = \det[J] d\xi d\eta \quad (43)$$

For this particular problem,  $\det[J]$  may be shown to be (Appendix A)

$$\det[J] = \frac{A^e}{4} \quad (44)$$

where  $A^e$  - area of the element

Elements of axial length become

$$dz = \frac{L^e}{2} \quad (45)$$

where  $L^e$  - axial length of the element

Utilization of these transformations makes the integrations required in equation (37) amenable to integration by numerical Gaussian quadrature.

## V. APPLICATION OF FEM TO GOVERNING FIELD EQUATIONS

In this chapter, equation (37) is applied to the governing field equations previously derived. The element matrices for each of the operators are developed so that the discretization of the spatial domain may be accomplished. The integrations required by the application of equation (37) are performed numerically using Gaussian quadrature.

### A. GAUSSIAN QUADRATURE

Prior to the application of equation (37), it is appropriate to discuss briefly the procedure used for the numerical integration. The product Gaussian quadrature formula is [16]

$$I_A = \int_{-1}^1 \int_{-1}^1 g(\xi, \eta) d\eta d\xi = \sum_{i=1}^m \sum_{j=1}^m W_i W_j g(\xi_i, \eta_j) \quad (46)$$

where

- $I_A$  - area integration
- $g(\xi, \eta)$  - any function of  $\xi$  and  $\eta$
- $W_{i,j}$  - weight associated with location  $i$  or  $j$
- $m$  - number of Gauss sampling points in one-dimension

The values of the weights associated with each Gauss point are given in Ref. [16]. Equation (42) may be simplified somewhat by combining the summations and weights

$$I_A = \sum_{k=1}^{m^2} W_k g(\xi_k, \eta_k) \quad (47)$$

where

$$k = i \times j$$

$$W_k = W_i \times W_j$$

For line integrations, the Gaussian quadrature formula involves only one summation

$$I_L = \int_{-1}^1 f(\eta) d\eta = \sum_{i=1}^m W_i f(\eta_i) \quad (48)$$

## B. NEUTRONIC FIELD EQUATIONS

The discretization of the spatial domain by the finite element method is accomplished by applying equation (37) to the governing field equations, using

$$\phi_k = \langle N_j \rangle^e \{ \psi_{kj} \}^e \quad j=1,2,\dots,8 \quad (49)$$

$$k=F,c,co$$

### 1. Fuel Region

The governing equation for the fuel region, equation (20) after applying equation (37) becomes

$$\begin{aligned} 2\pi \int \int \frac{N_i}{v} \frac{\partial \phi_F}{\partial z} r dr dz - 2\pi \int \int N_i \left( \frac{1}{r} \frac{\partial}{\partial r} (r D_F \frac{\partial \phi_F}{\partial r}) \right. \\ \left. + \frac{\partial}{\partial z} (D_F \frac{\partial \phi_F}{\partial z}) + \Sigma_{aF} \phi_F (1-\beta) [k_{\infty}^0 + \rho - b \ln(T_F/T_F^0)] \right. \\ \left. + \lambda \bar{\beta} \Sigma_{aF} \int_0^t e^{-\lambda_1(t-t')} (k_{\infty}^0 + \rho) \phi_F dt' + \lambda C^0 e^{-\lambda t} \right) r dr dz = 0 \end{aligned} \quad (50)$$

The second order terms in equation (50) may be reduced to a first order term by application of Green's Theorem or equivalently integration-by-parts (See Appendix B). Dividing through by  $2\pi$  and reducing the second order terms yields

$$\begin{aligned} & \int_z r N_i D_F \frac{\partial \phi_F}{\partial r} dz + \int_r r N_i D_F \frac{\partial \phi_F}{\partial z} dr + \int_r \int_z \frac{N_i}{v} \frac{\partial \phi_F}{\partial t} r dr dz \\ & + \int_r \int_z \left\{ D_F \left[ \frac{\partial N_i}{\partial r} \frac{\partial \phi_F}{\partial r} + \frac{\partial N_i}{\partial z} \frac{\partial \phi_F}{\partial z} \right] - N_i \Sigma_{aF} \phi_F (1-\beta) [k_{\infty}^* + \rho - b \ln(T_F/F_{F0})] \right. \\ & \left. - N_i \bar{\lambda} \bar{\beta} \Sigma_{aF} \int_0^t e^{-\lambda(t-t')} (k_{\infty}^* + \rho) \phi_F dt' - N_i \bar{\lambda} C^* e^{-\bar{\lambda} t} \right\} r dr dz = 0 \quad (51) \end{aligned}$$

From continuity and boundary conditions the line integrals are zero. Now using the approximate functions of equation (49) and noting that  $\{\psi_F\}^e$  is not a function of space, equation (51) may be written as

$$\begin{aligned} & \frac{1}{v} \iint_{r,z} \{N_i\}^e \langle N_j \rangle^e r dr dz \{\psi_F\}^e + \iint_{r,z} D_F \left[ \{N_{i,r}\}^e \langle N_{j,r} \rangle^e + \{N_{i,z}\}^e \langle N_{j,z} \rangle^e \right] r dr dz \{\psi_F\}^e \\ & - \iint_{r,z} \Sigma_{aF} (1-\beta) [k_{\infty}^* + \rho - b \ln(T_F/T_F^0)] \{N_i\}^e \langle N_j \rangle^e r dr dz \{\psi_F\}^e - \bar{\lambda} \bar{\beta} \Sigma_{aF} \int_0^t e^{-\bar{\lambda}(t-t')} (k_{\infty}^* + \rho) dt' \\ & \iint_{r,z} \{N_i\}^e \langle N_j \rangle^e r dr dz \{\psi_F\}^e - \bar{\lambda} C^* e^{-\bar{\lambda} t} \iint_{r,z} \{N_i\}^e r dr dz = 0 \quad (52) \end{aligned}$$

The integrations may not be easily carried out with a shift to local coordinates and with use of the previously derived transformations. Rearranging equation (52) and assuming the properties are constant for each time step gives

$$\begin{aligned}
 D_F \int_{-1}^1 \int_{-1}^1 & [(N_{1,\xi} J_{11}^*) \langle J_{11}^* N_{j,\xi} \rangle + (N_{1,\eta} J_{22}^*) \langle J_{22}^* N_{j,\eta} \rangle] r \det[J] d\xi d\eta (\psi_F)^e \\
 - \Sigma_{aF} (1-\beta) (k_\infty^0 + \rho) & \int_{-1}^1 \int_{-1}^1 (N_1) \langle N_j \rangle r \det[J] d\xi d\eta (\psi_F)^e \\
 - \Sigma_{aF} (1-\beta) b & \int_{-1}^1 \int_{-1}^1 \ln \frac{T_F}{T_F} (N_1) \langle N_j \rangle r \det[J] d\xi d\eta (\psi_F)^e \\
 - \bar{\lambda} \Sigma_{aF} f(t) & \int_{-1}^1 \int_{-1}^1 (N_1) \langle N_j \rangle r \det[J] d\xi d\eta (\psi_F)^e - \bar{\lambda} C^0 e^{-\bar{\lambda} t} \int_{-1}^1 \int_{-1}^1 (N_1) r \det[J] d\xi d\eta \\
 + \frac{1}{V} & \int_{-1}^1 \int_{-1}^1 (N_1) \langle N_j \rangle r \det[J] d\xi d\eta (\psi_F)^e = 0
 \end{aligned} \tag{53}$$

Since the element chosen has eight degrees of freedom (nodal points), the discretized matrices which result from the integration of equation (53) will be 8x8 matrices and the forcing function will be an 8x1 vector at the element level. Defining the matrices as

$$\begin{aligned}
 & \int_{-1}^1 \int_{-1}^1 [(N_{1,\xi} J_{11}^*) \langle J_{11}^* N_{j,\xi} \rangle + (N_{1,\eta} J_{22}^*) \langle J_{22}^* N_{j,\eta} \rangle] r \det[J] d\xi d\eta \\
 [H12_{ij}]_{8 \times 8} &= \frac{A^e}{4} \sum_{k=1}^8 [(N_{1,\xi})_k (N_{j,\xi})_k J_{11}^{*2} \\
 & + (N_{1,\eta})_k (N_{j,\eta})_k J_{22}^{*2}] r_k w_k
 \end{aligned} \tag{54}$$

where  $W_k = W_i W_j$  and  $r_k = \sum_{i=1}^8 r_i (N_i)_k$

$$\int_{-1}^1 \int_{-1}^1 \{N_i\} \langle N_j \rangle r \det[J] d\xi d\eta = [H3_{ij}]_{8 \times 8} = \frac{A^e m^2}{4} \sum_{k=1}^8 (N_i)_k (N_j)_k r_k W_k \quad (55)$$

$$\int_{-1}^1 \int_{-1}^1 \{N_i\} r \det[J] d\xi d\eta = \{F_i\}_{8 \times 1} = \frac{A^e}{4} \sum_{k=1}^8 (N_i)_k r_k W_k \quad (56)$$

$$\begin{aligned} \int_{-1}^1 \int_{-1}^1 \ln(T_F/T_D) \{N_i\} \langle N_j \rangle r \det[J] d\xi d\eta &= [H4_{ij}]_{8 \times 8} \\ &= \frac{A^e m^2}{4} \sum_{k=1}^8 \ln(T_F/T_{F^0})_k (N_i)_k (N_j)_k r_k W_k \end{aligned} \quad (57)$$

To carry out the summation of equation (57), the temperature  $T_F$  must be known; however, this temperature is exactly what is being sought. To alleviate this problem, a linearization is used.

In the solution technique, the temperature is predicted for the next time step. It is this temperature which is used for the determination of matrix  $H4$ .

Equation (53) simplifies to

$$\begin{aligned} (D_F [H12_{ij}] - [\Sigma_{aF} (1-\beta) (k_m^0 + \rho) + \lambda \bar{\beta} \Sigma_{aF} f(t)] [H3_{ij}] + \Sigma_{aF} (1-\beta) b [H4_{ij}]) \{\psi_F\}^e \\ - \lambda C^0 c^{-\bar{\lambda} t} \{F_i\}^e + \frac{1}{V} [H3_{ij}] \{\psi_F\} = 0 \end{aligned} \quad (58)$$

The function  $f(t)$  is evaluated by summing the values at each time step using the trapezoid rule for numerical integration.

$$f(t) = e^{-\bar{\lambda}t} \int_0^t e^{-\bar{\lambda}t'} [k_{\infty}^0 + \rho] dt' \quad (59)$$

Defining

$$I_1[g(t)] = \frac{1}{2} h_1 \{g(t_1) + g(t_{1-1})\} \quad (60)$$

$$g(t) = e^{\bar{\lambda}t} (k_{\infty}^0 + \rho)$$

$h_1$  - time step taken

$$g_0 = 0$$

The function may be expressed as

$$f(t) = e^{-\bar{\lambda}t} \sum_{i=1}^S I_1 [g(t)] \quad (61)$$

$S$  - number of time steps

## 2. Clad Region

Following the same procedure as with the fuel equation, the discretized form of equation (11) becomes

$$\{D_c[H12_{1j}] + \Sigma_{ac}[H3_{1j}]\}(\psi_c)^e + \frac{1}{V}[H3_{1j}](\dot{\psi}_c)^e = 0 \quad (62)$$

## 3. Coolant Region

The governing equation for the coolant region, equation (12), may be discretized into the form

$$\{D_{co}[H12_{1j}] + \Sigma_{aco}[H3_{1j}]\}(\psi_{co})^e + \frac{1}{V}[H3_{1j}](\dot{\psi}_{co})^e = 0 \quad (63)$$

Once the governing equations have been discretized at the element level, they are combined into a system of equations at the global level. On the global level the governing equation for neutron transport takes the form of

$$[H]_{n \times n} \{\psi\}_{n \times 1} + [P]_{n \times n} \{\dot{\psi}\}_{n \times 1} + \{F\}_{n \times 1} = 0 \quad (64)$$

where  $[H]$ ,  $[P]$ , and  $[F]$  represent the system matrices and  $n$  is the number of nodal points used in the discretization. There are, then,  $n$  simultaneous ordinary differential equations used to describe the neutron transport problem.

### C. HEAT TRANSPORT FIELD EQUATIONS

The spatial domain for the heat transport problem is discretized in the same manner as the domain for the neutronics problem. The same element matrices previously defined are valid. Let

$$T_k = \langle N_j \rangle^e \{\tau_{kj}\}^e \quad \begin{matrix} j=1,2,\dots,8 \\ k=F,c,co \end{matrix} \quad (65)$$

#### 1. Fuel Region

The governing field equation for the fuel, equation (24), is discretized by applying equation (37). Using an integration by part to lower the order of the second order terms allows equation (24) to be written as

$$\int_r [N_i k_F \frac{\partial T_F}{\partial z}]_0^z r dr dz + \int_z [N_i k_F \frac{\partial T_F}{\partial r}]_0^a dz - \int_r \int_z \{k_F [\frac{\partial N_i}{\partial r} \frac{\partial T_F}{\partial r} + \frac{\partial N_i}{\partial z} \frac{\partial T_F}{\partial z}] - e \Sigma_{tF} N_i \phi_F + N_i \rho_F C_{pF} \frac{\partial T_F}{\partial t}\} r dr dz = 0 \quad (66)$$

From continuity considerations the line integrals are zero except along the boundaries of a region. It is assumed that no heat is transferred from the cell in the axial direction (boundary condition 5); therefore, the first line integral of equation (66) is zero. In the neutron diffusion problem there was continuity of flux at the interfaces so that the line integrals were zero; however, the heat transfer at the interfaces is affected by the gap and film conductances. The fuel-clad interface condition, equation (29), may be rewritten as

$$-k_F \frac{\partial T_F}{\partial r} = H_{\text{gap}}(T_F - T_C) = -k_C \frac{\partial T_C}{\partial r} \quad (67)$$

Substituting equation (67) into (66), dividing by minus one and utilizing equation (65) yields

$$\begin{aligned} & \int_z [r H_{\text{gap}} \{N_1\}^{e^*} \langle N_j \rangle^{e^*} \Big|_0^a dz \{\tau_F\}^{e^*} - \int_z [r H_{\text{gap}} \{N_1\}^{e^*} \langle N_j \rangle^{e^*} \Big|_0^a dz \{\tau_C\}^{e^*} \\ & + \int_r \int_z k_F [\{N_1, r\}^{e^*} \langle N_j, r \rangle^{e^*} + \{N_1, z\}^{e^*} \langle N_j, z \rangle^{e^*}] r dr dz \{\tau_F\}^{e^*} \\ & - \int_r \int_z e \Sigma_{fF} \{N_1\}^{e^*} \langle N_j \rangle^{e^*} r dr dz \{\psi_F\}^{e^*} \\ & + \int_r \int_z \rho_F C_{pF} \{N_1\}^{e^*} \langle N_j \rangle^{e^*} r dr dz \{\dot{\tau}_F\}^{e^*} = 0 \end{aligned} \quad (68)$$

$e^*$  - element across the interface

Transforming to local coordinates and integrating by Gaussian quadrature yields the same element matrices as given for the neutron flux, equations (54) and (55), except for the line integrals between regions. It should be noted that the line integrals exist only on the interfaces, along which there is a discontinuity of temperature. For the fuel equation the interface corresponds to the local coordinate  $\xi=1$ . Define

$$\int_{-1}^1 \{N_i\} \{N_j\} d\eta = [k]_{ij} 8 \times 8 = \frac{1}{2} \sum_{k=1}^{m^2} (N_i)_k (N_j)_k W_k \quad (69)$$

where the  $N$ 's are evaluated at  $\xi=1$ . Many of the terms of  $K1$  will be zero since only the nodes on the  $\xi=1$  boundary will have shape functions which are non-zero. It is through  $K1$  that the temperatures for each region are coupled together. Equation (68) may now be written as

$$\begin{aligned} r_a H_{gap} \{ [K1] \{ \tau_F \}^e - [K1] \{ \tau_C \}^{e*} \} + k_F [H12] \{ \tau_F \}^e \\ - e \Sigma_{fF} [H3] \{ \psi_F \}^e + \rho_F C_{pF} [H2] \{ \dot{\tau}_F \} = 0 \end{aligned} \quad (70)$$

In obtaining this equation, it was assumed that material properties for each nodal point were constant at each time step. Perhaps a better assumption would have been to assume an average value for the properties of each element. The difference should not be significant, and the assumed constant nodal properties were numerically more tractable.

## 2. Clad Region

Applying equation (37) to the governing field equation for the clad, equation (25) gives the discretized form of the equation. Assuming no heat transfer in the axial direction on the boundaries (Boundary condition 5), equation (25) becomes

$$\begin{aligned}
 - \int_z [N_i r k_c \frac{\partial T_c}{\partial r}]_a^b dz + \int_r \int_z k_c [\frac{\partial N_i}{\partial r} \frac{\partial T_c}{\partial r} + \frac{\partial N_i}{\partial z} \frac{\partial T_c}{\partial z}] r dr dz \\
 + \int_r \int_z \rho_c c_{pc} N_i \frac{\partial T_c}{\partial t} r dr dz = 0
 \end{aligned} \quad (71)$$

In the cladding, there are two interfaces along which the line integral of equation (71) is not zero, along the fuel-clad interface and along the clad-coolant interface. For the fuel-clad interface, equation (61) applies. For the clad-coolant interface, the interface condition, equation (30), may be rewritten as

$$k_c \frac{\partial T_c}{\partial r} = h_{surf} (T_c - T_{co}) = -k_{co} \frac{\partial T_{co}}{\partial r} \quad (72)$$

Along the fuel-clad interface, the local coordinate corresponds to  $\xi = -1$ . Define the new element matrix

$$\int_{-1}^1 \int_{-1}^1 \{N_i\}^e \{N_j\}^e d\eta = [K2_{ij}]_{8 \times 8} = \frac{L}{2} \sum_{k=1}^{m^2} (N_i)_k (N_j)_k W_k$$

where the  $N$ 's are evaluated at  $\xi = -1$ . As with  $K1$ ,  $K2$  will have many zero values because the shape functions are evaluated at  $\xi = -1$ .

Along the clad-coolant interface, the local coordinate corresponds to  $\xi=1$  and the K1 matrix is appropriate.

Substituting equations (67) and (72), equation (71) becomes

$$\begin{aligned} \int_z [r h_{surf} N_1 (T_c - T_{co})]_b dz - \int_z [r h_{gap} N_1 (T_F - T_c)]_a dz \\ + \int_r \int_z k_c \left[ \frac{\partial N_1}{\partial r} \frac{\partial T_c}{\partial r} + \frac{\partial N_1}{\partial z} \frac{\partial T_c}{\partial z} \right] r dr dz \\ + \int_r \int_z \rho_c C_{pc} N_1 \frac{\partial T_c}{\partial t} r dr dz = 0 \end{aligned} \quad (73)$$

The governing equation for the clad region may now be written as

$$\begin{aligned} r_a h_{gap} \{ [K2] \{\tau_c\}^e - [K2] \{\tau_F\}^{e*} \} + r_b h_{surf} \{ [K1] \{\tau_c\}^e - [K1] \{\tau_{co}\}^{e*} \} \\ + k_c [H12] \{\tau_F\}^e + \rho_c C_{pc} [H3] \{\dot{\tau}_c\} = 0 \end{aligned} \quad (74)$$

The line integrals of equation (73) affect only nodes which are on one of the boundaries; therefore, the nodal inputs into K1 and K2 are zero unless the node is on one of the boundaries.

### 3. Coolant Region

The field equation governing the coolant may be discretized in the same manner as above. After applying the Galerkin method and performing an integration by parts

on the second order terms, equation (25) becomes

$$\begin{aligned}
 & - \int_z [r N_1 k_{co} \frac{\partial T}{\partial r}]_b^c dz + \int_r \int_z k_{co} \left[ \frac{\partial N_1}{\partial r} \frac{\partial T_{co}}{\partial r} + \frac{\partial N_1}{\partial z} \frac{\partial T_{co}}{\partial z} \right] r dr dz \\
 & + \int_r \int_z V_{co} \rho_{co} C_{pco} N_1 \frac{\partial T_{co}}{\partial z} r dr dz \\
 & + \int_r \int_z \rho_{co} C_{pco} N_1 \frac{\partial T_{co}}{\partial t} r dr dz = 0 \quad (75)
 \end{aligned}$$

The line integral, when evaluated at c, is zero (boundary condition 4). When evaluated at b, or correspondingly at  $\xi = -1$ , equation (72) is valid and K2 matrix is appropriate. All the terms of equation (75) have been defined except the flow term. Define

$$\begin{aligned}
 & \int_{-1}^1 \int_{-1}^1 \{N_1\}^e \langle N_{1,n} \rangle^e r \det[J] d\xi d\eta = [H5]_{ij}]_{6 \times 8} \\
 & = \frac{A^e m^2}{4} \sum_{k=1}^2 (N_1)_k (N_{1,n})_k r_k W_k \quad (76)
 \end{aligned}$$

Transforming to local coordinates and integrating reduces equation (75) to

$$\begin{aligned}
 & r_b h_{surf} \{ [K2] \{\tau_{co}\}^e - [K2] \{\tau_c\}^{e*} \} + k_{co} [H12] \{\tau_{co}\}^e \\
 & + V_{co} \rho_{co} C_{pco} [H5] \{\tau_{co}\}^e + \rho_{co} C_{pco} [H3] \{\dot{\tau}_{co}\}^e = 0 \quad (77)
 \end{aligned}$$

Now that the governing equations have been defined for each region on the element level, equations (70), (74), and (77), they may be assembled into a system equation on the global level. The equation will be in the general form of

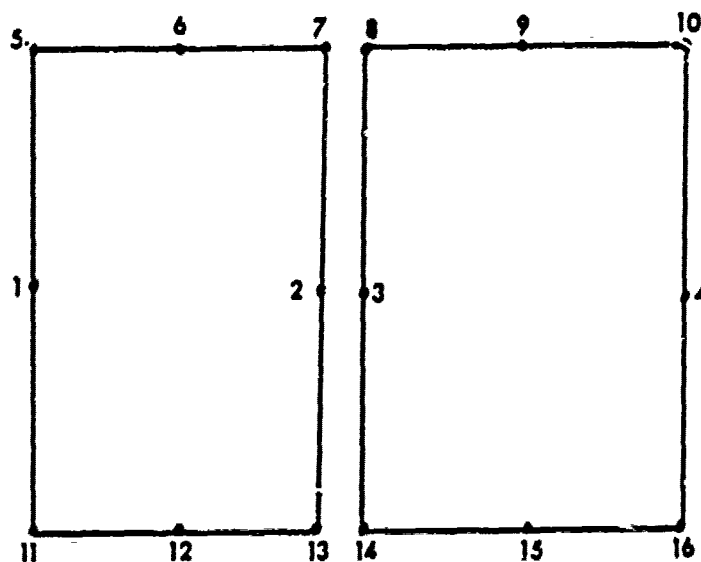
$$[K]_{n \times n} \{\tau\}_{n \times 1} + [M]_{n \times n} \{\psi\}_{n \times 1} + [G]_{n \times n} \{\dot{\tau}\}_{n \times 1} = 0 \quad (78)$$

#### D. DISCRETIZATION OF THE SPATIAL DOMAIN

Prior to the numerical solution of the governing equations, equations (64) and (78), the spatial domain must be divided into a number of elements. For this work the domain was subdivided as shown in figure 5.

Since there is a discontinuity of temperatures at the interfaces, as described by equations (29) and (30), a novel application of the FEM method was necessary. The common practice for handling these "flux" type boundary conditions is to define a constant reference temperature,  $T_{\infty}$ , as when working with a convection heat transfer problem [17], or to define a known function, as when working with a fracture mechanics problem [18]. In either case the reference condition was known. The novel application here lies in the use of a different field equation to describe the reference temperature, e.g., the clad equation (74) is the reference condition for heat transfer from the fuel across the gap interface.

The discontinuity of temperature at the interface necessitated another novel application of the FEM. Since there is a temperature drop along each interface, a single node there is not adequate. In the discretization of the domain, two nodes were used for each interface point (for example, points 62 and 63 in figure 6). This allows the temperature drop due to the gap and film conductances to be taken into consideration. Since two nodes are used, the governing equations for each region are not directly coupled together. The coupling of the regions is accomplished by the "flux" boundary or interface conditions since it is assumed that any heat flux leaving a region enters the adjacent region. Consider a typical set of elements on an interface



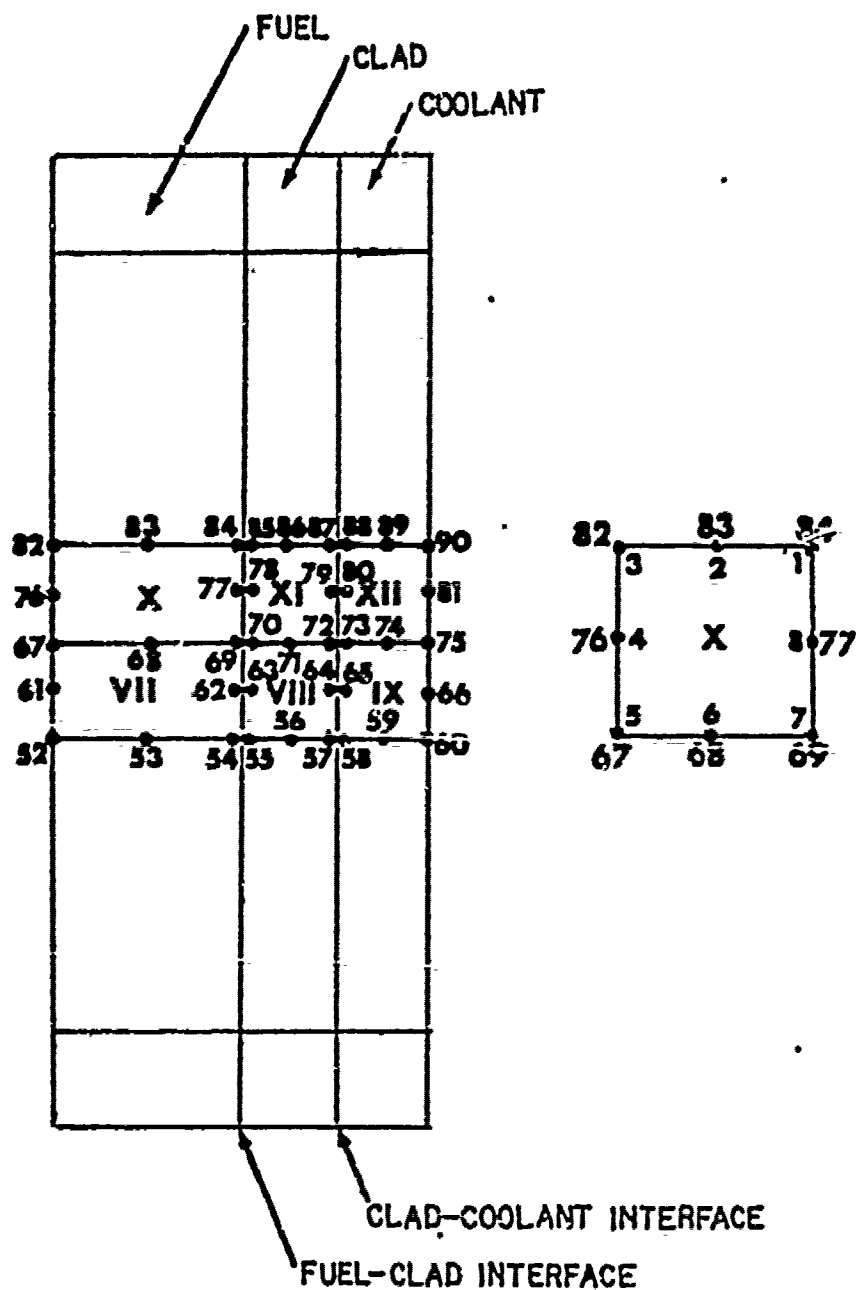


Figure 6. Finite Element Discretization

The coupling terms  $K_1$  and  $K_2$  may be combined into a system  $K$  matrix which shows the coupling. The  $K$  matrix for the simple set shown is

$$\begin{array}{c}
 \begin{array}{cccccccccccccccc}
 & 1 & 2 & 3 & 4 & 5 & 6 & 7 & 8 & \cdots & 13 & 14 & 15 & 16 \\
 \begin{array}{c} 1 \\ 2 \\ 3 \\ 4 \\ 5 \\ 6 \\ 7 \\ 8 \\ \vdots \\ 13 \\ 14 \\ 15 \\ 16 \end{array} & \left[ \begin{array}{cccccccccccccccc}
 & & & & & & & & & & & & & \\
 & a & -a & & & & & c & -c & & & c & -c & \\
 & -a & a & & & & & -c & c & & & -c & c & \\
 & & & & & & & & & & & & & \\
 & & & & & & & & & & & & & \\
 & & & & & & & & & & & & & \\
 & & c & -c & & & & b & -b & & & d & -d & \\
 & -c & c & & & & & -b & b & & & -d & d & \\
 & \vdots & & & & & & & & & & & & \\
 & & & & & & & & & & & & & \\
 & & c & -c & & & & d & -d & & & b & -b & \\
 & -c & c & & & & & -d & d & & & -b & b & \\
 & & & & & & & & & & & & & \\
 & & & & & & & & & & & & & 
 \end{array} \right]
 \end{array}
 \end{array}
 \quad
 \begin{array}{l}
 a = 16/15 \\
 b = 4/15 \\
 c = 2/15 \\
 d = 1/15
 \end{array}$$

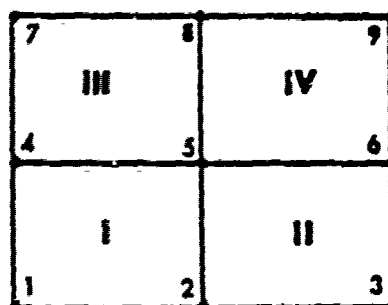
As can be seen, the nodes on the interface are coupled to the adjacent element interface nodes. For example, node 2 in element I is coupled to nodes 3, 8, and 14 in element II.

#### E. OPTIMUM COMPACTING SCHEME

The system matrices ( $H$ ,  $P$ , etc.) are  $n \times n$  matrices, where  $n$  is the number of nodal points used in the discretization of the domain. In terms of computer storage, these matrices may become excessively large if they are stored as  $n \times n$ . There are several techniques available to reduce this storage requirement. The most common method is the banded storage scheme, whereby only the banded portion of the matrices are stored. With judicious numbering of the nodes,

considerable savings may be realized. However, it is not the optimum storage scheme [8].

Since the shape functions,  $N_i$ , for the  $k^{\text{th}}$  nodal equation are nonzero over only the element containing  $k$ , the system matrices are not only banded but sparse as well. The sparseness is due to the non-consecutive numbering of the nodes surrounding the  $k^{\text{th}}$  node. The optimum compact storage (OCS) scheme compacts the matrices by storing only the non-zero elements of the matrices. The implementation of the OCS scheme requires two additional integer arrays, say JA and NAME. The NAME array identifies the nodal points which contribute to each nodal equation. The JA array acts as a pointer to indicate where the nodal equation starts in NAME. Consider the following simple 2x2 system with nodes as indicated



The NAME array starts with node 1 and identifies the nodes which contribute to node 1 (i.e., 5, 4, and 2). The NAME array would, then, give the nodes contributing to node 2 and so forth, so that

$$\begin{aligned}
 \text{and } \langle \text{NAME} \rangle &= \begin{matrix} 1234 & 5678910 & 11 & 1213 & 14 & \dots & \text{JC} \\ \langle 1542 : 254163 : 3 & 6 & 5 & 2 : \dots : 9856 \rangle \end{matrix} \\
 \text{and } \langle \text{JA} \rangle &= \begin{matrix} 1 & 2 & 3 \\ \langle 1 & 5 & 11 & \dots \rangle \end{matrix}
 \end{aligned}$$

The algorithm to assemble the element matrices into a compact storage vector is straightforward and represents a significant savings in computer storage [8]. The system matrices are stored as a vector rather than a two-dimensional array. For example, the value which would be stored in position (1,5) of the  $n \times n$  array is stored in position 2 of the system vector.

## VI. NUMERICAL SOLUTION

This section contains a brief description of possible solution techniques in addition to the solution technique chosen. Computer subroutines necessary to implement the technique are also described.

### A. SELECTION OF METHOD

The numerical solution of the system of implicit ordinary differential equations, equations (64) and (78), may be accomplished by any of a number of different techniques such as Houbolt's method, Crank-Nicolson's method, Gear's method, or implicit Gear's method. It was not the objective of this analysis to determine which of the numerical solution schemes is the most efficient. Each method has its advantages and disadvantages. The Crank-Nicolson method is a single-step, implicit equation solver and, therefore, does not require storage of previous time solutions. When analyzing neutronic problems, the system of equations which arises is commonly very stiff (i.e., a rapid change in flux over a short period of time). The Crank-Nicolson method has, in a past work [8], demonstrated difficulty in tracking these stiff systems. Gear's method was specifically developed for stiff systems and can handle the problem very well. However, Gear's method is a multi-step, predictor-corrector method requiring storage of previous time solutions. In addition to this disadvantage, Gear's method requires the

transformation of the developed implicit O.D.E.'s into an explicit system of O.D.E.'s. After this transformation is done, the system matrices are no longer sparse or banded, thus eliminating the use of the optimum compacting scheme. In an effort to overcome these difficulties, Gear's method was modified, Ref. [9], to treat the implicit system of equations as well as to allow use of the optimum compacting scheme. A previous work, Ref. [8], has shown that the implicit Gear's method is particularly attractive in solving the type problem developed in this analysis. Therefore, the implicit Gear's method is used for the solution of the system of O.D.E.'s arising in this analysis.

No attempt will be made here to give the mathematics involved in developing the implicit Gear's method. Reference [9] may be consulted if details are desired. A listing of the computer program developed will be given in the Computer Program section. In order to utilize the implicit Gear's method, several user supplied subroutines must be developed: 1) DIFFUN, 2) JACMAT, and 3) RUTSL.

## B. USER SUPPLIED SUBROUTINES TO IMPLEMENT THE IMPLICIT GEAR'S METHOD

### 1. DIFFUN

Subroutine DIFFUN evaluates equations (64) and (78) for a given time and for given values of  $\psi$ ,  $\dot{\psi}$ ,  $\tau$  and  $\dot{\tau}$ . Since at each nodal point,  $i$ , there is a solution for the flux and for the temperature, the solution was set equal to DYI and DYII, respectively. In addition to having flux and

temperature at each nodal point, there are also three different regions in the domain which have different governing equations. An integer array, ITYPE, was developed to indicate for each nodal point whether it was: 0) a fuel node not in an interface element, 1) a fuel node in an interface element, 2) a cladding node or, 3) a coolant node. Using ITYPE, the computer program is directed to a different section depending upon the type of node being considered. After all the nodes have been considered, boundary conditions are established by changing DYI and DYII for the appropriate boundary nodes. Since in this analysis there is continuity of flux at the interfaces, special considerations must be given to these nodes. At the fuel-clad interface, the value of DYI for the clad node was set to the value of the flux at that node minus the value of the flux at the adjacent node (i.e.,  $DYI_i = \psi_i - \psi_{i-1}$ ). Similarly, at the clad-coolant interface, the value of DYI for the coolant node was set to the value of the flux at that node minus the value of the flux at the adjacent node. During the solution of the problem, DYI is driven toward zero, which in the limit forces  $\psi_i$  to equal  $\psi_{i-1}$ . This is the desired continuity result.

## 2. JACMAT

Subroutine JACMAT, evaluates the Jacobian matrix (for Gear's method) at the given time and for the current values of the dependent variables. The Jacobian for an equation of the type,

$$F(y, \dot{y}, t) = 0 \quad (79)$$

may be represented as [19],

$$J = \left[ \frac{\partial F}{\partial y} - \frac{\alpha_0}{\beta_0 h} \frac{\partial F}{\partial \dot{y}} \right] \quad (80)$$

where  $\alpha_0$  and  $\beta_0$  are coefficients from Gear's method and  $h$  is the time step. Using the notation of DIFFUN, let DYI and DYII represent equations (64) and (78), respectively. The Jacobian matrix may, then, be written as (J is called PW in JACMAT.)

$$PW = \left[ \frac{\partial DYI}{\partial \psi} - \frac{\alpha_0}{\beta_0 h} \frac{\partial DYI}{\partial \dot{\psi}}, \frac{\partial DYII}{\partial \tau} - \frac{\alpha_0}{\beta_0 h} \frac{\partial DYII}{\partial \dot{\tau}} \right] \quad (81)$$

It is the form of equation (81) which is programmed in JACMAT. As in DIFFUN, the integer array ITYPE is used to indicate the appropriate section of the program to be utilized. The problem boundary conditions must also be accounted for in JACMAT. In DIFFUN, the value of DYI or DYII was set to zero for constant boundary conditions (i.e., zero). This cannot be done in JACMAT since a division by zero would occur. For a constant boundary condition at the  $i$ th node, the value of PW is set to one for the diagonal term and zero for all other terms of the  $i$ th equation.

### 3. NUITSL

Subroutine NUITSL solves the system of equations for the quasi-Newton iterates. In this analysis the system is solved using a successive over-relaxation (SOR) method. In this work, the optimum amount of over-relaxation was not determined. Since no effort was made to find the optimum,

it was felt a small over-relaxation would be best. The over-relaxation factor of 0.02 was used. For small values of this factor, the SOR method approaches the Gauss-Siedel iteration technique.

## VII. PROCEDURE

In this section, the method utilized to obtain a solution is described. The input data necessary to run the developed computer program will be documented.

Prior to initiating a transient overpower excursion, the steady-state conditions for the fuel cell must be known. Since the system of equations which were developed are not specifically designed to obtain a steady-state solution, the initial steady-state conditions must be part of the input data. The initial temperature distribution was obtained from the steady-state conditions given in Ref. [7].

The axial temperature distribution for the fuel centerline, fuel surface, clad, and coolant have been determined for several different fuel life cycles [7]. For this analysis, the beginning of life cycle for channel 10 was used. Although this distribution is somewhat artificial, it should be adequate for this analysis. It is the trends of the results which are considered important. The distribution within the fuel radially is taken to vary as the square of the radial distance; then

$$T_F(r,z,0) = T_F(0,z,0)\left(1 - \frac{r^2}{a^2}\right) + T_F(a,z,0)\left(\frac{r^2}{a^2}\right)$$

Within the cladding and the coolant, the initial radial temperature distribution is assumed to be constant.

The initial flux distribution is assumed to be radially constant, a flat flux assumption. In the axial direction the flux is assumed to vary as the shape of the sine function. The maximum flux, the flux at the axial center, is an input parameter. For this analysis, the maximum initial flux was taken to be  $10^{14}$  neutron/cm<sup>2</sup>sec.

To obtain a steady state flux distribution, the value of fission cross section for the fuel is varied. A trial-and-error method is used until a critical fission cross section,  $\Sigma_{ff}^{cr}$ , which gives a steady flux is obtained.

Once the steady-state conditions have been determined, the excess reactivity may be inserted. This starts the transient overpower excursion.

#### A. INPUT DATA

The first data card contains: the order of Gauss quadrature, the number of radial elements in the fuel, the number of axial elements, number of nodal points in the radial direction, and the height of the fuel rod. The next cards, one for each radial nodal point, contain the nodal radial distances. The next cards contain the fuel centerline, fuel surface, clad and coolant temperatures. There is one card for each axial node. The next card contains the maximum flux. The next four cards contain the physical parameters listed in Table I. The last input cards contain the time, end time, estimated initial time step, minimum time step, and maximum time step. A sample data deck is shown in figure 7.

TABLE I. Physical Parameters

Fuel Diffusion Coefficient (DCF)	0.93 [cm]
Doppler constant (B)	0.006
Energy release per fission (E)	$7.652 \times 10^{-12}$ [cal/fissions]
Fraction of delayed neutrons (BETA)	0.0064
Fraction of delayed neutrons for the ith group (BETAi)	0.0064
Decay constant for ith delayed neutron group (DCLAMI)	0.0784
Initial flux for delayed neutrons	$1 \times 10^{10}$ [neutron/cm <sup>2</sup> sec]
Average number of neutrons released per fission (ANU)	2.44
Neutron velocity (VEL)	$4.8 \times 10^8$ [cm/sec]
Fuel absorption cross section (SIGAF)	0.088 [cm <sup>-1</sup> ]
Critical fuel fission cross section (SIGFF)	0.0586875 [cm <sup>-1</sup> ]
Blanket absorption cross section (SIGAB)	0.0 [cm <sup>-1</sup> ]
Blanket fission cross section (SIGFB)	0.0 [cm <sup>-1</sup> ]
Step reactivity input (RHOA)	Variable
Ramp reactivity input (RHOB)	Variable
Fuel density (DENF)	10.9 [gm/cm <sup>3</sup> ]
Clad diffusion coefficient (DCC)	1.1 [cm]
Clad specific heat (CPC)	0.12 [cal/gm °C]
Clad density (DENC)	8.0 [gm/cm <sup>3</sup> ]
Clad thermal conductivity (TKC)	0.0526 [cal/cm sec °C]
Clad absorption cross section (SIGAC)	0.0015 [cm <sup>-1</sup> ]
Coolant diffusion coefficient (DCCO)	1.55 [cm]
Coolant absorption cross section (SIGACO)	0.00004 [cm <sup>-1</sup> ]
Coolant flow velocity (VCO)	396.0 [cm/sec]
Surface heat transfer coefficient (HSURF)	0.7 [cal/cm <sup>2</sup> sec °C]



### VIII. RESULTS

When using the finite element method, one of the first considerations must be given to the convergence of the method. To determine convergence, the results for a given point are compared for different finite element discretizations. As shown in figure 8, the results are comparable but no definite claim of convergence can be made. However, for this work, it was felt that these results were adequate. It was not the object of this analysis to arrive at the "final" result; it was the trends and methods that were of interest. Since the 66-element mesh appears to give a fair approximation of the results, the 66-element mesh was used as the discretized domain.

The next item of consideration was the determination of a neutronic steady-state condition. This proved to be a very time consuming task. The fission cross section for the fuel was varied by a trial-and-error method in an attempt to find the critical cross section which would give a steady state. As may be seen in figure 9, a change in cross section of less than one percent significantly affected the state of the problem. It was felt that the critical value was between the values of 0.05875 and 0.058625. Time did not permit investigation for critical value; therefore, it was assumed that the value for the critical fission cross section was half way between the values (i.e.,  $\Sigma_f^{cr} = 0.0586875$ ).

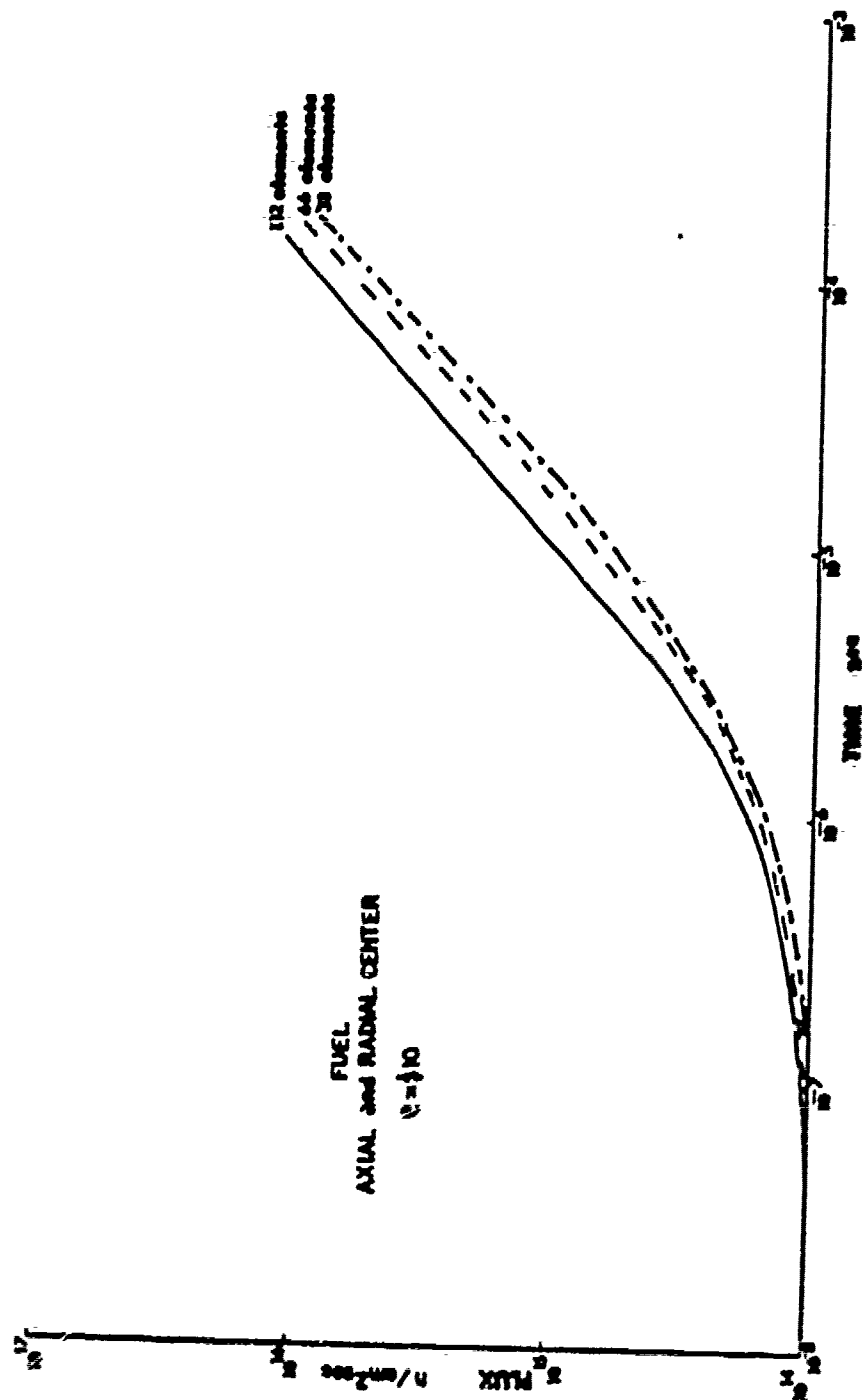


Figure 6. Convergence of Finite Element Method

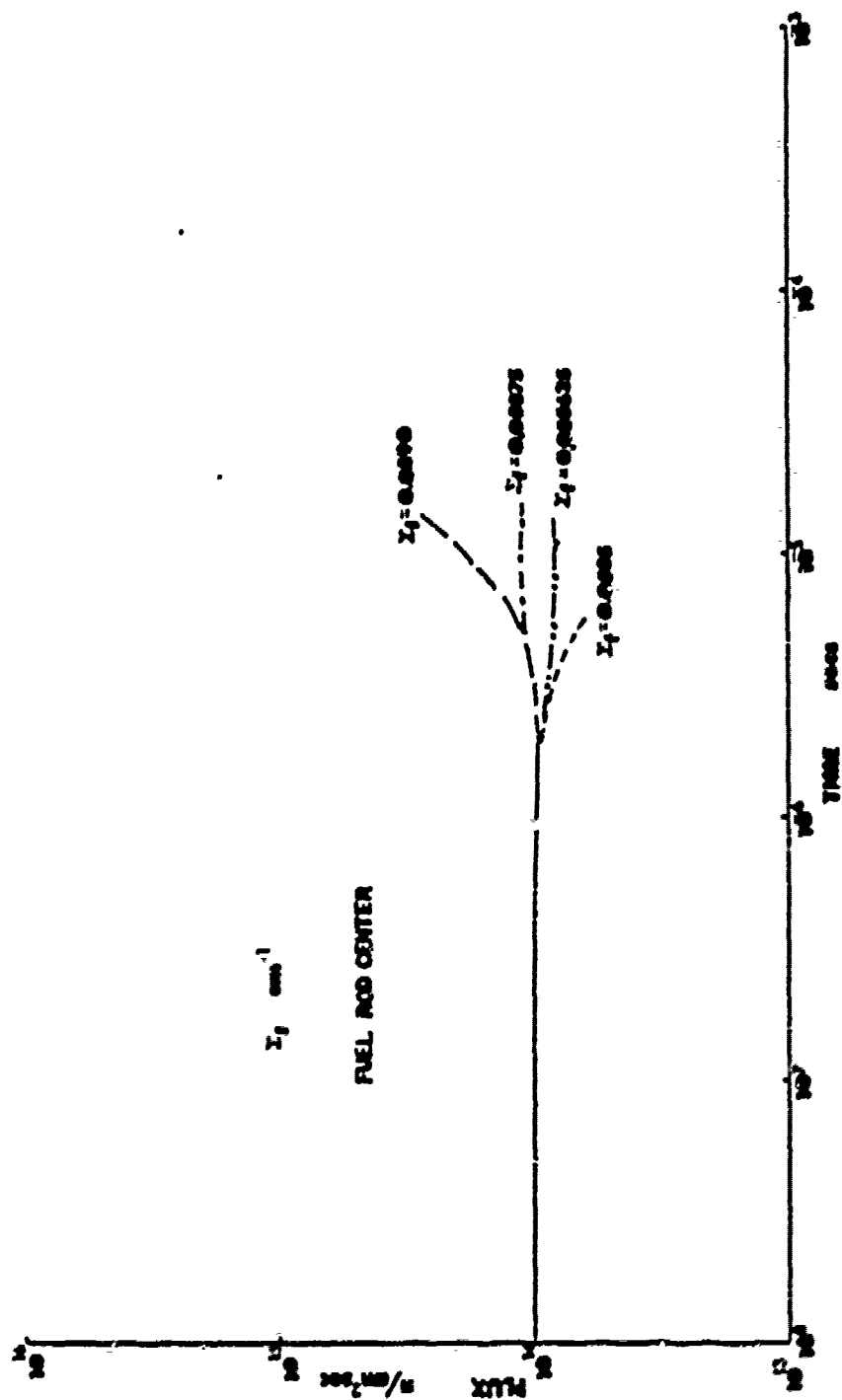


Figure 9. Determination of Critical Fission Cross Section

Even if this value is in error, which it most probably is, the net effect would only be a small decrease or increase in the proposed reactivity insertion. The reactivity insertion would, then, be an approximation of the actual reactivity of the problem.

The first test problem considered was a step increase in reactivity of approximately ten dollars. For the uranium dioxide fuel, one dollar of reactivity was taken to be 0.0064. Figure 10 shows the time history of the flux at the center of the fuel rod. Figure 11 gives the corresponding temperature profile. The temperatures were taken at the hottest point of each region at the axial center (i.e., the fuel centerline, clad inside surface, and coolant inside surface). As seen on the fuel temperature time history, the fuel rapidly reaches the fuel melting point. The model developed does not take into consideration melting of the fuel. This melting would tend to decrease the effect of the transient. The problem was allowed to continue despite this inconsistency in the mathematical model. A short time after fuel melting, the inside surface of the clad reaches its melting point. The temperature in the coolant experienced what is felt to be a numerical phenomenon. The coolant temperature decreased prior to the small rise at the end of the transient. Intuitively, this decrease does not seem to be realistic. A similar occurrence was observed while conducting sample tests on the developed computer program. Reference [20] reported the same phenomenon. It is felt that this

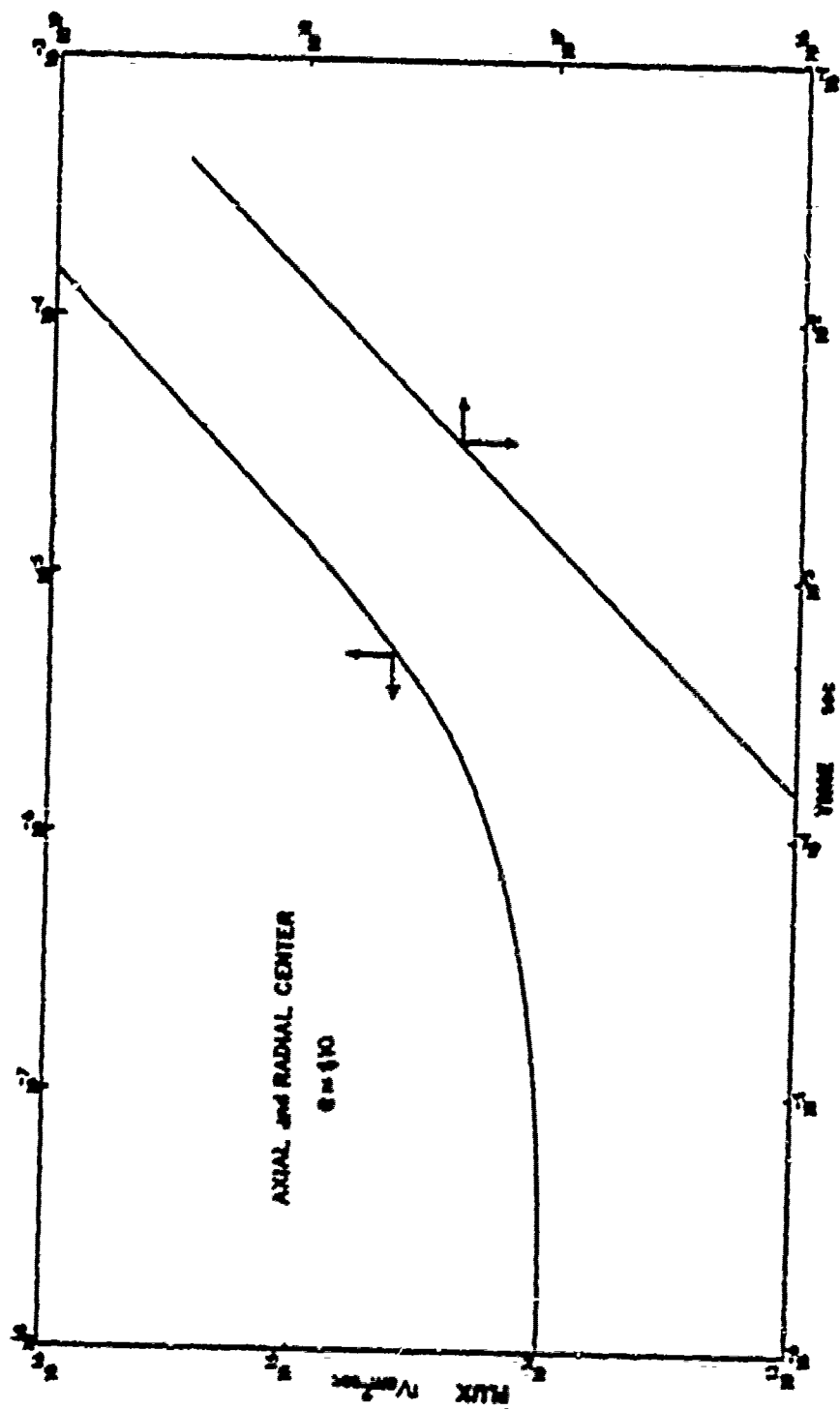


Figure 10. Flux Profile

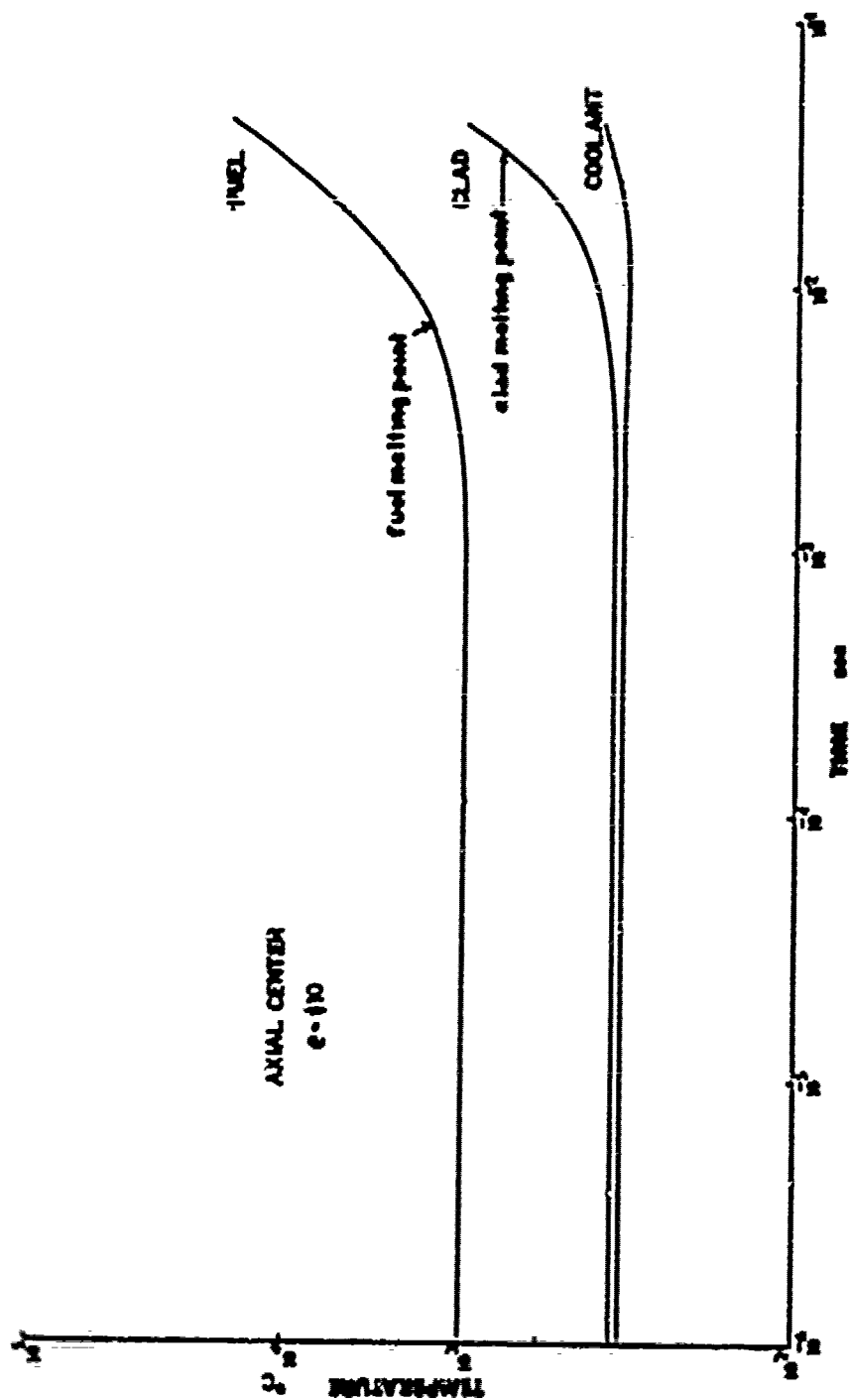


Figure 11. Temperature Profile

phenomenon is a quirk of the finite element method. The radial and axial distributions of the neutron flux are presented in figures 12 and 13 for time equal to  $7.39 \times 10^{-3}$  seconds. The distributions are, basically, as anticipated. The neutron flux peaks slightly before the axial center. It was expected to peak at the axial center. The radial and axial temperature distributions for the same time are presented in figures 14 and 15. As with the flux, the temperature profiles were, basically, as expected. The fuel temperature peaks slightly below the expected location, most likely in response to the peak in axial fluxes. The coolant unexpectedly drops near the outlet of the fuel rod. The finite element method characteristically has some problems on the boundaries of the domain; this may account for the drop in coolant temperature.

The temperature of the fuel and cladding do not appear to be as closely coupled as anticipated. As seen in figure 14, a significant increase in fuel temperature has resulted in a relatively small clad temperature increase. As noted in figure 11, there appears to be a time lag in temperature response for each region which may account for part of the apparent temperature disagreement. It is felt that the temperatures should be more closely related, which indicates a higher gap heat transfer coefficient should be utilized. Since values of the gap heat transfer coefficient were assumed, it is not unreasonable to believe the values used are too low.

FIGURE 12  
RADIAL FLUX

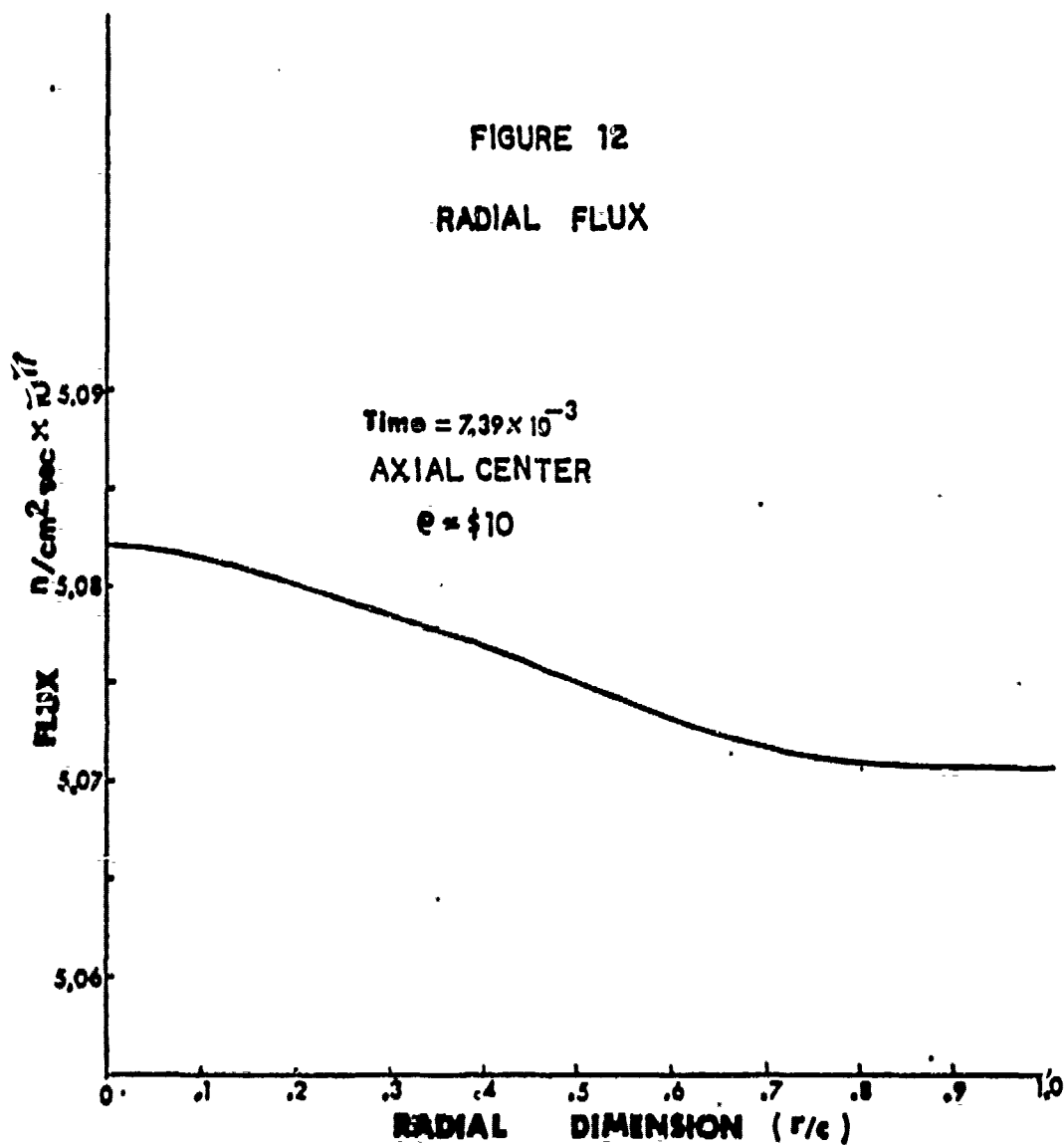


Figure 12. Radial Flux

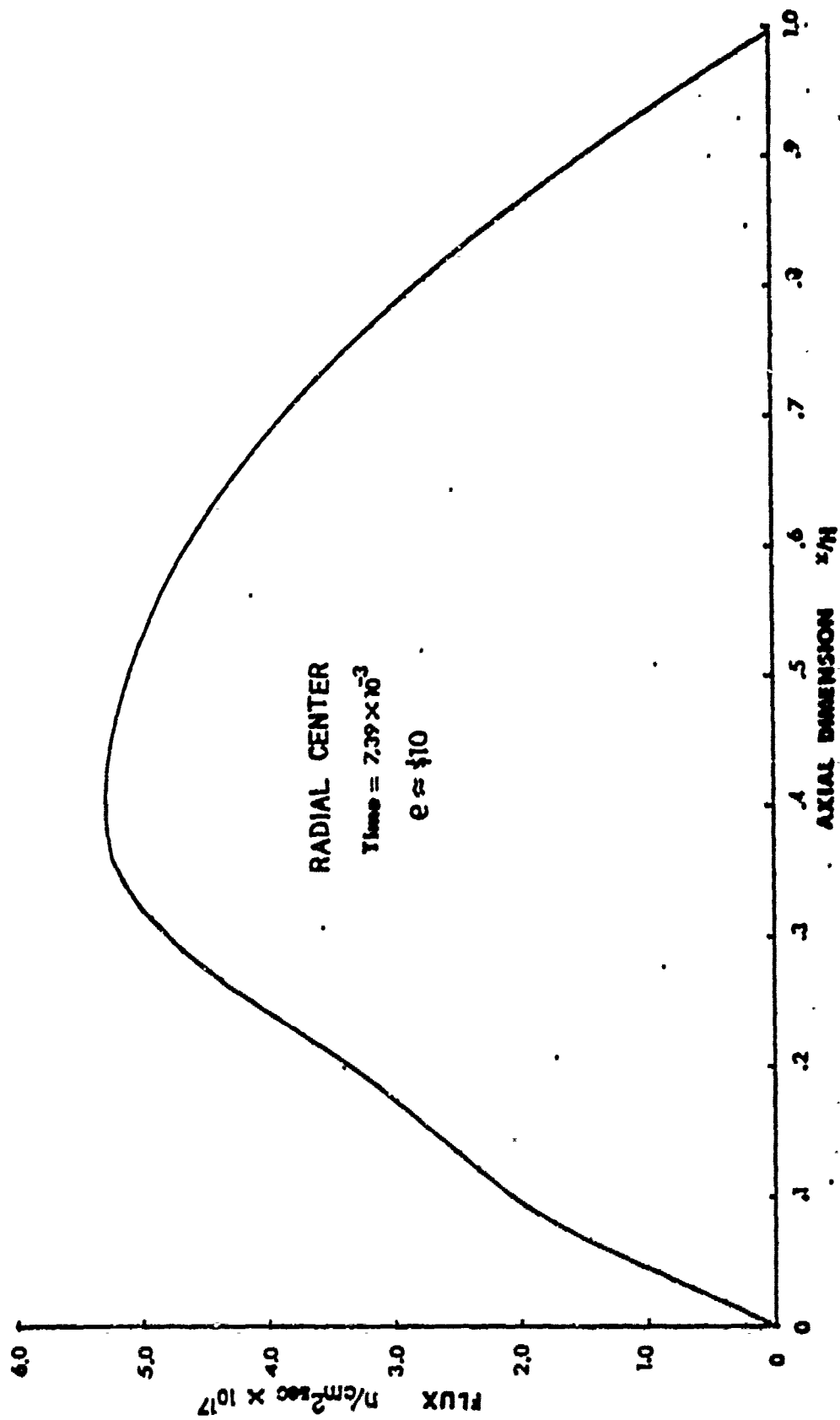


Figure 13. Axial Flux Profile

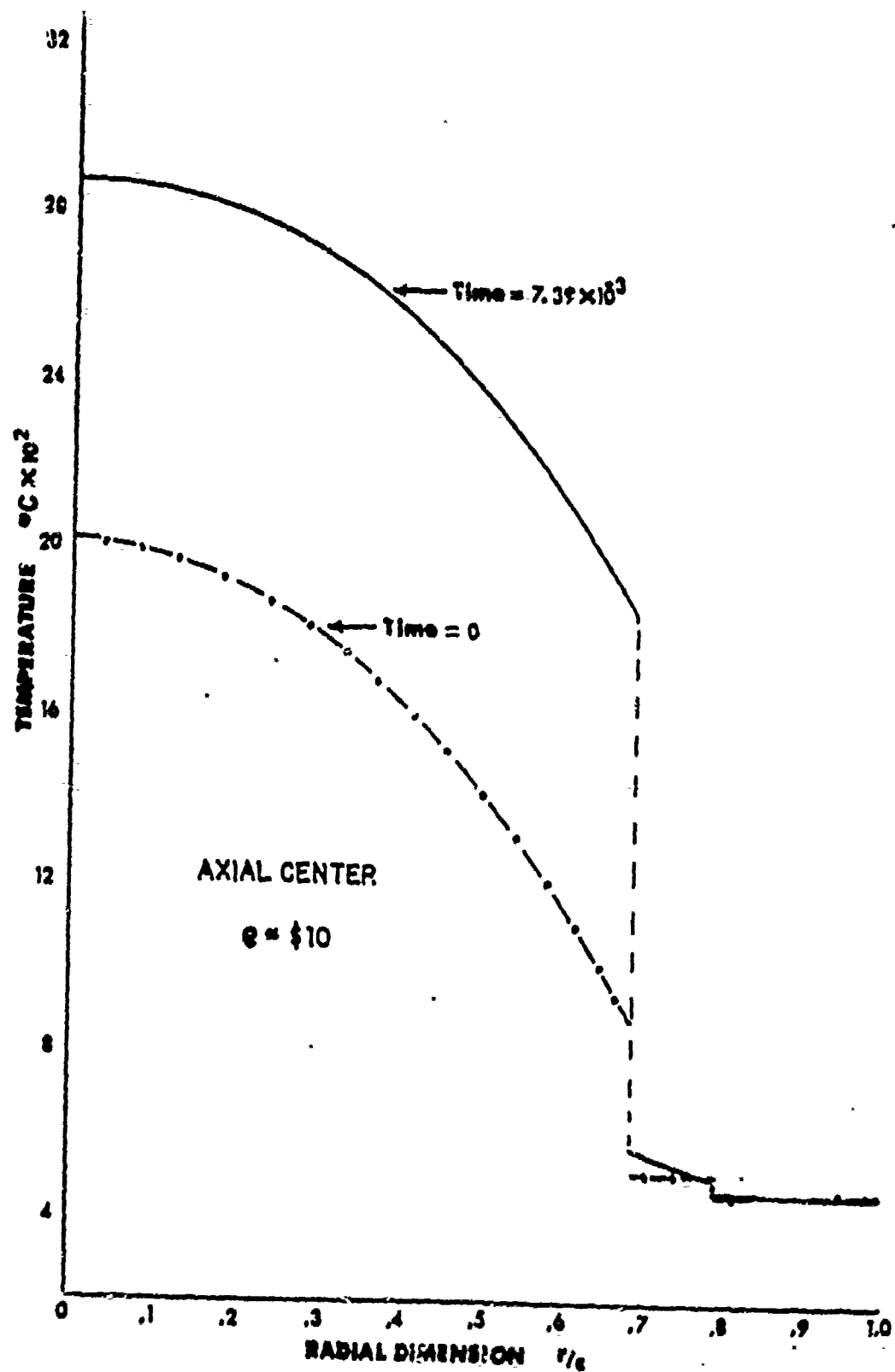


Figure 14. Radial Temperature Profile

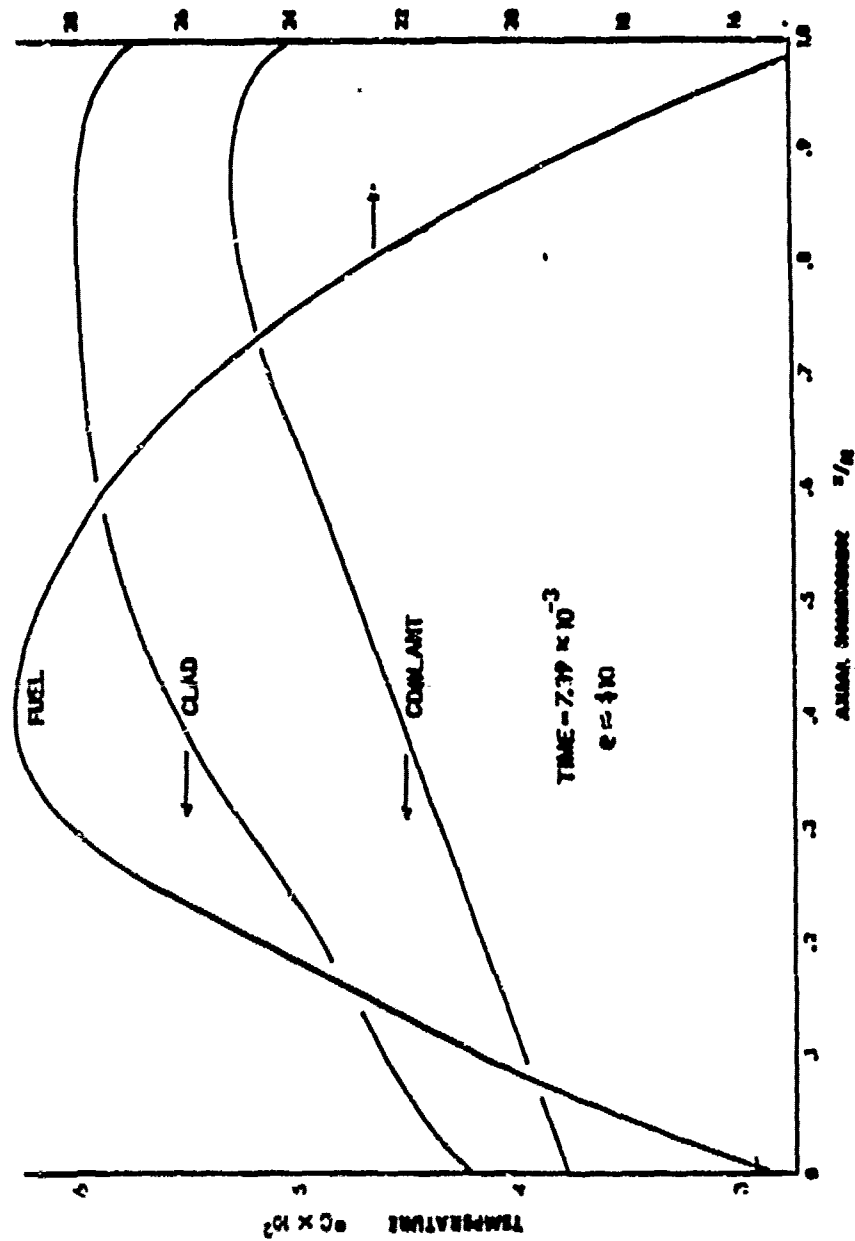


Figure 15. Axial Temperature Profile

Time did not permit investigation of other reactivity insertions. Other reactivity inputs may be investigated by students in the future.

This work does not represent a solution to the very complicated nuclear reactor problem. It does represent an application of a numerical technique which is relatively new to nuclear applications. Methods for implementing the finite element method have been discussed, and a computer code has been developed for the simplistic model considered.

## IX. RECOMMENDATIONS

For the model developed, perhaps the most important item to pursue is the critical fission cross section. A better determination of this value is necessary so that the reactivity insertion is more accurately known. Different test cases for the prompt critical and prompt subcritical reactor could then be conducted.

In further developing the model, more consideration should be given the gap heat transfer coefficient. As noted in the results, the value used appears to be too small. Sample problems for different gap heat transfer coefficients would give a better indication of the values to use.

Melting of the fuel during the transient would probably be the next major improvement on the model. With relatively few changes, the model could be adapted to allow melting element by element. This, too, would be an approximation but, still, an improvement to the model. Perhaps at the same time, a simplified model to take into consideration the fuel restructuring could be implemented.

Another improvement would be to consider reactivity feedbacks in addition to the Doppler feedback. Sodium voiding and fuel rod expansion are two of the more important feedback effects to consider.

On the numerical side, probably the most important thing to do would be to run the computer program on the

"H-compiler", which optimizes the program. However, on several runs using the H-compiler, erroneous results were obtained. With sufficient time, this could be corrected to allow use of the H-compiler. The use of the H-compiler results in a savings in computer time. The present program runs on a "G-compiler" and takes excessive amounts of computer time (two to four hours per run).

In addition to this, the optimum over-relaxation factor in the implicit Gear's method could be determined by trial-and-error.

Implementation of these recommendations should enhance the analysis and lead to a more efficient computer code.

# APPENDIX A DEVELOPMENT OF TRANSFORMATIONS

The Jacobian matrix [J] may be written (8) for two dimensions as

$$[J] = \begin{bmatrix} \sum_{i=1}^N N_{i,\xi} r_i & \sum_{i=1}^N N_{i,\xi} z_i \\ \sum_{i=1}^N N_{i,\eta} r_i & \sum_{i=1}^N N_{i,\eta} z_i \end{bmatrix} \quad (A1)$$

For a simple 2x2 matrix [A] the inverse is

$$[A] = \begin{bmatrix} a & b \\ c & d \end{bmatrix}$$

$$[A]^{-1} = \frac{1}{\det[A]} \begin{bmatrix} d & -b \\ -c & a \end{bmatrix}$$

Applying this fact to equation (A1) gives

$$[J]^{-1} = \frac{1}{\det[J]} \begin{bmatrix} \sum_{i=1}^N N_{i,\eta} z_i & - \sum_{i=1}^N N_{i,\xi} z_i \\ \sum_{i=1}^N N_{i,\eta} r_i & \sum_{i=1}^N N_{i,\xi} r_i \end{bmatrix} \quad (A2)$$

$$= \begin{bmatrix} J_{11}^* & J_{12}^* \\ J_{21}^* & J_{22}^* \end{bmatrix}$$

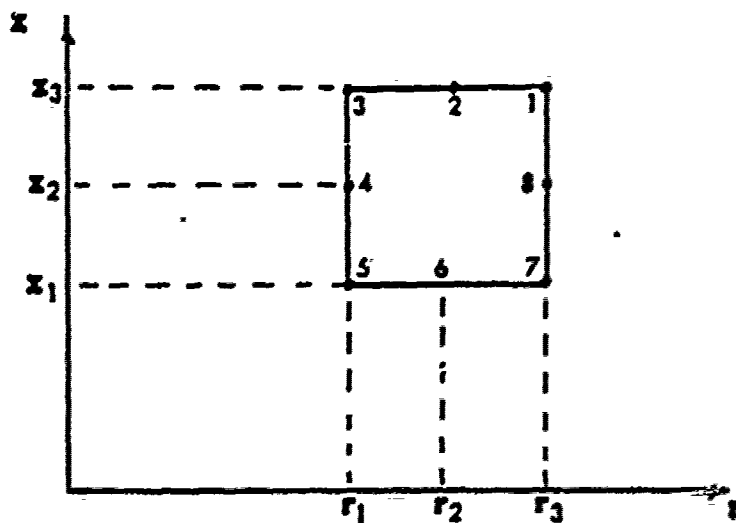
From matrix algebra

$$\det[J] = \sum_{i=1}^N N_{i,\xi} r_i \sum_{i=1}^N N_{i,\eta} z_i - \sum_{i=1}^N N_{i,\eta} r_i \sum_{i=1}^N N_{i,\xi} z_i \quad (A3)$$

The derivatives of the shape functions may be found from equations (38).

$$\begin{aligned} N_{1,\xi} &= \frac{1}{4}(1+\eta)(2\xi+\eta) & N_{1,\eta} &= \frac{1}{4}(1+\xi)(2\eta+\xi) \\ N_{2,\xi} &= -\xi(1-\eta) & N_{2,\eta} &= \frac{1}{2}(1-\xi^2) \\ N_{3,\xi} &= \frac{1}{4}(1+\eta)(2\xi-\eta) & N_{3,\eta} &= \frac{1}{4}(1-\xi)(2\eta-\xi) \\ N_{4,\xi} &= -\frac{1}{2}(1-\eta^2) & N_{4,\eta} &= -\eta(1-\xi) \\ N_{5,\xi} &= \frac{1}{4}(1-\eta)(2\xi+\eta) & N_{5,\eta} &= \frac{1}{4}(1-\xi)(2\eta+\xi) \\ N_{6,\xi} &= -\xi(1-\eta) & N_{6,\eta} &= -\frac{1}{2}(1-\xi^2) \\ N_{7,\xi} &= \frac{1}{4}(1-\eta)(2\xi-\eta) & N_{7,\eta} &= \frac{1}{4}(1+\xi)(2\eta-\xi) \\ N_{8,\xi} &= \frac{1}{2}(1-\eta^2) & N_{8,\eta} &= -\eta(1+\xi) \end{aligned} \quad (A4)$$

If one now considers an arbitrary element



with the midside nodes exactly at the midpoint (not a necessary criteria for the FEM) and substitutes into equation (A3),

the result is

$$\det[J] = \frac{(z_3 - z_1)(r_3 - r_1)}{4} = \frac{A^e}{4} \quad (A5)$$

Substituting into equation (A2) and using (A5) will yield

$$J_{11}^* = \frac{4}{A^e} \left[ \frac{1}{2}(z_3 - z_1) \right] = 2/r_3 - r_1, \quad (A6)$$

$$J_{12}^* = 0, \quad (A7)$$

$$J_{21}^* = 0, \quad (A8)$$

and  $J_{22}^* = \frac{4}{A^e} \left[ \frac{1}{2}(r_3 - r_1) \right] = 2/z_3 - z_1. \quad (A9)$

The inverse of the Jacobian matrix now becomes

$$[J]^{-1} = \begin{bmatrix} 2/r_3 - r_1 & 0 \\ 0 & 2/z_3 - z_1 \end{bmatrix} \quad (A10)$$

For integration along a line, the transformation used is

$$dz = \det[J'] d\eta \quad (A11)$$

in this case

$$\det[J'] = \sum_{i=1}^N N_{i,\eta} z_i \quad (A12)$$

Again considering the arbitrary element and substituting (A4) into (A12) will result in

$$\det[J'] = \frac{z_3 - z_1}{2} = \frac{L^e}{2} \quad (A13)$$

# APPENDIX B REDUCTION OF SECOND ORDER TERM

The second order term of the governing field equations may be reduced to first order by integration by parts. Consider, for example,

$$\int_r \int_z N_1 \left[ \frac{1}{r} \frac{\partial}{\partial r} \left( r D \frac{\partial \psi}{\partial r} \right) + \frac{\partial}{\partial z} \left( D \frac{\partial \psi}{\partial z} \right) \right] r dr dz \quad (B1)$$

which may be expanded as

$$\int_r \int_z \left[ N_1 r D \frac{\partial^2 \psi}{\partial r^2} + N_1 r \frac{\partial D}{\partial r} \frac{\partial \psi}{\partial r} + N_1 D \frac{\partial \psi}{\partial r} + N_1 r D \frac{\partial^2 \psi}{\partial z^2} + N_1 r \frac{\partial D}{\partial z} \frac{\partial \psi}{\partial z} \right] dr dz \quad (B2)$$

Integrating just the second order terms by parts will yield

$$\begin{aligned} \int_r \int_z N_1 D \frac{\partial^2 \psi}{\partial r^2} r dr dz &= \int_z \left[ N_1 r D \frac{\partial \psi}{\partial r} \right]_r dz \\ &\quad - \int_r \int_z \frac{\partial \psi}{\partial r} \left[ D N_1 + r N_1 \frac{\partial D}{\partial r} + r D \frac{\partial N_1}{\partial r} \right] dr dz \quad (B3) \end{aligned}$$

and

$$\int_r \int_z N_1 D \frac{\partial^2 \psi}{\partial z^2} r dr dz = \int_r \left[ N_1 D \frac{\partial \psi}{\partial z} \right]_z r dr - \int_r \int_z \frac{\partial \psi}{\partial z} \left[ \frac{\partial N_1}{\partial z} D + N_1 \frac{\partial D}{\partial z} \right] r dr dz \quad (B4)$$

Substituting the results of (B3) and (B4) into equation (B2) will give

$$\int_z \left[ N_1 r D \frac{\partial \psi}{\partial r} \right]_r dz + \int_r \left[ N_1 D \frac{\partial \psi}{\partial z} \right]_z r dr - \int_r \int_z D \left[ \frac{\partial N_1}{\partial r} \frac{\partial \psi}{\partial r} + \frac{\partial N_1}{\partial z} \frac{\partial \psi}{\partial z} \right] r dr dz \quad (B5)$$

## APPENDIX C

### LIST OF RELATIONS FOR MATERIAL THERMAL PROPERTIES

#### A. FUEL ( $UO_2$ )

1. Specific Heat, Ref. [19]

$$C_{pF} = [18.45 + 2.431 \times 10^{-3}T - 2.272 \times 10^{-5}T^2] / 270.07$$

[cal/gm °C]

$T$  - °C

2. Thermal Conductivity, Ref. [5]

$$Tk_F = [1 - 2.5(1 - \rho_{TD})] \times \left[ \frac{45.1}{135 + T} + 4.79 \times 10^{-13}T^3 \right] \times 0.239$$

[cal/cm sec °C]

$\rho_{TD}$  - percent theoretical density

$T$  - °K

#### B. CLAD (Stainless Steel)

Properties are assumed to be temperature independent, and average values from Ref. [5] were used for the clad properties.

#### C. COOLANT (Liquid Sodium)

1. Specific Heat, Ref. [5]

$$C_{pco} = 0.34574 - 0.79226 \times 10^{-4}T + 0.34086 \times 10^{-7}T^2$$

[cal/gm °C]

$T$  - °F

2. Density, Ref. [5]

$$\rho_{co} = [59.566 - 7.9504 \times 10^{-3}T - 0.2872 \times 10^{-6}T^2 + 0.05035 \times 10^{-9}T^3] \times 0.01601 \quad [\text{gm/cm}^3]$$

$T$  - °F

3. Thermal Conductivity, Ref. [5]

$$Tk_{co} = [54.306 - 1.878 \times 10^{-2}T + 2.0914 \times 10^{-6}T^2] \\ \times 4.134 \times 10^{-3} \quad [\text{cal/cm sec } ^\circ\text{C}]$$

$$T - ^\circ\text{F}$$

D. SURFACE HEAT-TRANSFER COEFFICIENT

$$h_{surf} = \frac{Tk_{co}}{De} [7.0 + 0.025 \left( \frac{De V_{co} \rho_{co} C_{pco}}{Tk_{co}} \right)^{0.8}] \\ [\text{BTU/hr ft}^2 ^\circ\text{F}]$$

$$Tk_{co} - [\text{BTU/hr ft } ^\circ\text{F}]$$

$$\rho_{co} - [\text{lbm/ft}^3]$$

$$V_{co} - [\text{ft/sec}]$$

$$C_{pco} - [\text{BTU/lbm } ^\circ\text{F}]$$

$$De - \text{equivalent diameter [ft]}$$

```

MAIN PROGRAM CALLS THE VARIOUS SUBROUTINES

1)FLICIT INTEGER*2(I-N)
INTEGER*4 NY,NL,MJSKE
REAL*8 SN,DESN,DXSN,WT,GP,STJ11,STJ22,DETJ,XW,XSN

THE FOLLOWING DIMENSION STATEMENTS MUST BE
CHANGED FOR EACH DIFFERENT PROBLEM CONSIDERED

CIPENSICN BIGH12(5525),BIGH3(5525),BIGH4(5525),BIGH5(5525),
1 BIGH(5525),NAME(5525)
CIPENSICN BIGF(350),R(350),Z(350),YIT(350),JA(350),JB(350),
1 ITYPE(350),NAME(26,350)
CIPENSICN Y(7,700),W(28000),NELCGA(11,66),NSTART(66),IBF(66)

AFFPROPRIATE DIMENSIONS ARE
BIGH12,BIGH3,BIGH4,BIGH5,BIGK,NAME-----JC
BIGF,R,Z,YIT,JA,JB,ITYPE-----NP
NAME(26,11),BY-----NP
NELCGA(11,66)-----NEL
NSTART,IBF-----NEL

Y,W AS REQUIRED BY FRANK'S SUBROUTINES BY THE ACDES
JC IS THE TOTAL NUMBER OF NODES
NP IS THE NUMBER OF LOCAL POINTS
NEL IS THE NUMBER OF ELEMENTS

ALL THE REST OF THE SUBROUTINES WILL HAVE THEIR DIMENSIONS
CHANGED THROUGH THE CALLING STATEMENTS SO THAT THE ABOVE
DIMENSIONS ARE THE ONLY ONES WHICH REQUIRE CHANGING

CIPENSICN DR(13)
CIPENSICN H12(8),H3(8,8),F(8)
CIPENSICN H4(8,8)
CIPENSICN GP(51),SN(8,25),DESN(8,25),DXSN(8,25),STJ11(25),XW(5)
CIPENSICN STJ22(25),XSN(5,5),WT(25)
CIPENSICN ADUM(3)
CIPENSICN XK1(8),XK2(8,8)
CCPMCN/CLAD/CCC,CPC,DENC,TKC,SIGAC,HGAP
CCPMCN/CCAN/ NP,NEL,JJC
CCPMCN/COOL/DCCO,SIGACC,VCO,HSURF
CCPMCN/FUEL/DCF,BIE,BETA,BETAI,CCLAMI,FFLUXC,AKINF,VEL,
1 SIGAF,SIGFF,SIGAB,SIGFB,DENF
CCPMCN/EP/ GP,NORC
CCPMCN/INP/DR,HEIGHT,NPR,NEZ,NFE
CCPMCN/JACINV/STJ11,STJ22,DETJ
CCPMCN/KIMAT/XK1,XK2
CCPMCN/MATRIX/H12,H3,F
CCPMCN/MTRXH4/H4
CCPMCN/REACT/RHGA,RFOB

```

```

CCMCON/SHAFUN/SN, DESN, DXSN
COMMON/WEIGHT/FF, RHG
FCRMAI(415,F10.5)
FCRMAI(0,9X,JSXF = ,15)
FCRMAI(8F10.5)
FCRMAI(0,8(8F15.6,/) )
1F RACIAL FUEL ELEMENTS IS,15,/,10X,NUMBER OF AXIAL FUEL ELEMENT
2S IS,15,/,10X,NUMBER OF RADIAL NODAL PCINTS IS,15,/,1CX,
3 FUEL ROD HEIGHT (CM) IS,F10.5)
FCRMAI(F10.5)
FCRMAI(0,14X,DCFF,10X,B,11X,E,5X,BETA,8X,BETA1,6X,
4C FORM,CCCLAMI,8X,NU,9X,KINF)
41 FCRMAI(0,9X,9E12.5)
42 FCRMAI(0,12X,FFLUXO,8X,VEL,8X,SIGAF,7X,SIGFF,7X,
43 SIGAB,7X,SIGAC,6X,SIGACC)
44 FCRMAI(0,14X,DCC,9X,CPC,8X,CENC,9X,TKC,3X,ECCC,
10X,VCO,8X,HSURF,8X,DENF)
FCRMAI(0,5X,RHC = RHCA + RHGR*1,/,6X,RHCA = ,F10.3,
1CX,RF0B = F10.3)
1 INPUT THE ORDER OF THE GAUSS QUADRATURE ---- 3,4, CR 5
INPUT THE NUMBER OF RADIAL ELEMENTS
INPUT THE NUMBER OF AXIAL ELEMENTS
INPUT THE NUMBER OF NODAL PCINTS IN THE RACIAL DIRECTION--2*NFE+7
REAL(5,10) NORO,AFE,NEZ,NPR,FEIGHT
WRITE(6,25) NORO,AFE,NEZ,NPR,FEIGHT
INPLT(5,30)(DR(1)) I = 1,NPR)
WRITE(6,35) (DR(1)) I = 1,NPR)
CALL GIANV(I,TYPE,NELCCN,NSTART,R,Z)
CALL CFCOMP(I,JP,JA,JB,NAME,NELCON,NSTART)
CALL INIT(1BP,NELCCN,R,Z,Y)
CALL SHAPE
45 I = 1,JC
EIGH12(I) = 0.0
EIGH13(I) = 0.0
EIGH15(I) = 0.0
EIGH(I) = 0.0
CCATINUE = 1,NP
DC50 I = C.0
EIGH(I) = C.0
SICRE YIT -- THE INITIAL TEMPERATURE DISTRIEUTION
YIT(I) = Y(I,I+NP)

```

CCCCC C

CC



```

SLROUTINE GINNY (ITYPE,NELCCN,ASTART,R,Z)
SUBROUTINE GINNY DEVELOPES THE SYSTEM MESH
IT ALLOWS FOR ONE OR TWO RADIAL ELEMENTS IN THE FUEL
AND ONE ELEMENT IN THE CLAD AND COCLANT
NEE SETS THE NUMBER OF RADIAL FUEL ELEMENTS
THE GENERATOR ALLOWS FOR ANY NUMBER OF AXIAL ELEMENTS DESIRED
NUMBER OF AXIAL ELEMENTS SET BY NEZ
THE GENERATOR WILL GIVE THE R AND Z DIMENSION FOR EACH NCCE
IT ALSO DEVELOPES THE CONNECTIVE MATRIX

ITYPE -- AN ARRAY USED TO INDICATE THE TYPE OF NCCE
0 -- FUEL NODE NOT IN AN INTERFACE ELEMENT
1 -- FUEL NODE IN AN INTERFACE ELEMENT
2 -- CLADDING NODE
3 -- COCLANT NODE
NELCON -- THE CONNECTIVE MATRIX
R -- RADIAL DIMENSION OF THE ITH NODE
Z -- AXIAL DIMENSION OF THE ITH NCCE

IAFLICIT INTEGER*2(I-N)
DIMENSION DR(13)
DIMENSION ITYPE(1)
DIMENSION NELCON(1,1)
DIMENSION NSTART(1)
DIMENSION R(1), Z(1)
COMMON/CCCN/ NP,NEL,JC
L1 = 0
L2 = 0
KK = 2*NFE + 1
MM = M + 4
NFE = N + 2
NEZ = NEZ*2
NACC = NEZ*NFE + 14
EZ = NEZ*HEIGHT/(2.0*EZ)
ZC 100 I = 1,NPZ
Y = 1
IF (KK.EQ. 1) GO TO 80
L1 = L1 + 1
NSTART(L1) = NP + 1
L2 = 70
J = 1,NPR
NFE = NP + 1
Z(NP) = Z1 + T
R(NP) = R(1)

```

99



[illegible]

```

SLROUTINE UPCOMP (IBP,JA,JB,NAME,NAME,NELCCN,NSTART)
SLROUTINE CFCOMP CALCULATES THE NAME ARRAY,
THE JA ARRAY, AND THE JB ARRAY WHICH
ARE USED IN THE OPTIMUM COMPACTING SCHEME

IBP -- AN ARRAY USED TO STORE THE FUEL-CLAC INTERFACE NODES
JA -- AN ARRAY WHICH INDICATES THE NUMBER OF NODES CONTRIBUTING
TO THE ITH NODE
JB -- THE POINTER ARRAY WHICH INDICATES WHERE THE ITH
EQUATION BEGINS IN NAME
NAME -- TWC-DIMENSIONAL ARRAY USED TO DEVELOP NAME
NAME -- THE ARRAY USED FOR THE OPTIMUM COMPACTING SCHEME
NELCCN -- CONNECTIVE MATRIX
NSTART -- AN ARRAY USED TO STORE CENTERLINE ACCAL FCINTS

IMPLICIT INTEGER*2(I-N)
DIMENSION DR(13)
DIMENSION IBP(1)
DIMENSION JA(1), JB(1), NAME(1), NAME(26,1)
DIMENSION NELCCN(1,1)
DIMENSION NSTART(1)
COMMON/BCUND/ NCCUNT
COMMON/CCNK/ NP,NEL,JC
COMMON/INP/DR,HEIGHT,NPR,NEZ,NFE
NELDOF = 8
WRITE (6,10) NP,NEL,NELDOF
FORMAT(/2X,15,5X,'NUMEL=',15,5X,'NELDOF=',15)
1C OC 42 I = 1, NP
JA(1) = 1
2C CONTINUE = 1,NP
CC 60 I = 1,26
CC 50 J = 1,26
NAME(J,I) = 0
3C CONTINUE
CC 65 I = 1,NP
NAME(I,1) = 1
4C CONTINUE
CC 100 I = 1,NEL
CC 50 J = 1,NELDOF
J = NELCCN(J,I)
CC 80 K = 1,NELDOF
IF (K.EQ.J) GC TO 80
KH = NELCCA(K,I)
JA(JJ) = JA(JJ)+1
JJA = JA(JJ)

```

```

7C 7C L=2,JAA
JJL=NAME(L,JJ) JA(JJ)=JA(JJ)-1
IF(JJL.EQ.KK) GO TO 80
IF(JJL.EQ.0) NAME(JAA,JJ)=KK
CCCONTINUE
EC
SC
1CC
C *** TC ACCUNT FOR THE INTERFACE CONCITIONS ***
ACCLNT = 3
IEP(1) = AF - 6
IEP(2) = NFE + 1
NAM = NFE + 7
NAM = 2+NFE
WRITE(4,1000) (NSTART(I),I=1,NEZ)
FCPWAT(10X,1115)
DO 300 I=1,NEZ
  IEF(NCUNT) = NSTART(I) + NUH
  IEF(I.EQ.NEZ) GC TO 300
  IEP(NCUNT + 1) = IEP(NCUNT) + AN
  NCCLNT = NCUNT + 2
  CCCONTINUE
  KK = 1
  WRITE(6,1000) (IBP(I),I=1,ACCUNT)
  CC 400 I = 1,ACCUNT
  JJ = IBP(I)
  IF (KK.EQ.0) GO TO 350
  IF (I.EQ.ACCUNT) GO TO 350
  IF (I.EQ.1) GO TO 350
  CC 325 J=1,13
  NAME(J+13,JJ) = NAME(J,JJ+1)
  NAME(J+13,JJ+1) = NAME(J,JJ)
  NAME(J+13,JJ+3) = NAME(J,JJ+4)
  NAME(J+13,JJ+4) = NAME(J,JJ+3)
  CCCONTINUE
  JA(JJ) = JA(JJ) + 13
  JA(JJ+1) = JA(JJ+1) + 13
  JA(JJ+3) = JA(JJ+3) + 13
  JA(JJ+4) = JA(JJ+4) + 13
  KK = 0
  GC TO 400
  CC 35C
  KK = 1
  J = 1,8
  CC 375 J=1,8
  NAME(J+8,JJ+1) = NAME(J,JJ+1)
  NAME(J+8,JJ+1) = NAME(J,JJ)

```

```

IF (I1.EQ.1).OR.(I1.EQ.NEZ1)) JJ = JJ + 1
NAME {J+8,JJ+2} = NAME {J,JJ+3}
NAME {J+8,JJ+3} = NAME {J,JJ+2}
IF (I1.EQ.1).OR.(I1.EQ.NEZ1)) JJ = JJ - 1
CCATINUE = JA (JJ) + 8
JA (JJ+1) = JA (JJ+1) + 8
IF (I1.EQ.1).OR.(I1.EQ.NEZ1)) JJ = JJ + 1
JA (JJ+2) = JA (JJ+2) + 8
JA (JJ+3) = JA (JJ+3) + 8
IF (I1.EQ.1) KK = C
CCATINUE

4CC
C***
C***

JE(I)=1
JC=C
CCZCO I = 1,NP
JA=JA(I)
JE(I+1)=JB(I)+JA(I)
JC=JC+JA(I)
CCATINUE
WRITE(7,5) {JA(I),I=1,NP},JC
WFORMAT(16,15)
WFORMAT(29,4)
WFORMAT(215) JC
WFORMAT(22X) JC=,I10)
DCZ50 I = 1,NP
JA=JA(I)
EL=JB(I)
JC=JB(I)+J-1
JA=JB(I)+J-1
NAME(JJ)=NAME(J,I)
CCATINUE
WRITE(7,5) (NAME(I),I=1,JC)
C
RETURN
END

```





```

C** TC REMAIN CONSTANT (FLAT FLUX ASSUMPTION)
C** AXIALLY THE FLUX ASSUMED TO VARY AS THE
C** SHAPE OF THE SINE FUNCTION
1001 REAC(S,1001) FMAX
      FCFMAT (F10.5)
      CC 700 P = 1,NP
      X = Z(M)*3.1415926/HEIGHT
      Y(1,M) = SIN(X) FMAX*S
700 CC CONTINUE
      WRITE (6,1050)
1050 FCFMAT (1,1,9X, 'NODAL',5X, 'INITIAL',3X, 'INITIAL',/,16X, 'POINT',5X,
      1 FLUX',6X, 'TEMP',//)
      CC 800 I = 1,NP
      WRITE (6,1100) I, Y(1,I),Y(1,I+NP)
800 CC CONTINUE
1100 FCFMAT (9X,14,E13.3,F10.3)
      RETURN
      END

```



109



```

140      XK2(5,5) = XK1(2,2)
      CC 160 I = 1,3
      CC 160 J = 2,3
      XK1(I,J) = 0.0
160      CC CONTINUE I = 1,8
      CC 180 J = 1,8
      XX I(J,I) = XK1(I,J)
      XX J(J,I) = XK2(I,J)
      CC CONTINUE
180      CC RETURN
      CC ENCL

```

```

SUBROUTINE JACOB (M,NELCON,R,Z)
JACOB EVALUATES THE JACOBIAN MATRIX,
ITS INVERSE, AND ITS DETERMINATE
FOR EACH OF THE GAUSS POINTS
M IS NUMBER OF THE ELEMENT UNDER CONSIDERATION
IMPLICIT INTEGER*2(I-N)
REAL*8 CR,DZ,DETJ,XJ11,XJ22,STJ11,STJ22
COMMON GP(5)
COMMON NELCON(11,1)
COMMON R(1),Z(1)
COMMON STJ11(25),STJ22(25)
COMMON GP/ GP,NORD
COMMON JACINV/ STJ11,STJ22,DETJ
COMMON CCN/ NP,NEL,JC
CALCULATE THE DETERMINATE OF THE JACOBIAN
L = NELCON(1,M)
KF = NELCON(3,M)
ZF = R(L) - R(KF)
ZF = Z(K) - Z(L)
DETJ = C*25*DR*DZ
XJ11 = 2*G/DR
XJ22 = 2*G/DZ
CC = 100*I = 1,NQ
CALCULATE THE INVERSE OF THE JACOBIAN MATRIX
STJ11(I) = XJ11
STJ22(I) = XJ22
RETURN
END

```

CCCCCCCC

C

C

ICC



```

      ZZZ = ZZZ + XXX*YYY*RR*WT(X)
      IF (J.NE.1) GO TO 60
      IF ((LE.EQ.2) .OR. (LE.EQ.3)) GO TO 60
      FF = FF + XXX*RR*WV(K)
      6C CCATINUE
      F12(I,J) = (ZX + ZZ)*DETJ
      F13(I,J) = ZZZ*DETJ
      F14(I,J) = ZY*DETJ
      F11(I,J) = FF*DETJ
      8C CCATINUE
      100 CCATINUE
      100 RETURN
      ENAC

```



```

CC 45 II = 118
LL = AELCCN(II,H)
WRITE(6,888) SN(II,K),Y(1,L3+NF),YIY(LL)
FCRMAT(3X,3G18.4,/)
CCATINUE = AELGG(TAUL)
TT = TAUL
HH = HH + XXX*VVY*RR*WT(K)*TT
CCATINUE = HH*DETJ
H4(I)INUE
ICC CCATINUE
FETURN
END
888
50
60
EC
ICC

```

```

CCCCCCCCCCCC
SLEFCUTINE SYSH12 (M,BIGH12,BIGH3,BIGH5,BIGF,JA,JB,NAME,NELCGN)
SLEFCUTINE SYSH12 DEVELOPES THE SYSTEM MATRICES
BIGH12, BIGH3, BIGH5, AND BIGF FROM THE ELEMENT
F12, F3, H3, H4, AND F MATRICES, RESPECTIVELY
BIGH12 -- SYSTEM MATRIX FOR THE LAPLACIAN TERM
BIGH3 -- D NI/OR X D NJ/DR + D A1/DZ X C A1/CZ
BIGH5 -- SYSTEM MATRIX FOR THE NI X NJ TERM
BIGF -- SYSTEM MATRIX FOR THE NI X D NJ/CZ TERM
IFLEICIT7 INTEGER*2(I=ND
DIMENSION BIGH12(1), BIGH3(1), BIGH5(1)
DIMENSION BIGHF(1)
DIMENSION H12(8,8), H3(8,8), F(8)
DIMENSION H4(8,8), JB(1), NAME(1)
DIMENSION NELCON(11,1)
DIMENSION COAN/ NP, NEL, JC
DIMENSION MATR1X/ H12, F3, F
DIMENSION MATR4/ H4
DOCC 120 K=1,8
KKK = NELCGN(K,M)
KKK = JA(KK)
LLL = JB(KK) - 1
CC 100 I=1,8
II = NELCGN(I,M)
CC 60 LL = 1, KKK
LLL = LLL + L
KKK = NAME(LL)
IF (II.EQ. KKK) GC TO 80
CCATINUE
BIGH12(LL) = BIGH12(LL) + H12(K,I)
BIGH3(LL) = BIGH3(LL) + H3(K,I)
BIGH5(LL) = BIGH5(LL) + H4(K,I)
CCATINUE
BIGF(KK) = BIGF(KK) + F(K)
CCATINUE
END
60 EC
100
120

```

```

CSCCSCC
SLEROUTINE: SYSH4 (M,JA,JB,NAME,NELCN,BIGH4)
SYSH4 DEVELOPES THE SYSTEM H4 MATRIX
FROM THE ELEMENT H4 MATRICES

BIGH4 --- SYSTEM MATRIX FOR THE TEMPERATURE DEPENDENT MATRIX
NATURAL LCG(I,TO) X NI X AJ
INTEGER*2(I-N)
IPLICIT IN BIGH4(I)
DIMENSION H4(8), JB(1), NAME(1)
DIMENSION JA(1), NELCN(11,1)
DIMENSION CCMN/CCMN/ NP, NEL, JC
CCMNCA/MT = 1, 8
CC 120 KCCN(K, H)
CC KKK = NELCN(K, H)
KKK = JA(KK)
LLL = JB(KK) - 1
CC 100 I = 1, 8
II = NELCN(I, H)
CC CCL = 1, KKK
LLL = LLL + I
KKK = NAME(LL)
IF (II.EQ. KKK) GC TO 80
CCATINUE
BIGH4(LL) = BIGH4(LL) + H4(K, 2)
CC CCATINUE
100 CCATINUE
120 RETRN
END

```

```

CCCCC
SUBROUTINE SYSK12 (M,JA,JB,NAME,NELCON,R,Z,BIGX)
  SYSK DEVELOPES THE SYSTEM K MATRIX
  FROM THE ELEMENT MATRICES
  BIGX -- SYSTEM MATRIX FOR THE THERMAL INTERFACE CCNCTIONS

  IMPLICIT INTEGER*2(I-N)
  DIMENSION BIGK(1), JB(1), NAME(1)
  DIMENSION NDUM(3), Z(1), XK1(N,M), XK2(8,8)
  DIMENSION R(1), Z(1), XK1(N,M), XK2(8,8)
  DIMENSION CCAN/CCAN/NP, NEL, JC
  COMMON/KIMAT/XK1,XK2
  NDUM(1) = 1
  NDUM(2) = 7
  NDUM(3) = 8
  NAME = NELCON(11,M)
  GO TO (1,2,3), MH
  DO 120 K=1,3
    NAME = NDUM(K)
    KK = NELCON(N,M)
    KKK = JAKK)/2
    LLL = JB(KK) - 1
    DO 100 I=1,3
      AA = NDUM(I)
      JJ = II + 1
      LL = 0
      DO 80 L=1, KKK
        LLL = LLL + KKK
        KKK = NAME(LL)
        IF (II - NE - KKK) GC TO 60
        BIGK(LL) = XK1(N,M)
        N1 = 1
        IF (JJ - NE - KKS) GC TO 70
        BIGK(LS) = BIGK(LS) - XK1(N,M)
        N2 = 1
        IF (N1 - EQ. 1) -AND. (N2 - EQ. 1) GO TO 100
        CC CONTINUE
        CC CONTINUE
        CC CONTINUE
        IF (MH - EQ. 1) GO TO 4

```

```

2 JE = NELCCN(3,M)
  CC 220 K = 3.5
  KKK = NELCCA(K,M)
  LLL = JA(KKK)/2 - 1
  CC 200 I = 3.5
  I I = I I + 1
  I I = 0
  N2 = 180 L = 1, KKK
  LLS = LLL + L
  KKK = LLL + KKK
  KKK = NAME(LLS)
  IF(I I .NE. KKK) GC TO 160
  BIGK(LL) = BIGK(LL) + XK2(K,I)
  N1 = I
  IF(I I .NE. KKK) GC TO 170
  BIGK(LS) = BIGK(LS) - XK2(K,I)
  N2 = I
  IF((N1 .EQ. 1) .AND. (N2 .EQ. 1)) GO TO 200
  CC CONTINUE
  CC CONTINUE
  CC RETURN
  160
  170
  180
  200
  220 4 END

```





```

24C CYII = CYII + (TKF*DBLE(BIGH12(J)) + RA*CONST*CBLE(BIGK(J))) *
2  - (E*SIGFF*DBLE(BIGH3(J))*Y(1,NA)
2 IF(K.EC.0) GO TO 250
J = J + JAA/2
AP = NAME(JJ)
DVI = CYI + (DCC*DBLE(BIGH12(JJ)) + SIGAC*DBLE(BIGH3(JJ))*Y(1,NM)
1 + VINV*HINV*DBLE(BIGH3(JJ))*Y(2,AP)
25C CCATINUE
CC TC 550

CETERMINE THE TYPE OF NODE BEING CONSIDERED
K = 1 NCDE NOT CN AN INTERFACE
K = 2 NCDE ON THE FUEL-CLAD INTERFACE
K = 3 NCDE ON THE CLAD-COOLANT INTERFACE

3CC K = 1
KCCC = C
DCC 320 IB = 1, NCCLNT
LEF = IEP(IB) + 1
IF(LBP.EC.1) GO TO 325
APF = LBP + 2
IF(NOCC.EC.C) GO TO 305
KCCF = AP - 1
KCCC = C
GCL TO 310
3CC ACCO = 1 EQ. 1) GG TC 33C
31C IF(LBP.EC.1) GO TO 33C
32C CCATINUE
22C K = 2
33C K = 3
34C CC 380 J = JBB, JAB
AP = NAME(J)
AP = AA + AP
IF(K.EC.2) GO TC 360
CYI = DVI + (DCC*DBLE(BIGH12(J)) + SIGAC*DBLE(BIGH3(J)) *Y(1,AA)
1 + VINV*HINV*DBLE(BIGH3(J))*Y(2,AA)
36C FCAF = (1000.0 + 247.9*CCO5(3.14159*(Z(NN)*H(C-0.01818)))*1.356E-4
FCAF = FCAF
IF(K.EC.3) H = FCAF
IF(K.EC.3) H = FCAF
RA = R(AN)
CYII = CYII + (TKC*DBLE(BIGH12(J)) + RA*F*Z)*CBLE(BIGK(J)) *
1Y(1,NA) + DENC*PC*DBLE(BIGH3(J))*HINV*Y(2,NA)
IF(K.EC.3) GO TO 380
J = J + JAA/2
AP = NAME(JJ)

```



C\*\*

APF = AP + 1  
AP = NPF\*2  
AP = NPF - NN  
CC 600 I = NN, NP  
CY(I) = 0.0  
CCCONTINUE

600

C\*\*

C\*\*

C

C

C\*\*

C\*\*

TC ACCOUNT FOR THE TEMP BOUNDARY CONDITIONS  
(CCASTANT COOLANT INLET TEMPERATURES)

AP = AP - 2  
CC 700 I = NN, NP  
CY(I+NP) = 0.0  
CCCONTINUE  
RETURN  
END

700

C

```

C***
C***
C***
C
      SLROUTINE FUNC(T,F,INV)
      CALCULATES TIME DEPERCENT FUNCTIONALS
      FOR THIS ANALYSIS DELAYED NEUTRON GROUPS
      TAKEN TO BE ONE AVERAGED GROUP
      CCMCN/FUEL/DCF,B,E,BETA,BETAI,DCLAMI,FFLUXC,AKINF,VEL,
      1 SIGAF,SIGFF,SIGAB,SIGFB,DENF
      CCMCN/REACT/RHOA,RHCB
      CCMCN/REACT/F,G,RHPC
      DATA ECLE/I,O,I,IGLC/C,O/I FI/O.C/
      CALCULATE REACTIVITY INPUT
      RHCB = RHOA + RHOB*I
      RHCLD = RHCA + RHCB*TOLC
      CALCULATE THE G FUNCTION
      CII = BETAI*AKINF+SIGAF*FFLUXO/DCLAMI
      X) = DCLAMI*T
      EE = EXP(X)
      EE = EXP(-X)
      G = CII*DCLAMI*EE
      CALCULATE THE F FUNCTION
      CC = DCLAMI*BETAI*EE
      CC = AKINF + RHO
      CCCLD = AKINF + RHCLD
      FI = FI + 0.5*(EOLD*CCOLD + EX*CC)/FINV
      F = C*FI
      TCLO = F
      ECLE = EX
      RETURN
      ENC
C***
C**
C**
C***

```

```

SUBROUTINE JACMAT (Y,YL,T,HINV,A2,A,NY,EPS,Y,F1,P,BIGH12,BIGH3,
1 EIGH4,BIGH5,BIGK,IBP,ITYPE,JA,JB,NAME,NELCCN,R,Z)

```

CCCCC

SUBROUTINE JACMAT CALCULATES THE JACOBIAN MATRIX OF THE  
 FLUX JACOBIAN STORED IN THE FIRST JC ELEMENTS OF THE  
 PA ARRAY AND THE TEMPERATURE JACOBIAN STORED IN  
 THE SECOND JC ELEMENTS OF THE PA ARRAY

```

1 IFLGICIT INTEGER*2(I-N)
  IATEGERICIT 4 NINHY12(1), BIGH3(1), BIGH5(1)
  DIMENSION BIGH4(1)
  DIMENSION BIGK(1)
  DIMENSION IBP(13), ITYPE(1)
  DIMENSION JA(1), JB(1), NAME(1)
  DIMENSION NELCCN(1,1), Z(1)
  DIMENSION Y(7,1), DY(1), PW(1)
  DIMENSION RCUND/ NCGUAT
  COMMON/CLAD/ DCC,CPC,DENC,TKC,SIGAC,HGAP
  COMMON/CLAN/ NP,NELCCN
  COMMON/CCOL/ DCCO,SIGACC,VCO,PSURF
  COMMON/CFUEL/ DCCF1,BE,BETA,BETAI,DCLAMI,FFLU... INF,VEL,
  COMMON/CFI/ SIGFF1,SIGAB,SIGEB,DENF
  COMMON/IMP/ DR,HEI,IGHT,NPR,NEZ,NFE
  COMMON/TIME/ F,G,RMC
  A1 = -A2*HINV
  Z1 = Z(1) - Z(1BP(1))
  VIAV = 1.0/VEL
  B1GFF = 1.0 - BETA
  SIGAFF = SIGFF1
  SIGAST1 = SIGAFF*B1 - 1.0
  SIGAST2 = SIGAFF*B1*NHO
  TC = 0.58
  PMCD = 1.0/(0.55*+EIGHT)
  CC500 = 1.0
  JAA = JA(1)
  JJB = JB(1)
  JAE = JAA/2
  JAZ = JAE + JJB
  IT = ITYPE(1) + 1
  GC TC (100,200,300,400),IT
  CC 150 JJB,JAB
  ANA = NAME(J) + NP
  PA(J) = DCCF*BIGH12(J) - ((CONST1+F)*SIGAF+CCNST2-AH*VINV)*BIGH3(J)

```

10C



```

IF(LBP, EC, I) GC TC 325
NEF = LBP + 2
IF (ACCC - EQ, 0) GC TO 305
NEF = NEF - I
ACCC = C
GC TO 310
ACCC = 1
IF(NEP, EQ, I) GO TO 330
305 CCATINUE
GC TO 340
325 K = 2
GC TO 340
330 K = 3
CC 380 J = JBB, JAB
NA = NAME(J)
NA = NAME(J) + NP
RF = R(AN)
PA(J) = 0.0
IF(K, EC, 2) GO TO 360
PA(J) = CC*BIGH12(J) + (SIGAC + AH*VINV)*BIGH3(J)
F-GAP = (1000.0 + 247.0*COS(3.14159*(Z(INN)*MCC-C*B1818)))*1.356E-4
360 F = HGAF
IF(K, EC, 3) H = HSURF
PA(J+JC) = TKC*BIGH12(J)+RA*H*Z1*EIGK(J)+AH*CEMC*CFC*BIGH3(J)
IF(K, NE, 3) GO TO 380
IF(J, LT, JA3) GC TC 380
J = JAB + J - JA3 + 1
PA(J) = CC*CO*BIGH12(J) + (SIGACC + AH*VINV)*BIGH3(J)
IF(J, NE, JA3) GC TC 380
PA(JBB) = PA(JBB) + PA(J)
PA(J) = 0.0
CCATINUE
380 IF(K, NE, 2) GO TO 500
PA(JBB) = 1.0
PA(JA3) = -1.0
GC TO 500
380
CCCCC
DETERMINE THE TYPE CF NCDE BEING CONSIDERED
K = 1
K = 2
NCDE NOT ON CLAD-COOLANT INTERFACE
NCDE ON THE CLAD-COOLANT INTERFACE
400 K = 1
ACCC = C
DC 420 IB = 1, NCGLNT
LEF = IEP(18) + 4
IF(ACCD, EC, 0) GC TO 410
LEF = LBP - 1
ACCC = C

```

```

410 GC TO 415
411 ACCE = 1
412 IF (UBP - EC - 1) GG TO 425
420 CC CONTINUE
421 GC TC 420
422 K = 2
423 CC 48C J = JBB, JAD
424 AA = AAPE(J)
425 AA = AAPE(J) + NP
426 PA(J) = 0.0
427 IF (K - EC - 2) GO TO 450
428 PA(J) = R(NN)
429 TCF = 1.8 * Y(1, NN) + 32.0
430 TKCO = (54.306 - 1.878E-2 * TCF + 2.0914E-5 * TCF**2) * 4.134E-3
431 CECC = C.34574 - 0.79222E-4 * TDF + C.34086E-7 * TCF**2
432 DEACC = C.155566 - 7.9504E-3 * TDF - 0.2872E-6 * TDF**2 +
1 C.66C35E-9 * TDF**3) * 0.016C1
433 A = DEACC * CPCO
434 PA(J+JC) = TKCO * BIGH12(J) + VCO * BIGH5(J) + AA * BIGH3(J)
435 1 + RB * HSURF * Z1 * BIGH(J)
436 CC CONTINUE
437 IF (K - AE - 2) GO TO 500
438 PA(JBB) = 1.0
439 PA(JA3) = -1.0
440 CC CONTINUE
500 C**
501 C**
502 C**
503 C**
504 C**
505 C**
506 C**
507 C**
508 C**
509 C**
510 C**
511 C**
512 C**
513 C**
514 C**
515 C**
516 C**
517 C**
518 C**
519 C**
520 C**
521 C**
522 C**
523 C**
524 C**
525 C**
526 C**
527 C**
528 C**
529 C**
530 C**
531 C**
532 C**
533 C**
534 C**
535 C**
536 C**
537 C**
538 C**
539 C**
540 C**
541 C**
542 C**
543 C**
544 C**
545 C**
546 C**
547 C**
548 C**
549 C**
550 C**
551 C**
552 C**
553 C**
554 C**
555 C**
556 C**
557 C**
558 C**
559 C**
560 C**
561 C**
562 C**
563 C**
564 C**
565 C**
566 C**
567 C**
568 C**
569 C**
570 C**
571 C**
572 C**
573 C**
574 C**
575 C**
576 C**
577 C**
578 C**
579 C**
580 C**
581 C**
582 C**
583 C**
584 C**
585 C**
586 C**
587 C**
588 C**
589 C**
590 C**
591 C**
592 C**
593 C**
594 C**
595 C**
596 C**
597 C**
598 C**
599 C**
600 C**
601 C**
602 C**
603 C**
604 C**
605 C**
606 C**
607 C**
608 C**
609 C**
610 C**
611 C**
612 C**
613 C**
614 C**
615 C**
616 C**
617 C**
618 C**
619 C**
620 C**
621 C**
622 C**
623 C**
624 C**
625 C**
626 C**
627 C**
628 C**
629 C**
630 C**
631 C**
632 C**
633 C**
634 C**
635 C**
636 C**
637 C**
638 C**
639 C**
640 C**
641 C**
642 C**
643 C**
644 C**
645 C**
646 C**
647 C**
648 C**
649 C**
650 C**
651 C**
652 C**
653 C**
654 C**
655 C**
656 C**
657 C**
658 C**
659 C**
660 C**
661 C**
662 C**
663 C**
664 C**
665 C**
666 C**
667 C**
668 C**
669 C**
670 C**
671 C**
672 C**
673 C**
674 C**
675 C**
676 C**
677 C**
678 C**
679 C**
680 C**
681 C**
682 C**
683 C**
684 C**
685 C**
686 C**
687 C**
688 C**
689 C**
690 C**
691 C**
692 C**
693 C**
694 C**
695 C**
696 C**
697 C**
698 C**
699 C**
700 C**
701 C**
702 C**
703 C**
704 C**
705 C**
706 C**
707 C**
708 C**
709 C**
710 C**
711 C**
712 C**
713 C**
714 C**
715 C**
716 C**
717 C**
718 C**
719 C**
720 C**
721 C**
722 C**
723 C**
724 C**
725 C**
726 C**
727 C**
728 C**
729 C**
730 C**
731 C**
732 C**
733 C**
734 C**
735 C**
736 C**
737 C**
738 C**
739 C**
740 C**
741 C**
742 C**
743 C**
744 C**
745 C**
746 C**
747 C**
748 C**
749 C**
750 C**
751 C**
752 C**
753 C**
754 C**
755 C**
756 C**
757 C**
758 C**
759 C**
760 C**
761 C**
762 C**
763 C**
764 C**
765 C**
766 C**
767 C**
768 C**
769 C**
770 C**
771 C**
772 C**
773 C**
774 C**
775 C**
776 C**
777 C**
778 C**
779 C**
780 C**
781 C**
782 C**
783 C**
784 C**
785 C**
786 C**
787 C**
788 C**
789 C**
790 C**
791 C**
792 C**
793 C**
794 C**
795 C**
796 C**
797 C**
798 C**
799 C**
800 C**
801 C**
802 C**
803 C**
804 C**
805 C**
806 C**
807 C**
808 C**
809 C**
810 C**
811 C**
812 C**
813 C**
814 C**
815 C**
816 C**
817 C**
818 C**
819 C**
820 C**
821 C**
822 C**
823 C**
824 C**
825 C**
826 C**
827 C**
828 C**
829 C**
830 C**
831 C**
832 C**
833 C**
834 C**
835 C**
836 C**
837 C**
838 C**
839 C**
840 C**
841 C**
842 C**
843 C**
844 C**
845 C**
846 C**
847 C**
848 C**
849 C**
850 C**
851 C**
852 C**
853 C**
854 C**
855 C**
856 C**
857 C**
858 C**
859 C**
860 C**
861 C**
862 C**
863 C**
864 C**
865 C**
866 C**
867 C**
868 C**
869 C**
870 C**
871 C**
872 C**
873 C**
874 C**
875 C**
876 C**
877 C**
878 C**
879 C**
880 C**
881 C**
882 C**
883 C**
884 C**
885 C**
886 C**
887 C**
888 C**
889 C**
890 C**
891 C**
892 C**
893 C**
894 C**
895 C**
896 C**
897 C**
898 C**
899 C**
900 C**
901 C**
902 C**
903 C**
904 C**
905 C**
906 C**
907 C**
908 C**
909 C**
910 C**
911 C**
912 C**
913 C**
914 C**
915 C**
916 C**
917 C**
918 C**
919 C**
920 C**
921 C**
922 C**
923 C**
924 C**
925 C**
926 C**
927 C**
928 C**
929 C**
930 C**
931 C**
932 C**
933 C**
934 C**
935 C**
936 C**
937 C**
938 C**
939 C**
940 C**
941 C**
942 C**
943 C**
944 C**
945 C**
946 C**
947 C**
948 C**
949 C**
950 C**
951 C**
952 C**
953 C**
954 C**
955 C**
956 C**
957 C**
958 C**
959 C**
960 C**
961 C**
962 C**
963 C**
964 C**
965 C**
966 C**
967 C**
968 C**
969 C**
970 C**
971 C**
972 C**
973 C**
974 C**
975 C**
976 C**
977 C**
978 C**
979 C**
980 C**
981 C**
982 C**
983 C**
984 C**
985 C**
986 C**
987 C**
988 C**
989 C**
990 C**
991 C**
992 C**
993 C**
994 C**
995 C**
996 C**
997 C**
998 C**
999 C**
1000 C**

```

```

CC 700 I = NN,NP
FA(JB(I)+JC) = 1.0
JS = JB(I) + 1 + JC
JE 700 J = JA(I) - 1 + JC
EC 700 J = JS,JE
FA(J) = 0.0
CCATINUE
RETURN
END
700

```









[illegible]

```

CIPERASIGN Y(7,1), YL(1), SAVE(7,1), YMAX(1), ER(1), YLSV(1), FI(1) LDA 1340
1 / EQUIVALENCE (A(18),END), (A(9),ER), (A(10),E), (A(11),EDN), LDA 1350
2 / A(12),ENQ1), (A(13),ENQ2), (A(14),ENQ3), (A(15),EUP), LDA 1360
3 / A(16),ENQ4), (A(17),ENQ5), (A(18),ENQ6), (A(19),ENQ7), LDA 1370
4 / A(20),ENQ8), (A(21),ENQ9), (A(22),ENQ10), (A(23),ENQ11), LDA 1380
5 / A(24),ENQ12), (A(25),ENQ13), (A(26),ENQ14), (A(27),ENQ15), LDA 1390
6 / A(28),ENQ16), (A(29),ENQ17), (A(30),ENQ18), (A(31),ENQ19), LDA 1400
7 / A(32),ENQ20), (A(33),ENQ21), (A(34),ENQ22), (A(35),ENQ23), LDA 1410
8 / A(36),ENQ24), (A(37),ENQ25), (A(38),ENQ26), (A(39),ENQ27), LDA 1420
9 / A(40),ENQ28), (A(41),ENQ29), (A(42),ENQ30), (A(43),ENQ31), LDA 1430
10 / A(44),ENQ32), (A(45),ENQ33), (A(46),ENQ34), (A(47),ENQ35), LDA 1440
11 / A(48),ENQ36), (A(49),ENQ37), (A(50),ENQ38), (A(51),ENQ39), LDA 1450
12 / A(52),ENQ40), (A(53),ENQ41), (A(54),ENQ42), (A(55),ENQ43), LDA 1460
13 / A(56),ENQ44), (A(57),ENQ45), (A(58),ENQ46), (A(59),ENQ47), LDA 1470
14 / A(60),ENQ48), (A(61),ENQ49), (A(62),ENQ50), (A(63),ENQ51), LDA 1480
15 / A(64),ENQ52), (A(65),ENQ53), (A(66),ENQ54), (A(67),ENQ55), LDA 1490
16 / A(68),ENQ56), (A(69),ENQ57), (A(70),ENQ58), (A(71),ENQ59), LDA 1500
17 / A(72),ENQ60), (A(73),ENQ61), (A(74),ENQ62), (A(75),ENQ63), LDA 1510
18 / A(76),ENQ64), (A(77),ENQ65), (A(78),ENQ66), (A(79),ENQ67), LDA 1520
19 / A(80),ENQ68), (A(81),ENQ69), (A(82),ENQ70), (A(83),ENQ71), LDA 1530
20 / A(84),ENQ72), (A(85),ENQ73), (A(86),ENQ74), (A(87),ENQ75), LDA 1540
21 / A(88),ENQ76), (A(89),ENQ77), (A(90),ENQ78), (A(91),ENQ79), LDA 1550
22 / A(92),ENQ80), (A(93),ENQ81), (A(94),ENQ82), (A(95),ENQ83), LDA 1560
23 / A(96),ENQ84), (A(97),ENQ85), (A(98),ENQ86), (A(99),ENQ87), LDA 1570
24 / A(100),ENQ88), (A(101),ENQ89), (A(102),ENQ90), (A(103),ENQ91), LDA 1580
25 / A(104),ENQ92), (A(105),ENQ93), (A(106),ENQ94), (A(107),ENQ95), LDA 1590
26 / A(108),ENQ96), (A(109),ENQ97), (A(110),ENQ98), (A(111),ENQ99), LDA 1600
27 / A(112),ENQ100), (A(113),ENQ101), (A(114),ENQ102), (A(115),ENQ103), LDA 1610
28 / A(116),ENQ104), (A(117),ENQ105), (A(118),ENQ106), (A(119),ENQ107), LDA 1620
29 / A(120),ENQ108), (A(121),ENQ109), (A(122),ENQ110), (A(123),ENQ111), LDA 1630
30 / A(124),ENQ112), (A(125),ENQ113), (A(126),ENQ114), (A(127),ENQ115), LDA 1640
31 / A(128),ENQ116), (A(129),ENQ117), (A(130),ENQ118), (A(131),ENQ119), LDA 1650
32 / A(132),ENQ120), (A(133),ENQ121), (A(134),ENQ122), (A(135),ENQ123), LDA 1660
33 / A(136),ENQ124), (A(137),ENQ125), (A(138),ENQ126), (A(139),ENQ127), LDA 1670
34 / A(140),ENQ128), (A(141),ENQ129), (A(142),ENQ130), (A(143),ENQ131), LDA 1680
35 / A(144),ENQ132), (A(145),ENQ133), (A(146),ENQ134), (A(147),ENQ135), LDA 1690
36 / A(148),ENQ136), (A(149),ENQ137), (A(150),ENQ138), (A(151),ENQ139), LDA 1700
37 / A(152),ENQ140), (A(153),ENQ141), (A(154),ENQ142), (A(155),ENQ143), LDA 1710
38 / A(156),ENQ144), (A(157),ENQ145), (A(158),ENQ146), (A(159),ENQ147), LDA 1720
39 / A(160),ENQ148), (A(161),ENQ149), (A(162),ENQ150), (A(163),ENQ151), LDA 1730
40 / A(164),ENQ152), (A(165),ENQ153), (A(166),ENQ154), (A(167),ENQ155), LDA 1740
41 / A(168),ENQ156), (A(169),ENQ157), (A(170),ENQ158), (A(171),ENQ159), LDA 1750
42 / A(172),ENQ160), (A(173),ENQ161), (A(174),ENQ162), (A(175),ENQ163), LDA 1760
43 / A(176),ENQ164), (A(177),ENQ165), (A(178),ENQ166), (A(179),ENQ167), LDA 1770
44 / A(180),ENQ168), (A(181),ENQ169), (A(182),ENQ170), (A(183),ENQ171), LDA 1780
45 / A(184),ENQ172), (A(185),ENQ173), (A(186),ENQ174), (A(187),ENQ175), LDA 1790
46 / A(188),ENQ176), (A(189),ENQ177), (A(190),ENQ178), (A(191),ENQ179), LDA 1800
47 / A(192),ENQ180), (A(193),ENQ181), (A(194),ENQ182), (A(195),ENQ183), LDA 1810
48 / A(196),ENQ184), (A(197),ENQ185), (A(198),ENQ186), (A(199),ENQ187), LDA 1820
49 / A(200),ENQ188), (A(201),ENQ189), (A(202),ENQ190), (A(203),ENQ191), LDA 1830
50 / A(204),ENQ192), (A(205),ENQ193), (A(206),ENQ194), (A(207),ENQ195), LDA 1840
51 / A(208),ENQ196), (A(209),ENQ197), (A(210),ENQ198), (A(211),ENQ199), LDA 1850
52 / A(212),ENQ200), (A(213),ENQ201), (A(214),ENQ202), (A(215),ENQ203), LDA 1860
53 / A(216),ENQ204), (A(217),ENQ205), (A(218),ENQ206), (A(219),ENQ207), LDA 1870
54 / A(220),ENQ208), (A(221),ENQ209), (A(222),ENQ210), (A(223),ENQ211), LDA 1880
55 / A(224),ENQ212), (A(225),ENQ213), (A(226),ENQ214), (A(227),ENQ215), LDA 1890
56 / A(228),ENQ216), (A(229),ENQ217), (A(230),ENQ218), (A(231),ENQ219), LDA 1900
57 / A(232),ENQ220), (A(233),ENQ221), (A(234),ENQ222), (A(235),ENQ223), LDA 1910
58 / A(236),ENQ224), (A(237),ENQ225), (A(238),ENQ226), (A(239),ENQ227), LDA 1920
59 / A(240),ENQ228), (A(241),ENQ229), (A(242),ENQ230), (A(243),ENQ231), LDA 1930
60 / A(244),ENQ232), (A(245),ENQ233), (A(246),ENQ234), (A(247),ENQ235), LDA 1940
61 / A(248),ENQ236), (A(249),ENQ237), (A(250),ENQ238), (A(251),ENQ239), LDA 1950
62 / A(252),ENQ240), (A(253),ENQ241), (A(254),ENQ242), (A(255),ENQ243), LDA 1960
63 / A(256),ENQ244), (A(257),ENQ245), (A(258),ENQ246), (A(259),ENQ247), LDA 1970
64 / A(260),ENQ248), (A(261),ENQ249), (A(262),ENQ250), (A(263),ENQ251), LDA 1980
65 / A(264),ENQ252), (A(265),ENQ253), (A(266),ENQ254), (A(267),ENQ255), LDA 1990
66 / A(268),ENQ256), (A(269),ENQ257), (A(270),ENQ258), (A(271),ENQ259), LDA 2000
67 / A(272),ENQ260), (A(273),ENQ261), (A(274),ENQ262), (A(275),ENQ263), LDA 2010
68 / A(276),ENQ264), (A(277),ENQ265), (A(278),ENQ266), (A(279),ENQ267), LDA 2020
69 / A(280),ENQ268), (A(281),ENQ269), (A(282),ENQ270), (A(283),ENQ271), LDA 2030
70 / A(284),ENQ272), (A(285),ENQ273), (A(286),ENQ274), (A(287),ENQ275), LDA 2040
71 / A(288),ENQ276), (A(289),ENQ277), (A(290),ENQ278), (A(291),ENQ279), LDA 2050
72 / A(292),ENQ280), (A(293),ENQ281), (A(294),ENQ282), (A(295),ENQ283), LDA 2060
73 / A(296),ENQ284), (A(297),ENQ285), (A(298),ENQ286), (A(299),ENQ287), LDA 2070
74 / A(300),ENQ288), (A(301),ENQ289), (A(302),ENQ290), (A(303),ENQ291), LDA 2080
75 / A(304),ENQ292), (A(305),ENQ293), (A(306),ENQ294), (A(307),ENQ295), LDA 2090
76 / A(308),ENQ296), (A(309),ENQ297), (A(310),ENQ298), (A(311),ENQ299), LDA 2100
77 / A(312),ENQ300), (A(313),ENQ301), (A(314),ENQ302), (A(315),ENQ303), LDA 2110
78 / A(316),ENQ304), (A(317),ENQ305), (A(318),ENQ306), (A(319),ENQ307), LDA 2120
79 / A(320),ENQ308), (A(321),ENQ309), (A(322),ENQ310), (A(323),ENQ311), LDA 2130
80 / A(324),ENQ312), (A(325),ENQ313), (A(326),ENQ314), (A(327),ENQ315), LDA 2140
81 / A(328),ENQ316), (A(329),ENQ317), (A(330),ENQ318), (A(331),ENQ319), LDA 2150
82 / A(332),ENQ320), (A(333),ENQ321), (A(334),ENQ322), (A(335),ENQ323), LDA 2160
83 / A(336),ENQ324), (A(337),ENQ325), (A(338),ENQ326), (A(339),ENQ327), LDA 2170
84 / A(340),ENQ328), (A(341),ENQ329), (A(342),ENQ330), (A(343),ENQ331), LDA 2180
85 / A(344),ENQ332), (A(345),ENQ333), (A(346),ENQ334), (A(347),ENQ335), LDA 2190
86 / A(348),ENQ336), (A(349),ENQ337), (A(350),ENQ338), (A(351),ENQ339), LDA 2200
87 / A(352),ENQ340), (A(353),ENQ341), (A(354),ENQ342), (A(355),ENQ343), LDA 2210
88 / A(356),ENQ344), (A(357),ENQ345), (A(358),ENQ346), (A(359),ENQ347), LDA 2220
89 / A(360),ENQ348), (A(361),ENQ349), (A(362),ENQ350), (A(363),ENQ351), LDA 2230
90 / A(364),ENQ352), (A(365),ENQ353), (A(366),ENQ354), (A(367),ENQ355), LDA 2240
91 / A(368),ENQ356), (A(369),ENQ357), (A(370),ENQ358), (A(371),ENQ359), LDA 2250
92 / A(372),ENQ360), (A(373),ENQ361), (A(374),ENQ362), (A(375),ENQ363), LDA 2260
93 / A(376),ENQ364), (A(377),ENQ365), (A(378),ENQ366), (A(379),ENQ367), LDA 2270
94 / A(380),ENQ368), (A(381),ENQ369), (A(382),ENQ370), (A(383),ENQ371), LDA 2280
95 / A(384),ENQ372), (A(385),ENQ373), (A(386),ENQ374), (A(387),ENQ375), LDA 2290
96 / A(388),ENQ376), (A(389),ENQ377), (A(390),ENQ378), (A(391),ENQ379), LDA 2300
97 / A(392),ENQ380), (A(393),ENQ381), (A(394),ENQ382), (A(395),ENQ383), LDA 2310
98 / A(396),ENQ384), (A(397),ENQ385), (A(398),ENQ386), (A(399),ENQ387), LDA 2320
99 / A(400),ENQ388), (A(401),ENQ389), (A(402),ENQ390), (A(403),ENQ391), LDA 2330
100 / A(404),ENQ392), (A(405),ENQ393), (A(406),ENQ394), (A(407),ENQ395), LDA 2340
101 / A(408),ENQ396), (A(409),ENQ397), (A(410),ENQ398), (A(411),ENQ399), LDA 2350
102 / A(412),ENQ400), (A(413),ENQ401), (A(414),ENQ402), (A(415),ENQ403), LDA 2360
103 / A(416),ENQ404), (A(417),ENQ405), (A(418),ENQ406), (A(419),ENQ407), LDA 2370
104 / A(420),ENQ408), (A(421),ENQ409), (A(422),ENQ410), (A(423),ENQ411), LDA 2380
105 / A(424),ENQ412), (A(425),ENQ413), (A(426),ENQ414), (A(427),ENQ415), LDA 2390
106 / A(428),ENQ416), (A(429),ENQ417), (A(430),ENQ418), (A(431),ENQ419), LDA 2400
107 / A(432),ENQ420), (A(433),ENQ421), (A(434),ENQ422), (A(435),ENQ423), LDA 2410
108 / A(436),ENQ424), (A(437),ENQ425), (A(438),ENQ426), (A(439),ENQ427), LDA 2420
109 / A(440),ENQ428), (A(441),ENQ429), (A(442),ENQ430), (A(443),ENQ431), LDA 2430
110 / A(444),ENQ432), (A(445),ENQ433), (A(446),ENQ434), (A(447),ENQ435), LDA 2440
111 / A(448),ENQ436), (A(449),ENQ437), (A(450),ENQ438), (A(451),ENQ439), LDA 2450
112 / A(452),ENQ440), (A(453),ENQ441), (A(454),ENQ442), (A(455),ENQ443), LDA 2460
113 / A(456),ENQ444), (A(457),ENQ445), (A(458),ENQ446), (A(459),ENQ447), LDA 2470
114 / A(460),ENQ448), (A(461),ENQ449), (A(462),ENQ450), (A(463),ENQ451), LDA 2480
115 / A(464),ENQ452), (A(465),ENQ453), (A(466),ENQ454), (A(467),ENQ455), LDA 2490
116 / A(468),ENQ456), (A(469),ENQ457), (A(470),ENQ458), (A(471),ENQ459), LDA 2500
117 / A(472),ENQ460), (A(473),ENQ461), (A(474),ENQ462), (A(475),ENQ463), LDA 2510
118 / A(476),ENQ464), (A(477),ENQ465), (A(478),ENQ466), (A(479),ENQ467), LDA 2520
119 / A(480),ENQ468), (A(481),ENQ469), (A(482),ENQ470), (A(483),ENQ471), LDA 2530
120 / A(484),ENQ472), (A(485),ENQ473), (A(486),ENQ474), (A(487),ENQ475), LDA 2540
121 / A(488),ENQ476), (A(489),ENQ477), (A(490),ENQ478), (A(491),ENQ479), LDA 2550
122 / A(492),ENQ480), (A(493),ENQ481), (A(494),ENQ482), (A(495),ENQ483), LDA 2560
123 / A(496),ENQ484), (A(497),ENQ485), (A(498),ENQ486), (A(499),ENQ487), LDA 2570
124 / A(500),ENQ488), (A(501),ENQ489), (A(502),ENQ490), (A(503),ENQ491), LDA 2580
125 / A(504),ENQ492), (A(505),ENQ493), (A(506),ENQ494), (A(507),ENQ495), LDA 2590
126 / A(508),ENQ496), (A(509),ENQ497), (A(510),ENQ498), (A(511),ENQ499), LDA 2600
127 / A(512),ENQ500), (A(513),ENQ501), (A(514),ENQ502), (A(515),ENQ503), LDA 2610
128 / A(516),ENQ504), (A(517),ENQ505), (A(518),ENQ506), (A(519),ENQ507), LDA 2620
129 / A(520),ENQ508), (A(521),ENQ509), (A(522),ENQ510), (A(523),ENQ511), LDA 2630
130 / A(524),ENQ512), (A(525),ENQ513), (A(526),ENQ514), (A(527),ENQ515), LDA 2640
131 / A(528),ENQ516), (A(529),ENQ517), (A(530),ENQ518), (A(531),ENQ519), LDA 2650
132 / A(532),ENQ520), (A(533),ENQ521), (A(534),ENQ522), (A(535),ENQ523), LDA 2660
133 / A(536),ENQ524), (A(537),ENQ525), (A(538),ENQ526), (A(539),ENQ527), LDA 2670
134 / A(540),ENQ528), (A(541),ENQ529), (A(542),ENQ530), (A(543),ENQ531), LDA 2680
135 / A(544),ENQ532), (A(545),ENQ533), (A(546),ENQ534), (A(547),ENQ535), LDA 2690
136 / A(548),ENQ536), (A(549),ENQ537), (A(550),ENQ538), (A(551),ENQ539), LDA 2700
137 / A(552),ENQ540), (A(553),ENQ541), (A(554),ENQ542), (A(555),ENQ543), LDA 2710
138 / A(556),ENQ544), (A(557),ENQ545), (A(558),ENQ546), (A(559),ENQ547), LDA 2720
139 / A(560),ENQ548), (A(561),ENQ549), (A(562),ENQ550), (A(563),ENQ551), LDA 2730
140 / A(564),ENQ552), (A(565),ENQ553), (A(566),ENQ554), (A(567),ENQ555), LDA 2740
141 / A(568),ENQ556), (A(569),ENQ557), (A(570),ENQ558), (A(571),ENQ559), LDA 2750
142 / A(572),ENQ560), (A(573),ENQ561), (A(574),ENQ562), (A(575),ENQ563), LDA 2760
143 / A(576),ENQ564), (A(577),ENQ565), (A(578),ENQ566), (A(579),ENQ567), LDA 2770
144 / A(580),ENQ568), (A(581),ENQ569), (A(582),ENQ570), (A(583),ENQ571), LDA 2780
145 / A(584),ENQ572), (A(585),ENQ573), (A(586),ENQ574), (A(587),ENQ575), LDA 2790
146 / A(588),ENQ576), (A(589),ENQ577), (A(590),ENQ578), (A(591),ENQ579), LDA 2800
147 / A(592),ENQ580), (A(593),ENQ581), (A(594),ENQ582), (A(595),ENQ583), LDA 2810
148 / A(596),ENQ584), (A(597),ENQ585), (A(598),ENQ586), (A(599),ENQ587), LDA 2820
149 / A(600),ENQ588), (A(601),ENQ589), (A(602),ENQ590), (A(603),ENQ591), LDA 2830
150 / A(604),ENQ592), (A(605),ENQ593), (A(606),ENQ594), (A(607),ENQ595), LDA 2840
151 / A(608),ENQ596), (A(609),ENQ597), (A(610),ENQ598), (A(611),ENQ599), LDA 2850
152 / A(612),ENQ600), (A(613),ENQ601), (A(614),ENQ602), (A(615),ENQ603), LDA 2860
153 / A(616),ENQ604), (A(617),ENQ605), (A(618),ENQ606), (A(619),ENQ607), LDA 2870
154 / A(620),ENQ608), (A(621),ENQ609), (A(622),ENQ610), (A(623),ENQ611), LDA 2880
155 / A(624),ENQ612), (A(625),ENQ613), (A(626),ENQ614), (A(627),ENQ615), LDA 2890
156 / A(628),ENQ616), (A(629),ENQ617), (A(630),ENQ618), (A(631),ENQ619), LDA 2900
157 / A(632),ENQ620), (A(633),ENQ621), (A(634),ENQ622), (A(635),ENQ623), LDA 2910
158 / A(636),ENQ624), (A(637),ENQ625), (A(638),ENQ626), (A(639),ENQ627), LDA 2920
159 / A(640),ENQ628), (A(641),ENQ629), (A(642),ENQ630), (A(643),ENQ631), LDA 2930
160 / A(644),ENQ632), (A(645),ENQ633), (A(646),ENQ634), (A(647),ENQ635), LDA 2940
161 / A(648),ENQ636), (A(649),ENQ637), (A(650),ENQ638), (A(651),ENQ639), LDA 2950
162 / A(652),ENQ640), (A(653),ENQ641), (A(654),ENQ642), (A(655),ENQ643), LDA 2960
163 / A(656),ENQ644), (A(657),ENQ645), (A(658),ENQ646), (A(659),ENQ647), LDA 2970
164 / A(660),ENQ648), (A(661),ENQ649), (A(662),ENQ650), (A(663),ENQ651), LDA 2980
165 / A(664),ENQ652), (A(665),ENQ653), (A(666),ENQ654), (A(667),ENQ655), LDA 2990
166 / A(668),ENQ656), (A(669),ENQ657), (A(670),ENQ658), (A(671),ENQ659), LDA 3000
167 / A(672),ENQ660), (A(673),ENQ661), (A(674),ENQ662), (A(675),ENQ663), LDA 3010
168 / A(676),ENQ664), (A(677),ENQ665), (A(678),ENQ666), (A(679),ENQ667), LDA 3020
169 / A(680),ENQ668), (A(681),ENQ669), (A(682),ENQ670), (A(683),ENQ671), LDA 3030
170 / A(684),ENQ672), (A(685),ENQ673), (A(686),ENQ674), (A(687),ENQ675), LDA 3040
171 / A(688),ENQ676), (A(689),ENQ677), (A(690),ENQ678), (A(691),ENQ679), LDA 3050
172 / A(692),ENQ680), (A(693),ENQ681), (A(694),ENQ682), (A(695),ENQ683), LDA 3060
173 / A(696),ENQ684), (A(697),ENQ685), (A(698),ENQ686), (A(699),ENQ687), LDA 3070
174 / A(700),ENQ688), (A(701),ENQ689), (A(702),ENQ690), (A(703),ENQ691), LDA 3080
175 / A(704),ENQ692), (A(705),ENQ693), (A(706),ENQ694), (A(707),ENQ695), LDA 3090
176 / A(708),ENQ696), (A(709),ENQ697), (A(710),ENQ698), (A(711),ENQ699), LDA 3100
177 / A(712),ENQ700), (A(713),ENQ701), (A(714),ENQ702), (A(715),ENQ703), LDA 3110
178 / A(716),ENQ704), (A(717),ENQ705), (A(718),ENQ706), (A(719),ENQ707), LDA 3120
179 / A(720),ENQ708), (A(721),ENQ709), (A(722),ENQ710), (A(723),ENQ711), LDA 3130
180 / A(724),ENQ712), (A(725),ENQ713), (A(726),ENQ714), (A(727),ENQ715), LDA 3140
181 / A(728),ENQ716), (A(729),ENQ717), (A(730),ENQ718), (A(731),ENQ719), LDA 3150
182 / A(732),ENQ720), (A(733),ENQ721), (A(734),ENQ722), (A(735),ENQ723), LDA 3160
183 / A(736),ENQ724), (A(737),ENQ725), (A(738),ENQ726), (A(739),ENQ727), LDA 3170
184 / A(740),ENQ728), (A(741),ENQ729), (A(742),ENQ730), (A(743),ENQ731), LDA 3180
185 / A(744),ENQ732), (A(745),ENQ733), (A(746),ENQ734), (A(747),ENQ735), LDA 3190
186 / A(748),ENQ736), (A(749),ENQ737), (A(750),ENQ738), (A(751),ENQ739), LDA 3200
187 / A(752),ENQ740), (A(753),ENQ741), (A(754),ENQ742), (A(755),ENQ743), LDA 3210
188 / A(756),ENQ744), (A(757),ENQ745), (A(758),ENQ746), (A(759),ENQ747), LDA 3220
189 / A(760),ENQ748), (A(761),ENQ749), (A(762),ENQ750), (A(763),ENQ751), LDA 3230
190 / A(764),ENQ752), (A(765),ENQ753), (A(766),ENQ754), (A(767),ENQ755), LDA 3240
191 / A(768),ENQ756), (A(769),ENQ757), (A(770),ENQ758), (A(771),ENQ759), LDA 3250
192 / A(772),ENQ760), (A(773),ENQ761), (A(774),ENQ762), (A(775),ENQ763), LDA 3260
193 / A(776),ENQ764), (A(777),ENQ765), (A(778),ENQ766), (A(779),ENQ767), LDA 3270
194 / A(780),ENQ768), (A(781),ENQ769), (A(782),ENQ770), (A(783),ENQ771), LDA 3280
195 / A(784),ENQ772), (A(785),ENQ773), (A(786),ENQ774), (A(787),ENQ775), LDA 3290
196 / A(788),ENQ776), (A(789),ENQ777), (A(790),ENQ778), (A(791),ENQ779), LDA 3300
197 / A(792),ENQ780), (A(793),ENQ781), (A(794),ENQ782), (A(795),ENQ783), LDA 3310
198 / A(796),ENQ784), (A(797),ENQ785), (A(798),ENQ786), (A(799),ENQ787), LDA 3320
199 / A(800),ENQ788), (A(801),ENQ789), (A(802),ENQ790), (A(803),ENQ791), LDA 3330
200 / A(804),ENQ792), (A(805),ENQ793), (A(806),ENQ794), (A(807),ENQ795), LDA 3340
201 / A(808),ENQ796), (A(809),ENQ797), (A(810),ENQ798), (A(811),ENQ799), LDA 3350
202 / A(812),ENQ800), (A(813),ENQ801), (A(814),ENQ802), (A(815),ENQ803), LDA 3360
203 / A(816),ENQ804), (A(817),ENQ805), (A(818),ENQ806), (A(819),ENQ807), LDA 3370
204 / A(820),ENQ808), (A(821),ENQ809), (A(822),ENQ810),
```

```

LCCFYY = 7*NY
LCCFYL = NL
NL = MINO(M,NY)
EPS = Sqrt(FLOAT(M1))*RMSEPS
MAXCER = MINO(MAXOR,6)
IF (IPRT.LE.0) GC TO 120
PRINT 3, N,NL,RMSEPS,TEND,H
PRINT 4
PS = C
12C AM = 0
C
CC 130 J=1,NY
YMAX(J) = AMAX1(1.,ABS(Y(1,J)))
13C Y(2,J) = Y(2,J)*F
C
AC = 1
ER = 1.
ASSIGN 150 TO IRET
SET COEFFICIENTS FOR THE ORDER CURRENTLY BEING USED.
E IS A TEST FOR ERRORS OF THE CURRENT ORDER AC
EUF IS TO TEST FOR INCREASING THE ORDER, ECU FOR DECREASING THE
ORDER.
14C K = NC*(NC-1)/2
CALL CGPYZ (A(2),CGF(K+1),NC)
K = AC+1
ICCU = AC
ENQ1 = .5/NC
ENQ2 = .5/K
ENQ3 = .5/(NQ+2)
PEPSH = EPS**2
EUP = FERT(NC,1)*PEPSH
ECU = PERT(NC,2)*PEPSH
ECU = PERT(NC,3)*PEPSH
BACVAL = (EPS*ENQ3)**2
15C IREVAL = 1
CALL IRET, (190,200,45C,570)
IF (F-EC.HAEW) GO TO 190
C
IF CALLER HAS CHANGED F, RESCALE DERIVATIVES TO REFLECT THAT FNEW
WAS USED ON THE LAST CALL.
C
R = H/HAEW
ASSIGN 190 TO IRET
GC TO 610
C
SET JSTART TO NQ, THE CURRENT ORDER OF THE METHCC, BEFORE EXIT,

```

```

C 160 AND SAVE THE CURRENT STEPSIZE IN INEW.
      JSTART = NC
      FAEW = F
      RETURN
C 170 NS = INPT.LE.O) GO TO 180
      IF (IPRT.LE.O) GO TO 180
      PRINT DATA IF DESIRED BY USER
C 180 PRINT 1, NS,NW,NQ,F,T,(Y(1,1),I=1,NY)
      CONTINUE
      IF (KFLAG.LI.O) GO TO 160
      IF (T.GE.YEND) GO TO 160
      TAKE ANOTHER STEP IF T < YEND
      JSTART = 1
      SAVE DATA FOR TRIAL WITH A SMALLER TIMESTEP IF THIS STEP FAILS
C 190 CALL CCOPYZ (SAVE,Y,LCCOPY)
      CALL CCOPYZ (YLSV,Y,LCCPYL)
      RACUM = 1.
      KFLAG = 1.
      FCLC = F
      NCCLC = NO
      TCLC = T
      T = T+H
      FINV = 1./F
C 200 CCMPUTE PREDICTED VALUES BY EFFECTIVELY MULTIPLYING DERIVATIVE
      VECTOR BY PASCAL TRIANGLE MATRIX
      CC 210 J=2,K
      JJ = K+J-1
      CC 210 J1=J,K
      JJ = J3-J1
      CC 210 I=1,NY
      Y(J2,I) = Y(J2,1)+Y(J2+1,I)
      CC 220 I=1,NY
      EN(I) = 0.

```

```

LDA 2310
LCA 2310
LDA 2320
LCA 2320
LDA 2330
LCA 2330
LDA 2340
LCA 2340
LDA 2350
LCA 2350
LDA 2360
LCA 2360
LDA 2370
LCA 2370
LDA 2380
LCA 2380
LDA 2390
LCA 2390
LDA 2400
LCA 2400
LDA 2410
LCA 2410
LDA 2420
LCA 2420
LDA 2430
LCA 2430
LDA 2440
LCA 2440
LDA 2450
LCA 2450
LDA 2460
LCA 2460
LDA 2470
LCA 2470
LDA 2480
LCA 2480
LDA 2490
LCA 2490
LDA 2500
LCA 2500
LDA 2510
LCA 2510
LDA 2520
LCA 2520
LDA 2530
LCA 2530
LDA 2540
LCA 2540
LDA 2550
LCA 2550
LDA 2560
LCA 2560
LDA 2580
LCA 2580
LDA 2590
LCA 2590
LDA 2600
LCA 2600
LDA 2610
LCA 2610
LDA 2620
LCA 2620
LDA 2630
LCA 2630
LDA 2640
LCA 2640
LDA 2650
LCA 2650
LDA 2660
LCA 2660
LDA 2670
LCA 2670
LDA 2680
LCA 2680
LDA 2690
LCA 2690
LDA 2700
LCA 2700
LDA 2710
LCA 2710
LDA 2720
LCA 2720
LDA 2730
LCA 2730
LDA 2740
LCA 2740
LDA 2750
LCA 2750
LDA 2760
LCA 2760
LDA 2770
LCA 2770
LDA 2780
LCA 2780

```

```

CCCCCCCCCCCC
CC LP TC THREE CORRECTOR ITERATIONS. CONVERGENCE IS OBTAINED WHEN
CHANGES ARE LESS THAN BND WHICH IS DEPENDENT ON THE ERCCR TEST
CCCONSTANT. THE SUM OF CORRECTIONS IS ACCUMULATED IN ER(I). IT IS
ECCAL TC THE K-TH DERIVATIVE OF Y TIMES F**K/(K-FACTCRIAL*(A(K))) IS
AND THUS IS PROPORTIONAL TO THE ACTUAL ERCCFS TC THE LOWEST FCWER
CF F PRESENT, WHICH IS F**K.
LDA 2750
LDA 2800
LDA 2810
LDA 2820
LDA 2830
LDA 2840
LDA 2850
LDA 2860
LDA 2870
LDA 2880

CC 270 L=1,3
CALL DIFFUN (Y,YL,T,HINV,DY,BIGH12,BIGH3,BIGH4,BIGH5,BIGF,BIGF,
1 IEPI,ITYPE,JA,JB,NAME,NELCON,RR,Z,YIT)
IF (INEVAL.LT.1) GC TC 230
LDA 2900
LDA 2910
LDA 2920
LDA 2930
LDA 2940
LDA 2950
LDA 2960
LDA 2970

IF THERE HAS BEEN A CHANGE OF CRCCR OR THERE HAS BEEN TRCUBLE
WITH CONVERGENCE, PW IS RE-EVALUATED PRIOR TC STARTING THE
CORRECTOR ITERATION. INEVAL IS THEN SET TC -1 AS AN INDICATOR
THAT IT HAS BEEN DONE. NEWPW IS SET NONZERO TO INDICATE TO
SUBROUTINE NUTSL THAT A NEW PW HAS BEEN PROVIDED.
LDA 3000
LDA 3010
LDA 3020

CALL JACMAT (Y,YL,T,HINV,A(2),N,NY,EPS,DY,F1,PW,BIGH12,BIGH3,
1 BIGH4,BIGH5,BIGK,IBF,ITYPE,JA,JB,NAME,NELCON,RR,Z)
KFLAG = 1
INEVAL = -1
NEWPW = 1
NEWFW = 1
230 CALL NUTSL (PW,DY,F1,N,NY,EPS,YMAX,NEWPW,KFRET,EIGH3,ITYPE,
1 JA,JB,NAME,NELCON)
IF (KFRET.NE.0) GC TO 600
IF (NL.LE.0) GO TO 250
LDA 3050
LDA 3060
LDA 3070
LDA 3080
LDA 3090
LDA 3100
LDA 3110
LDA 3120
LDA 3130
LDA 3140
LDA 3150
LDA 3160
LDA 3170
LDA 3180
LDA 3190
LDA 3200
LDA 3210
LDA 3220
LDA 3230

CC 240 I=1,NL
24C VL(I) = YL(I)-F1(I+NY)
C
25C CCATINUE
DEL = 0.
C
CC 260 I=1,NY
Y(I,I) = Y(I,I)-F1(I)
Y(I,I) = Y(I,I)+A(2)*F1(I)
ER(I) = ER(I)+F1(I)
DEL = DEL+(F1(I)/AMAX1(YMAX(I),ABS(Y(I,I))))**2
26C CCATINUE
C
IF (L.GE.2) BR = AMAX1(.9*BR,DEL/CELL)
DEL = DEL
IF (AMIN1(DEL,BR*DEL*2.).LE.BND) GO TO 330
270 CCATINUE

```

```

C C C C C C C C
28C THE CORRECTOR ITERATION FAILED TO CONVERGE IN 3 TRIES. VARICUS
29C POSSIBILITIES ARE CHECKED FOR. IF H IS ALREADY HPIA AND PH PAS
30C ALREADY BEEN RE-EVALUATED, A NO CONVERGENCE EXIT IS TAKEN.
31C OTHERWISE THE MATRIX PH IS RE-EVALUATED AND/CR (IN THAT CR CER) THE
32C STEP IS REDUCED TO TRY AND GET CONVERGENCE.
33C
34C T = TOLD
35C IF (IMEVAL) 280,300,290
36C IF (H.LE.HMIN*.1-0.00001) GO TO 310
37C RACUM = RACUM*.25
38C CCATINJE
39C GO TO 560
40C KFLAG = -3
41C
42C RESTORE Y AND YL AFTER CONVERGENCE FAILURE
43C
44C CALL COPYZ (Y,SAVE,LCCPYZ)
45C CALL COPYZ (YL,YLSV,LCCPYL)
46C I = HOLD
47C NC = NCCLC
48C GO TO 170
49C
50C THE CORRECTOR CONVERGED, SO NOW THE ERROR TEST IS MADE.
51C
52C C = 0.
53C
54C CC 340 I=1,M1
55C YP = ANAXI(ABS(Y(1,I)),YMAX(I))
56C C = D+(ER(I)/YM)**2
57C
58C IMEVAL = 0
59C IF (D.GT.E) GO TO 380
60C
61C THE ERROR TEST IS OKAY, SO THE STEP IS ACCEPTED. IF IDOUB
62C NOW BECOMES NEGATIVE, A TEST IS MADE TO SEE IF CR CAN INCREASE.
63C CAN BE INCREASED AT THIS CR CER OR ONE HIGHER CR CAN INCREASE.
64C THE CHANGE IS MADE ONLY IF THE STEP CAN BE INCREASED BY AT
65C LEAST 10%. IDOUB IS SET TO NO TO PREVENT FURTHER TESTING
66C FOR A WHILE. IF AC CHANGE IS MADE, IDOUB IS SET TO 5.
67C
68C IF (K.LT.3) GO TO 360
69C
70C CC 350 J=3,X
71C
72C CC 350 I=1,NY
73C Y(J,I) = Y(J,I)+A(J)*ER(I)

```

```

C 36C KFLAG = 1 ICCUB-1
      ICCUB = 1000UB) 410,37C,510
C 37C CALL CCPYZ (ESV,ER,M1)
      GC TO 510
C
C-----THE ERROR TEST FAILED. IF JSTART = 0, THE DERIVATIVES IN THE
C-----SAVE ARRAY ARE UPDATED. TESTS ARE THEN MADE TO FIX THE STEPSIZE
C-----AND PERHAPS REDUCE THE ORDER. AFTER REENTERING AND SCALING THE
C-----Y VARIABLES, THE STEP IS RETRIED.
C-----
C 38C IF (JSTART.GT.0) GC TO 400
C
C 39C DC 350 I=1,NY
C 39C SAVE(2,I) = Y(2,I)
C
C 40C KFLAG = KFLAG-2
      IF (H.LE.HMIN) GC TO 550
      I = IOLL
C 41C IF (KFLAG.LE.-5) GC TO 530
      FF2 = (C/E)**ENQ2*1.2
      L = 0
      IF (NQ.LE.-1) GC TO 430
      D = 0.
C
C 42C DC 420 J=1,M1
      YP = AMAX1(ABS(Y(1,J)),YMAX(J))
      C = C+(Y(K,J)/YM)**2
C
C 43C PRI = (C/EDWN)**ENCI*1.3
      IF (PRI.GE.PR2) GO TO 430
      PR2 = PRI
      L = -1
      IF (KFLAG.LT.0.OR.NC.GE.MAXCER) GC TO 45C
      D = 0
C
C 44C DC 440 J=1,M1
      YP = AMAX1(ABS(Y(1,J)),YMAX(J))
      C = C+((ER(J)-ESV(J))/YM)**2
C
C 45C PRI = (C/EUP)**ENC3*1.4
      IF (PRI.GE.PR2) GO TO 450
      PR2 = PRI
      L = 1
      R = 1/AMAX1(PR2,1.E-5)
      IF (KFLAG.LT.0.OR.R.GE.1.1) GO TC 460
      ICCUB = 9

```

```

46C GC TC 510
    NEWC = AQ+L
    K = NEWC+1
    IF (NEWC-LE,NQ) GC TO 480
    RI = A(NEWC)/FLOAT(NEWC)
C
C 47C DC 470 J=1,NY
    Y(K,J) = ER(J)*RI
C
C 48C CCATINUE
C
C 49C IF THE STEP WAS OKAY, SCALE THE Y VARIABLES IN ACCORDANCE
    WITH THE NEW VALUE OF P. IF KFLAG < 0, HOWEVER, USE THE
    SAVED VALUES (IN SAVE AND YLSV). IN EITHER CASE, IF THE ORDER
    HAS CHANGED IT IS NECESSARY TO FIX CERTAIN PARAMETERS BY CALLING
    THE PROGRAM SEGMENT AT STATEMENT NUMBER 140.
C
C 50C ICCLB = NQ
    IF (NEWC-EC,NQ) GC TO 450
    AC = NEWC
    ASSIGN 450 TO IRET
    GC TO 140
C
C 51C IF (KFLAG-GE,0) GC TO 500
    RACUM = RACUM*R
    GC TO 560
C
C 52C R = AMAXI(AMINI,HMAX/H,R),HMIN/H)
    IREVAL = 1
    ASSIGN 510 TO IRET
    GC TO 610
C
C 53C DC 520 I=1,N1
    YMAX(I) = (MAX1(ABS(Y(1,I)),YMAX(1)))
C
C 54C GC TO 170
    THE ERROR TEST HAS NOW FAILED THREE TIMES, SO THE CEFFIVATIVES ARE
    IN BAD SHAPE. RETURN TO FIRST ORDER METHOD AND TRY AGAIN. CF
    COURSE, IF NQ = 1 ALREADY, THEN THERE IS NO PCPE AND WE EXIT WITH
    KFLAG = -4.
C
C 55C IF (NQ-EG-1) GO TC 540
    AC = 1
    ICCLB = 1
    ASSIGN 570 TO IRET
    GC TO 140
C
C 56C ACCLD = 1
    KFLAG = -4

```

```

LDA 4200
LDA 4210
LDA 4220
LDA 4230
LDA 4240
LDA 4250
LDA 4260
LDA 4270
LDA 4280
LDA 4290
LDA 4300
LDA 4310
LDA 4320
LDA 4330
LDA 4340
LDA 4350
LDA 4360
LDA 4370
LDA 4380
LDA 4390
LDA 4400
LDA 4410
LDA 4420
LDA 4430
LDA 4440
LDA 4450
LDA 4460
LDA 4470
LDA 4480
LDA 4490
LDA 4500
LDA 4510
LDA 4520
LDA 4530
LDA 4540
LDA 4550
LDA 4560
LDA 4570
LDA 4580
LDA 4590
LDA 4600
LDA 4610
LDA 4620
LDA 4630
LDA 4640
LDA 4650
LDA 4660
LDA 4670

```



CCCCC

C

CCC

```

TC RESTART THE USER FIRST CALLS LCARST TO RESTORE THE VALUES SAVED
BY LCASAV, THEN RE-ENTERS LDASUB WITH JSTART = 0, AND WITH THE
OTHER PARAMETERS THE SAME AS RETURNED FROM THE LAST ENTRY TO
LDASUB, PARTICULARLY THOSE ARRAYS MENTIONED ABOVE.
ENTRY LCASAV(SAV)
LCCPYS = 25
CALL COPYZ (SAV,A,LCCPYS)
CALL COPYZ (SAVE,V,LCCPYV)
CALL COPYZ (YLSV,YL,LCCPYL)
RETURN
ENTRY LCARST(SAV)
LCCPYR = 25
CALL COPYZ (A,SAV,LCCFYR)
RETURN
1 FCRMAT (215,12,1P2E10-2,7E14-6/132X,7E14-6)
2 FCRMAT (32X,1P7E14-6)
3 FCRMAT (1,1,13,0 RMSEPS =,1PES-2,0 TENC =,
  ES-2,0 H =,ES-2//) H,8X,0T '8X,Y(1,0) AND YL(0,0)//
4 FCRMAT (1,1,13,0 RMSEPS =,1PES-2,0 TENC =,
  ES-2,0 H =,ES-2//) H,8X,0T '8X,Y(1,0) AND YL(0,0)//
END
LDA 517C
LDA 518C
LDA 519C
LDA 520C
LDA 521C
LDA 522C
LDA 523C
LDA 524C
LDA 525C
LDA 526C
LDA 527C
LDA 528C
LDA 529C
LDA 530C
LDA 531C
LDA 532C
LDA 533C
LDA 534C
LDA 535C
LDA 536C
LDA 537C
LDA 538C
LDA 539C
LDA 540C
LDA 541C
LDA 542C
LDA 543C

```



[illegible]



14C PRINT 1, JSKF  
STOP

C  
C

1 FCFORMAT ('QUIT IS AN ERRGR TO ENTER SOESOL WITH JSKF = ',110//  
' RUN HAS BEEN TERMINATED.')  
END

SDE 131C  
SDE 1320  
SDE 1330  
SDE 1340  
SDE 1350  
SDE 1360  
SDE 1370

```

SUBROUTINE COPYZ(S,Y,L)
DIMENSION S(1),Y(1)
-----
THIS SUBROUTINE COPIES THE ARRAY Y, OF LENGTH L, INTO THE ARRAY S
-----
IF(L.LE.0)RETURN
DO 100 J=1,L
S(J) = Y(J)
100 CONTINUE
RETURN
END

```

```

COP 10
COP 20
COP 30
COP 40
COP 50
COP 60
COP 70
CCF 80
COP 90
COP 100
CCF 110
COP 120

```



```

C      DIMENSION Y(7,1), YL(1), W(1)
      DC 100 I=1,NY
      W(2*N+1) = AMAX1(ABS(Y(1,1)),1.0)
      100 Y(3,1) = 0.
      HIAV = 16.0**20
      KERET = 0
      EPS2 = NY/1.E5
      EPS = SCRT(EPS2)
      CC 140 IT=1,10
      DC 110 I=1,NY
      110 Y(2,I) = Y(3,I)/HIAV
      CALL DIFFUN(Y,YL,I,F,INV,W,BIGH12,BIGH3,BIGH4,BIGH5,BIGH6,BIGH7,
      1 IF,ITYPE,JA,JB,NAME,NELCON,R,Z,YIT)
      CALL JACMA(Y,YL,I,F,INV,W,BIGH3,BIGH4,BIGH5,BIGH6,BIGH7,
      1 BIGH8,BIGH9,BIGH10,BIGH11,BIGH12,BIGH13,BIGH14,BIGH15,
      1 AEMPW=1)
      CC 120 I=1,NY
      120 Y(1,I) = Y(2,I)*HINV
      CALL NUTISL(W(3*N+1),W,W(N+1),NY,NY,EPS,A(2*N+1),AEMPW,KRET,
      1 BIGH3,ITYPE,JA,JB,NAME,NELCON)
      IF (KRET.NE.0) GC 10 170
      EF = 0.
      CC 130 I=1,NY
      Y(3,1) = Y(3,1)-W(N+1)
      W(2*N+1) = AMAX1(ABS(Y(3,1)),1.0)
      130 ER = ER+(W(N+1)/AMAX1(ABS(Y(3,1)),1.0))**2
      140 IF (ER-1.EPS2) GC 10 50
      CC CONTINUE
      GC TO 170
      CC 150 I=1,NY
      Y(2,I) = Y(3,I)
      150 Y(2,I) = Y(3,I)
      170 RETURN
      KERET = 1
      RETURN
      END

```

```

380 DER
390 DER
400 DER
410 DER
420 DER
430 DER
440 DER
450 DER
470 DER
480 DER
490 DER
500 DER
510 DER
520 DER
530 DER
560 DER
570 DER
580 DER
590 DER
600 DER
620 CER
630 DER
640 DER
650 DER
660 CER
670 CER
680 CER
690 CER
700 CER
710 CER
720 CER
730 CER
740 CER
750 CER
760 CER
770 CER
780 CER
790 CER

```

## LIST OF REFERENCES

1. Apostolakis, G. E., "Analytical Estimate of the Error in Conventional Point-Kinetic Reactivity Due to Spatial Effects," Nucl. Sci. Engr., 53, p. 141-152, 1974.
2. Yasinsky, J. B., "On the Use of Point Kinetics for the Analysis of Rod Ejection Accidents," Nucl. Sci. Engr., 39, p. 241-256, 1970.
3. Jackson, J. F. and Kastenburger, W. S., "Space-time Dynamics Studies in Large LMFBR's with Feedback," Nucl. Sci. Engr., 42, p. 278-294, 1970.
4. Nguyen, D. H. and D. Salinas, "Finite Element Solution of Space-Time Nonlinear Reactor Dynamics," Nucl. Sci. Engr., 60, p. 120-130, 1976.
5. Hanford Engineering Development Laboratory Report HEDL-TME 92-128, User's Guide for GAPCON: A Computer Program to Predict Fuel-to-Cladding Heat Transfer Coefficients in Oxide Fuel Pins, by G. R. Horn and F. E. Panisko, 1972.
6. Hanford Engineering Development Laboratory Report HEDL-TME 74-47, Melt III-A Neutronics Thermal-Hydraulic Computer Program for Fast Reactor Safety, v. 1, by A. S. Walter and others, 1974.
7. Hanford Engineering Development Laboratory Report HEDL-TME 75-50, An Analysis of the Unprotected Transient Overpower Accident in the FTR, by A. S. Walter and others, 1975.
8. Naval Postgraduate School Report NPS-69Zc-76111, An Optimal Compact Storage Scheme for Nonlinear Reactor Problems by FEM, by D. Salinas, D. H. Nguyen, and R. Franke, 1976.
9. Naval Postgraduate School Report NPS-53Fe-76051, A Program for the Numerical Solution of Large Sparse Systems of Algebraic and Implicitly Defined Stiff Differential Equations, by R. Franke, 1976.
10. Lamarsh, J. R., Introduction to Nuclear Reactor Theory, Addison, Wesley, 1972.
11. Salinas, D., D. H. Nguyen and T. W. Southworth, "Finite Element Solution of a Nonlinear Nuclear Reactor Dynamics Problem," International Conference on Computational Methods in Nonlinear Mechanics, Austin, Texas, p. 541-550, 1974.

12. Semenze, L. A., Lewis, E. E., and Rossow, E. C., "The Application of the Finite Element Method to the Multi-group Neutron Diffusion Equation," Nucl. Sci. Engr., 47, p. 302-310, 1972.
13. Zienkiewicz, O. C., The Finite Element Method in Engineering Science, McGraw-Hill, 1970.
14. Zlamal, M., "On the Finite Element Method," Numer. Meth., 12, p. 394-409, 1968.
15. Personal conversation with Dr. G. Cantin of the Naval Postgraduate School, 1976.
16. Cook, R. D., Concepts and Applications of Finite Element Analysis, Wiley, 1974.
17. Zienkiewicz, O. C. and C. J. Parekh, "Transient Field Problems: Two-Dimensional and Three-Dimensional Analysis by Isoparametric Finite Elements," Int. J. for Numer. Meth. in Engr., v. 2, p. 61-71, 1970.
18. Barsoum, R. S., "On the Use of Isoparametric Finite Elements in Linear Fracture Mechanics," Int. J. for Numer. Meth. in Engr., v. 10, no. 1, p. 25-37, 1976.
19. Belle, J., Uranium Dioxide: Properties and Nuclear Applications, Naval Reactors, Div. of Reactor Development, U. S. Atomic Energy Commission, p. 189, 1961.
20. Lew, G. T., A Three Dimensional Solution of the Transient Field Problem Using Isoparametric Finite Elements, Masters Thesis, Naval Postgraduate School, 1972.

# INITIAL DISTRIBUTION LIST

	No. Copies
1. Defense Documentation Center Cameron Station Alexandria, Virginia 22314	2
2. Library, Code 0142 Naval Postgraduate School Monterey, California 93940	2
3. Department Chairman, Code 69 Department of Mechanical Engineering Naval Postgraduate School Monterey, California 93940	1
4. Dr. D. H. Nguyen (thesis advisor) 4625 Larchmont NE Albuquerque, New Mexico 87115	1
5. Assoc. Professor D. Salinas (thesis advisor) Department of Mechanical Engineering Naval Postgraduate School Monterey, California 93940	1
6. Assoc. Professor R. Franke (second reader) Department of Mathematics Naval Postgraduate School Monterey, California 93940	1
7. Professor Gilles Cantin Department of Mechanical Engineering Naval Postgraduate School Monterey, California 93940	1
8. LT R. E. Kasdorf, USN (student) 129 Redondo Ct. Marina, California 93933	2